

General Disclaimer

One or more of the Following Statements may affect this Document

- This document has been reproduced from the best copy furnished by the organizational source. It is being released in the interest of making available as much information as possible.
- This document may contain data, which exceeds the sheet parameters. It was furnished in this condition by the organizational source and is the best copy available.
- This document may contain tone-on-tone or color graphs, charts and/or pictures, which have been reproduced in black and white.
- This document is paginated as submitted by the original source.
- Portions of this document are not fully legible due to the historical nature of some of the material. However, it is the best reproduction available from the original submission.



(NASA-CR-150058) VIBRATION OF A FLEXIBLE
SPACECRAFT WITH MOMENTUM EXCHANGE
CONTROLLERS (California Univ.) 168 p
HC A08/MF A01

N77-11096

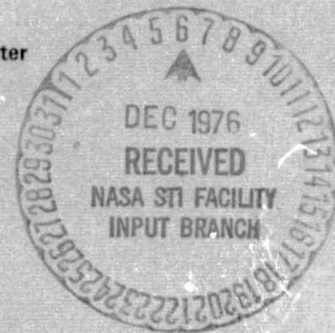
CSSL 22B

Unclas

G3/18

56142

Prepared for the George C. Marshall Space Flight Center
Marshall Space Flight Center, Alabama 35812
Under Contract No. NAS8-28358, Mod 12
Contract Type: CR



UCLA-ENG-7631
JUNE 1976

VIBRATION OF A FLEXIBLE SPACECRAFT WITH MOMENTUM EXCHANGE CONTROLLERS

J.R. CANAVIN

VIBRATION OF A FLEXIBLE SPACECRAFT WITH
MOMENTUM EXCHANGE CONTROLLERS

Joseph Reed Canavin

Principal Investigator: P.W. Likins

Prepared for
the George C. Marshall Space Flight Center
Marshall Space Flight Center, Alabama 35812
Under Contract No. NAS8-28358, Mod 12
Contract Type: CR

School of Engineering and Applied Science
University of California
Los Angeles, California

ABSTRACT

Significant problems are presented in the vibration and rotation analysis of spacecraft with distributed structural flexibility and momentum exchange controllers. These systems exhibit gyroscopic coupling which depends on the rotor speed and orientation, which must remain explicit in the analysis as control variables.

An investigation is made into floating reference frames in order to allow first order vibration analysis in the presence of large system rotations. When the deformations of an elastic continuum are expanded in terms of the free-free modes of an unconstrained system, the rigid body modes are found to be fixed relative to the Tisserand frame, with respect to which the relative momentum is zero. The proof presented for this is based on the orthogonality condition for modes with distinct natural frequencies. This result also guarantees the independence of coordinates for all modes with nonzero natural frequencies. A Modified Tisserand Constraint is introduced in order to define a floating reference frame with similar properties for an elastic body which contains a spinning rotor.

Finite element equations of motion are derived for a completely flexible spacecraft with momentum exchange controllers, using a Modified Tisserand Frame. The deformable systems covered in this application are assumed to undergo only small rotations, and therefore the rotor torques must formally be small, although in engineering applications it may be possible to relax this constraint. A modal analysis is performed for the system and the resulting set of equations is reduced in number by a truncation procedure for more efficient system simulation.

In order to gain insight into system behavior, a continuum analysis is performed for a simple physical system consisting of a uniform beam and an axisymmetric rotor. Equations are derived using Hamilton's principle and closed form solutions are obtained using generalized methods of separation of variables.

Numerical examples are presented for both the finite element and continuum equations of motion.

TABLE OF CONTENTS

	<u>Page</u>
LIST OF FIGURES	vii
CHAPTER 1. INTRODUCTION.	1
1.1 Statement of Problem	1
1.2 Motivation and Objectives.	3
1.3 Scope of the Dissertation.	4
CHAPTER 2. FLOATING REFERENCE FRAMES	7
2.1 Chapter Summary.	7
2.2 Floating Frames for Deformable Bodies.	7
2.3 Description of Specific Floating Frames.	10
2.4 Example of Frame Motion.	16
2.5 Historical Perspective	23
CHAPTER 3. THE TISSERAND FRAME FOR A DEFORMABLE BODY	27
3.1 Chapter Summary.	27
3.2 Mode Shape Constraint.	28
3.3 Discussion and Example of the Mode Shape Constraint	36
3.4 Modified Tisserand Constraint.	40
CHAPTER 4. FINITE ELEMENT EQUATIONS OF MOTION.	47
4.1 Chapter Summary.	47
4.2 System Kinetic Energy.	49
4.3 Constraint Equations	56
4.4 Equations of Motion-Discrete Coordinates	57
4.5 Modal Analysis	62
CHAPTER 5. CONTINUUM ANALYSIS.	67
5.1 Chapter Summary.	67
5.2 Governing Partial Differential Equations	69
5.3 Solution of the Partial Differential Equations	80
5.4 Numerical Solutions.	92
CHAPTER 6. NUMERICAL RESULTS FOR THE FINITE ELEMENT MODEL.	103
6.1 Chapter Summary.	103
6.2 Example Problem and Modal Analysis	104
6.3 Numerical Integration and Truncation Procedure	117

TABLE OF CONTENTS (Cont'd)

	<u>Page</u>
CHAPTER 7. SUMMARY, CONTRIBUTIONS AND FUTURE WORK.	129
BIBLIOGRAPHY.	135
APPENDIX A. NOMENCLATURE.	137
APPENDIX B. COORDINATE TRANSFORMATIONS.	143
APPENDIX C. VECTOR-DYADIC RELATIONSHIPS	147
APPENDIX D. HYBRID COORDINATE METHOD USING ASSUMED MODE SHAPES FOR ELASTIC CONTINUUM.	149

LIST OF FIGURES

	Page
2.1 Example System	17
2.2 Coordinate Systems	19
3.1 Rotational Rigid Body Modes.	31
3.2 Example Problem Mode Shapes.	38
4.1 Location of Generic Mass Element	51
5.1 Uniform Beam with Tip Mounted Rotor.	70
5.2 Geometry of the Beam Element	73
5.3 First Natural Frequency.	94
5.4 Second Natural Frequency	95
5.5 First Mode Shapes.	96
5.6 Second Mode Shapes	97
5.7 Third Mode Shapes.	98
5.8 Fourth Mode Shapes	99
5.9 Fifth Mode Shapes.	100
5.10 Motion of the Tip of the Rotor Shaft	101
6.1 Finite Element Model	106
6.2 Bending Mode Shapes.	114
6.3 Torsion Mode Shapes.	116
6.4 Initial Conditions	118
6.5 Numerical Results at Quarter Period Point.	122
6.6 Numerical Results at Half Period Point	123
6.7 Numerical Results at Three Quarter Period Point.	124
6.8 Numerical Results at One Period Point.	125
6.9 Motion of the Tip of the Rotor Shaft	126

CHAPTER 1
INTRODUCTION

1.1 Statement of Problem

Modern spacecraft design relies on the successful dynamic analysis of the system in order to provide attitude stabilization. This is true for both active and passive attitude control systems. Present systems emphasize active control techniques with momentum exchange controllers being the most popular because of their greater accuracy potential.

Momentum exchange controllers fall into three general categories: dual spin, momentum (or reaction) wheel and control moment gyro systems. The dual spin spacecraft typically has a large rotor spinning at a nearly constant speed and a despun platform. For communications satellites, the antennas are mounted on the despun platform, which is aimed at a point on the earth. The platform orientation about one axis is controlled by changes in the rotor speed, and orientation about the other two axes is passively controlled by a nutation damper. An example of this type of system is the Intelsat IV spacecraft. The second type is the momentum wheel or reaction wheel system. The reaction wheel has a nominal spin rate near zero. There may be three or more rotors, and control about each axis is accomplished actively by controlling rotor speeds. This is often referred to as a type of a three axis stabilized system. An example of this system is the Orbiting Astronomical Observatory (OAO). The third type of system uses the control moment gyro (CMG). This device consists of a gimballed constant speed rotor. Torques are applied to the vehicle by driving the gimbals and changing

the orientation of the rotor. An example of a spacecraft with this system is SKYLAB. A mixture of the above and active control using gas jets has also been incorporated in spacecraft design.

To analyze these systems, many powerful techniques and formulations are available. If the system is treated as a group of interconnected rigid bodies, Newton's laws may be used to solve for the equations of motion. Advanced formulations exist for general classes of configurations which use nested body techniques to eliminate the constraint forces. An example of this is the Hooker-Margulies-Hooker system of equations. If the bodies are not rigid, flexibility of terminal appendages may also be analyzed by using the "hybrid coordinate" method. This approach utilizes a combination of discrete and modal coordinates. The underlying finite element formulation allows truncation of the number of degrees of freedom after a modal analysis and therefore has the very great advantage of computational ease. Appendix D contains a simplified example of this approach.

Ongoing developments are causing the rigid body model of a spacecraft to be less acceptable. The effects of distributed structural flexibility need to be included to reduce spacecraft weights and to meet ever more stringent accuracy requirements. The increase in size of spacecraft due to the advent of the Space Shuttle will also make rigid body models less precise. This research was motivated by the attitude control problems associated with the proposed Large Space Telescope (LST).

The incorporation of distributed structural flexibility for the entire vehicle introduces great complexity to the dynamic analysis. The

linearized equations of motion for a finite element model with momentum exchange controllers contain time varying coefficients. Thus, an eigenvalue analysis to find vehicle normal modes is not possible. If the spin speeds are constant, a modal analysis results in complex modes; that is, the eigenvectors are represented by complex numbers. If a continuum model is adopted, the resulting partial differential equations are coupled and have time varying boundary conditions.

1.2 Motivation and Objectives

The motivation for this study was a desire to address the difficulties posed by spacecraft of the next level of complexity. A review of the present techniques does not indicate an appropriate course of action for the dynamic analysis of spacecraft with both distributed flexibility and momentum exchange controllers. A finite element model must be adopted to allow for arbitrary mass and stiffness properties. A modal analysis will allow the introduction of distributed coordinates and the truncation to a smaller number of coordinates. A modal analysis can be accomplished only for nearly constant speeds, and then the complex mode shapes depend on the chosen spin speed and rotor orientation. A method of staging mode shapes for different ranges of spin speeds or orientations would have to be devised to handle a general system. This is not an attractive method.

The hybrid coordinate method is frustrated by the lack of a central rigid body. For this method, the modal coordinates are coupled to each other through the motion of the central rigid body. If a rigid body is designated from among the rigid bodies in the finite element model, perhaps the body to which the rotor is mounted, then the mass

properties of the body will influence the determination of the modal coordinates. This casts the validity of the truncation procedure into doubt.

The principal objectives of this research on the vibration of spacecraft with distributed flexibility and momentum exchange controllers are:

1. Provide the advantage of a first order vibration analysis by adopting a floating reference frame which somehow "moves" with the flexible body.
2. Develop equations of motion for use in spacecraft dynamics and control analysis.
3. Gain insight into system behavior through analysis of simple physical systems.

1.3 Scope of the Dissertation

The body of the work pursued in the dissertation is broken into two main parts. The first part consists of the introduction and analysis of various floating reference frames. The second part consists of the formulation of equations of motion for the class of spacecraft characterized by distributed flexibility and momentum exchange controllers, using both finite element and continuum models. Numerical examples are developed for both classes of models, using eigenvalue analysis and numerical integration for the finite element model and closed form solutions for the continuum model. The two parts of the dissertation are interrelated by the use of a floating reference frame in the finite element analysis of a system with momentum exchange controllers. In order to aid in understanding the organization of the dissertation, a brief summary of each chapter is presented.

Chapter one introduces the problem area and presents the motivation for the studies undertaken. The difficult aspects of the problem are identified and the existing solution techniques are reviewed. The topics covered by the dissertation are discussed.

Chapter two introduces the concept of a floating reference frame. For an elastic body free to rotate, these frames are introduced in order to ensure the validity of a first order vibration analysis. A review is made of several distinct ways of defining a floating reference frame. They all provide for frame motion which somehow "follows" the overall body. In order to demonstrate how this is accomplished, a very simple example problem is worked out to illustrate the motion of specific frames when the body is deformed. The chapter concludes with a brief historical perspective of the use of floating frames to solve problems in the physical sciences.

Chapter three deals with a specific floating frame, the Tisserand frame, which is defined in terms of angular momentum relative to the frame. An examination of the constraint relationship reveals a rather elegant solution form which involves the free-free modes of an unconstrained system. This is called the Mode Shape Constraint. An example is worked out in order to illustrate the application of the Mode Shape Constraint to a simple problem. The last section of the chapter expands the concept of the Tisserand frame to systems containing spinning rigid rotors. This is done with the introduction of the Modified Tisserand Constraint.

Chapter four begins the second main part of the dissertation. The focus now turns to the derivation of equations of motion for systems

containing a spinning rigid rotor. System behavior is limited by the requirement that variations in rotor angular momentum be first order. The deformable body is also assumed to undergo only small, first order rotations. This chapter uses a Finite Element Model and applies the Modified Tisserand Constraint. A modal analysis leads to a system of equations which are still coupled, but which may be truncated to a smaller number of coordinates.

Chapter five defines a very simple physical system consisting of a uniform beam and axisymmetric rotor for analysis as a continuum. Hamilton's Principle is used to derive the governing partial differential equations with boundary conditions. Generalized separation of variables techniques are used in order to solve for the system natural frequencies and system normal modes. Numerical solutions are provided for a specific choice of parameters in order to illustrate the system behavior.

Chapter six presents numerical results for the Finite Element Model equations of motion. The strategy is quite simple. The simple physical system introduced in Chapter five is modeled by finite elements and initial conditions are chosen for a vehicle normal mode as determined by the continuum analysis. Numerical integration of the Finite Element Model equations of motion should then demonstrate periodic behavior corresponding to the system natural frequency. The method of truncation to a smaller number of modal coordinates is investigated.

Chapter seven summarizes the dissertation problem, techniques and contributions. The principal conclusions of the research are assembled and areas of future work are outlined.

CHAPTER 2

FLOATING REFERENCE FRAMES

2.1 Chapter Summary

The problem of specifying a set of axes for a deformable body is a difficult one. The use of a moving or "floating" set of axes is introduced here. The choice of a floating reference system is not unique and several alternative methods are described. In particular, there are the locally attached frame, the principal axis frame, the Tisserand and Buckens frames, and the rigid body mode frame. The advantages of each different type of floating frame are discussed and a simple example is used to illustrate the motion of the different floating frames. The historical origin of the principal axis and Tisserand reference frames is briefly discussed to demonstrate their application to past problems in the physical sciences.

2.2 Floating Frames for Deformable Bodies

For the problems discussed here, we are concerned with small deformations of elastic bodies. Specifically, we will define a deformable body to be a body for which the relative displacements are so small that only first order terms need be retained in the analysis. The body is allowed overall motion which is completely unrestricted; that is, the body has complete freedom of motion in responding to impressed moments and forces.

For such a body, it is difficult to specify a set of axes from which to measure deformations. If an inertially fixed set of axes is chosen, the displacements relative to these axes may grow large if the body undergoes any appreciable rotation due to an externally applied

moment. Then the dynamic analysis of the system using these displacements would require more than a first order analysis. In order to simplify the analysis, the idea presents itself to use a frame that somehow moves with the body. If a frame moves with the body, or "floats", in the proper way, then the displacements measured relative to this floating frame will be small. The dynamic analysis of the system may then be pursued using a first order analysis. It is this property, the use of a first order analysis, that makes a floating frame attractive.

There are five types of floating frames that will be treated here; they are:

- Locally attached frame
- Principal axis frame
- Tisserand frame
- Buckens frame
- Rigid body mode frame.

Before these different types of frames are discussed in detail, several general characteristics of floating frames will be discussed. A deformable body experiences relative displacement and therefore the system inertia quantities do not remain constant. In the formulation of equations of motion, the system angular momentum and kinetic energy are a function of the relative displacements and possess a more complicated structure than for rigid bodies. The system angular momentum for a deformable body about its center of mass is written as:

$$\underline{H} = \int_D \underline{\rho} \times \dot{\underline{\rho}} \, dm \quad (2.1)$$

where

$\underline{\rho}$ = vector from the center of mass to a generic mass element

$\dot{\underline{\rho}}$ = $\frac{d}{dt} \underline{\rho}$ = time derivative of $\underline{\rho}$ relative to inertial space

dm = generic mass element

D = integration over the deformable body

\underline{H} = angular momentum of the system about the center of mass.

If a floating frame, f , is introduced with its origin at the center of mass, then

$$\dot{\underline{\rho}} = \dot{\underline{\rho}}^{\circ} + \underline{\omega}^{fi} \times \underline{\rho} \quad (2.2)$$

where

$\dot{\underline{\rho}}^{\circ} = \frac{d}{dt} \underline{\rho}$ = time derivative of $\underline{\rho}$ relative to floating frame f .

$\underline{\omega}^{fi}$ = angular velocity of frame f relative to inertial space.

Using this relationship to evaluate the angular momentum yields

$$\underline{H} = \underline{I} \cdot \underline{\omega}^{fi} + \int_D \underline{\rho} \times \dot{\underline{\rho}} dm \quad (2.3)$$

since

$$\int_D \underline{\rho} \times (\underline{\omega}^{fi} \times \underline{\rho}) dm = \underline{I} \cdot \underline{\omega}^{fi} \quad (2.4)$$

where \underline{I} is the inertia dyadic for the mass center. The second quantity in Equation (2.3) is the angular momentum relative to the floating frame. This is referred to as the internal angular momentum. The first term of Equation (2.3) is structurally identical to the rigid body angular momentum, but since the body is deformable, the inertia dyadic is not constant. It should be noted that for small (first order) displacements relative to the floating frame, the variations in the inertia dyadic will be first and higher order terms.

The kinetic energy of a body with an inertially fixed center of mass may be written

$$T = \frac{1}{2} \int_D \dot{\underline{\rho}} \cdot \dot{\underline{\rho}} \, dm \quad (2.5)$$

Using the relationship for the time derivative in Equation (2.2) allows the kinetic energy to be rewritten using a floating frame as

$$T = \frac{1}{2} \underline{\omega}^{fi} \cdot \underline{\square} \cdot \underline{\omega}^{fi} + \underline{\omega}^{fi} \cdot \int_D (\underline{\rho} \times \dot{\underline{\rho}}) \, dm + \frac{1}{2} \int_D \dot{\underline{\rho}} \cdot \dot{\underline{\rho}} \, dm \quad (2.6)$$

where

$$\frac{1}{2} \underline{\omega}^{fi} \cdot \underline{\square} \cdot \underline{\omega}^{fi} = \frac{1}{2} \int_D (\underline{\omega}^{fi} \times \underline{\rho}) \cdot (\underline{\omega}^{fi} \times \underline{\rho}) \, dm.$$

The first term of this equation has the same structural form as the kinetic energy of a rigid body. Again, this quantity differs from the rigid body quantity because the inertia dyadic is not constant. The second term includes the same internal angular momentum expression found earlier in Equation (2.3). The last term could be called the internal kinetic energy, since it represents kinetic energy contributed by the dot product of velocities relative to the frame.

2.3 Description of Specific Floating Frames

This next section will now deal with the specific definitions for the most commonly available floating frames. The first type to be discussed is the locally attached frame. For this frame, a sub-body or mass element is identified in the deformable body, and a frame is defined that follows the motion of this sub-body or mass element. An example of this type of frame may be associated with a spacecraft with a rigid central body and a flexible appendage. A reference frame may be attached to the central rigid body. Also, if the appendage is

driven, that is, its orientation relative to the central rigid body varies as a specific function of time in addition to small displacements, a floating reference frame may be attached to a mass element in the appendage. This would most commonly be a set of axes fixed in the appendage at the mounting point. The angular momentum and kinetic energy for a locally attached frame would be given by equations (2.3) and (2.6) respectively. As a general rule, no simplification of these expressions could be guaranteed for the locally attached reference frame.

The next type of floating reference, the principal axis frame, does offer some simplification of the expressions for angular momentum and kinetic energy. For this frame, the origin of the axes would be the center of mass and the orientation of the axes would be such that the inertia matrix of the deformable body would be diagonal. This defines the location of the principal axes of inertia. The components of a diagonal inertia matrix are called the moments of inertia for principal axes and the products of inertia are all zero. Because the inertia matrix contains only three components, the calculations for angular momentum and kinetic energy are simplified. However, this is done at the expense of introducing three constraint relationships that require the products of inertia all to be zero. The constraint relationships are

$$\begin{aligned}
 I_{12} = I_{21} &= - \int_D \rho_1 \rho_2 \, dm = 0 \\
 I_{13} = I_{31} &= - \int_D \rho_1 \rho_3 \, dm = 0 \\
 I_{23} = I_{32} &= - \int_D \rho_2 \rho_3 \, dm = 0
 \end{aligned} \tag{2.7}$$

where (ρ_1, ρ_2, ρ_3) are the components of $\underline{\rho}$ in the floating frame

For the Tisserand frame, the expressions for angular momentum and kinetic energy are structurally simplified by moving the axes so as to set the internal angular momentum always to zero. The requirement is also made that the internal linear momentum be zero. This is accomplished by the simple requirement that the origin of the frame be located at the center of mass. In order to set the internal angular momentum to zero, a constraint relationship is introduced:

$$\int_D \underline{\rho} \times \dot{\underline{\rho}} \, dm = 0 \quad (2.8)$$

Referring back to Equation (2.3), the angular momentum is thus

$$\underline{H} = \underline{I} \cdot \underline{\omega}^{fi} \quad (2.9)$$

This is structurally identical to the rigid body form, although as noted, the inertia matrix is not a constant for a deformable body as it would be for a rigid body relative to axes fixed in that body. Going back to the constraint relationship, let us evaluate this in greater detail. First we introduce a new expression for the position relative to the center of mass

$$\underline{\rho} = \bar{\underline{\rho}} + \underline{u} \quad (2.10)$$

where $\bar{\underline{\rho}}$ is the position of a generic mass element in the undeformed state. This vector, $\bar{\underline{\rho}}$, is fixed in the floating reference frame and may be thought of as the station location of a mass element. The vector \underline{u} represents the deformation of a generic mass element. For a deformable body, this will be a first order quantity. The derivative

of the position of a generic mass element relative to the center of mass is then written as

$$\underline{\dot{\rho}} = \underline{\dot{\bar{\rho}}} + \underline{\dot{u}} = \underline{\dot{u}} \quad (2.11)$$

since $\underline{\bar{\rho}}$ is fixed in the frame and has no derivative relative to the frame. The constraint relationship is then

$$\int_D \underline{\rho} \times \underline{\dot{u}} \, dm = 0 \quad (2.12)$$

This is equivalent to the three scalar equations

$$\begin{aligned} \int_D \dot{u}_3(y + u_2) - \dot{u}_2(z + u_3) \, dm &= 0 \\ \int_D \dot{u}_1(z + u_3) - \dot{u}_3(x + u_1) \, dm &= 0 \\ \int_D \dot{u}_2(x + u_1) - \dot{u}_1(y + u_2) \, dm &= 0 \end{aligned} \quad (2.13)$$

where (x, y, z) are components of $\underline{\bar{\rho}}$ in the floating frame. The next step in our examination of the constraint relationship is to introduce a separation of variables for the deformations. Then the deformations may be written as

$$\begin{aligned} u_1 &= \sum_{i=1}^n \phi_1^i(\underline{\bar{\rho}}) \eta_i(t) \\ u_2 &= \sum_{i=1}^n \phi_2^i(\underline{\bar{\rho}}) \eta_i(t) \\ u_3 &= \sum_{i=1}^n \phi_3^i(\underline{\bar{\rho}}) \eta_i(t) \end{aligned} \quad (2.14)$$

where the variables $(\phi_1^i, \phi_2^i, \phi_3^i)$ are the components of the mode shape $\underline{\phi}^i$ and depend only on the spatial variables. The variable η_i is the modal

coordinate and depends on the time. This separation of variables may be written in vector form as

$$\underline{u} = \sum_{i=1}^n \underline{\phi}^i \dot{\eta}_i \quad (2.15)$$

Using the separation of variables in the constraint relationship yields

$$\sum_{j=1}^n \int_D \left[\left(\underline{\bar{\rho}} + \sum_{i=1}^n \underline{\phi}^i \eta_i \right) \times \underline{\phi}^j \right] dm \dot{\eta}_j = 0 \quad (2.16)$$

This is a vector constraint of the Pfaffian form

$$\sum_{j=1}^n \underline{a}_j(\eta) \dot{\eta}_j = 0 \quad (2.17)$$

where

$$\underline{a}_j(\eta) = \int_D \left[\left(\underline{\bar{\rho}} + \sum_{i=1}^n \underline{\phi}^i \eta_i \right) \times \underline{\phi}^j \right] dm. \quad (2.18)$$

If the constraint relationship (Equation (2.16)) possesses an integral, then the constraint is holonomic. It is important to note that if a Tisserand constraint is used in a Lagrangian formulation, then the equations of motion must include Lagrange multipliers for the general case. The Tisserand frame is a general concept and may be applied to a system where the deformations are large. In the case of a deformable body as previously defined, the relative displacements are small and may be treated analytically as first order quantities. The analysis may then proceed using first order quantities and may ignore second and higher order terms. It is proceeding in this direction which leads us to introduce the Buckens frame. The Buckens constraint relationship is simply a first order Tisserand constraint. It may be written as

$$\int_D \bar{\rho} \times \dot{\underline{u}} \, dm = 0 , \quad (2.19)$$

Again the origin of the system is placed at the center of mass. The Buckens constraint is identical to the Tisserand constraint if this relationship holds

$$\int_D \underline{u} \times \dot{\underline{u}} \, dm = 0 \quad (2.20)$$

The justification for the above is that second order quantities may be ignored for a deformable body. Introducing a separation of variables again yields a constraint of the Pfaffian form

$$\sum_{j=1}^n \int_D \bar{\rho} \times \underline{\phi}^j \, dm \, \dot{\eta}_j = 0 \quad (2.21)$$

The difference is that now the coefficients of the constraint relationship are constant and the expression always possesses an integral. Thus, the Buckens or first order Tisserand constraint is a holonomic constraint. Since the Buckens and Tisserand constraints are identical for a deformable body as defined above, they will both be referred to as the Tisserand constraint. This choice is made because of the historical precedence of the Tisserand constraint and the fact that it is more common in the literature. This is not to minimize the contribution made by Buckens, for it is the first order form which will allow the greater use of the Tisserand frame that is explored in the next chapter.

The last frame to be described is the rigid body mode frame. This concept arises in structural dynamics for semidefinite systems. A semidefinite system is one for which the strain energy may be zero

without the motion being zero. Unrestrained systems, or systems without supports, are typical examples of semidefinite systems. A rigid body mode is defined as a displacement which results in zero strain energy. The rigid body mode frame follows the displacement which results in zero strain energy. There is an essential difference between the rigid body mode and the equilibrium position of a body. The rigid body mode is associated with zero strain energy which results in the equilibrium position of the body at rest. The body must be inertially at rest both translationally and rotationally. If a body is spinning at a given rate, the equilibrium position will not coincide with the rigid body mode (equilibrium at rest) since the centrifugal forces may be thought of as inducing a nonzero strain energy at equilibrium. The presence of environmental forces such as thermal gradients can complicate the notion of a rigid body mode. The dictum of zero strain energy must still be followed in this case, but the effects of environmental forces on the strain energy can be neglected.

The constraint relationship associated with the rigid body mode is simply that the strain energy be zero. The difficulty of working with this constraint is circumvented by showing a relationship between the Tisserand frame for deformable bodies and the rigid body mode frame. This allows the rigid body mode to be easily applied. This is pursued in the next chapter.

2.4 Example of Frame Motion

In order to give insight into the concept of a floating reference frame, a simple example problem has been formulated. This example system is shown in Figure 2.1 and consists of two uniform rigid bodies

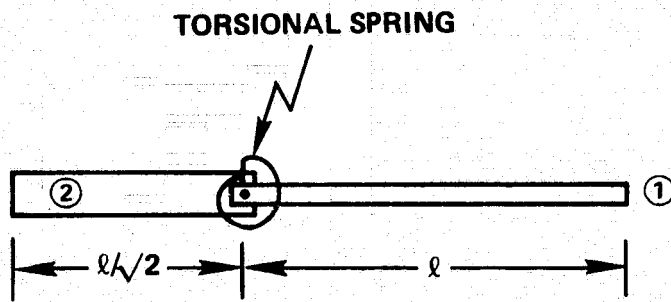


Figure 2.1. Example System.

that are connected by a line hinge. All motion is planar. In the undeformed position, the two bodies are aligned in a straight line. The length of body one is ℓ and the length of body two is $\ell/\sqrt{2}$. The mass per unit length of body two is twice that of body one. This places the center of mass for the undeformed body at the hinge point. The above system is made non-uniform in order to separate the motion of the principal axis and Tisserand frames. If the bodies were identical, the two frames would move in the same manner. The coordinate systems for the example are shown in Figure 2.2. The deformation of the system is specified by the angle α between the two bodies. A set of axes, with respect to which unit vectors \hat{b}_1 , \hat{b}_2 , and \hat{b}_3 are fixed, is fixed in body two with its origin at the hinge point. The location of the hinge point relative to the center of mass is specified by the vector \underline{R} . A floating frame, in which unit vectors \hat{f}_1 , \hat{f}_2 , and \hat{f}_3 are fixed, has its origin at the center of mass and makes an angle β with the body fixed axes. A mass element is located by a vector \underline{x} relative to the hinge point with the subscript specifying the associated body. The center of mass is defined by

$$\int_D \underline{\rho} \, dm = 0 \quad (2.22)$$

This becomes for the example

$$\int_0^\ell (\underline{R} + \underline{x}_1) \, m \, dx + \int_0^{\frac{\ell}{\sqrt{2}}} (\underline{R} + \underline{x}_2) \, 2m \, dx = 0 \quad (2.23)$$

where

$$\begin{aligned} \underline{x}_1 &= x(\cos\alpha \hat{b}_1 + \sin\alpha \hat{b}_2) \\ \underline{x}_2 &= -x \hat{b}_1 \end{aligned} \quad (2.24)$$

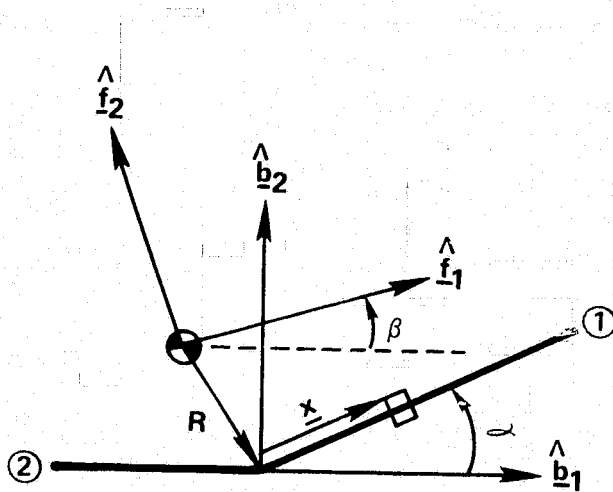


Figure 2.2. Coordinate Systems.

This yields the position vector of the hinge point relative to the center of mass

$$\underline{R} = \hat{b}_1 \left[\frac{\ell}{4} (1 - \cos\alpha) \right] - \hat{b}_2 \left(\frac{\ell}{4} \sin\alpha \right) \quad (2.25)$$

Note that the center of mass is at the hinge point for zero deformations.

The Tisserand frame will have its origin at the center of mass and will obey the constraint relationship

$$\int_D \underline{\rho} \times \dot{\underline{\rho}} \, dm = 0 \quad (2.26)$$

where

$$\begin{aligned} \underline{\rho}_1 &= \underline{R} + \underline{x}_1 \\ \underline{\rho}_2 &= \underline{R} + \underline{x}_2 \end{aligned} \quad (2.27)$$

The constraint then becomes

$$\int_0^\ell m \left(\rho_{1x} \dot{\rho}_{1y} - \rho_{1y} \dot{\rho}_{1x} \right) dx + \int_0^{\frac{\ell}{\sqrt{2}}} 2m \left(\rho_{2x} \dot{\rho}_{2y} - \rho_{2y} \dot{\rho}_{2x} \right) dx = 0 \quad (2.28)$$

Evaluating the vectors in Equation (2.27) in the floating reference frame so as to facilitate the derivatives involved yields

$$\begin{aligned} \underline{\rho}_1 &= \{\hat{f}\}^T \begin{Bmatrix} \frac{\ell}{4} \cos\beta + \left(x - \frac{\ell}{4}\right) \cos(\alpha-\beta) \\ -\frac{\ell}{4} \sin\beta + \left(x - \frac{\ell}{4}\right) \sin(\alpha-\beta) \\ 0 \end{Bmatrix} \\ \underline{\rho}_2 &= \{\hat{f}\}^T \begin{Bmatrix} -\left(x - \frac{\ell}{4}\right) \cos\beta - \frac{\ell}{4} \cos(\alpha-\beta) \\ \left(x - \frac{\ell}{4}\right) \sin\beta - \frac{\ell}{4} \sin(\alpha-\beta) \\ 0 \end{Bmatrix} \end{aligned} \quad (2.29)$$

where $\{\hat{f}\}$ is the 3×1 array of vectors $\hat{f}_1, \hat{f}_2, \hat{f}_3$.

With these relationships and the derivatives of the components, the constraint relationship may be evaluated. After the necessary algebra and integrations, Equation (2.28) becomes

$$(.2342 + .0991 \cos\alpha)\dot{\alpha} - (.3333 + .1982 \cos\alpha)\dot{\beta} = 0 \quad (2.30)$$

This constraint is in the Pfaffian form and since it possesses an integral, the Tisserand constraint here is holonomic. If the deformations are small, then the constraint shows that the frame must move relative to the bodies in a specific manner, that is

$$\dot{\beta} = .586 \dot{\alpha} \quad (2.31)$$

For a Buckens frame, the constraint relationship is

$$\int_D \bar{\rho} \times \dot{\bar{\rho}} \, dm = 0 \quad (2.32)$$

where

$$\begin{aligned} \bar{\rho}_1 &= x \hat{f}_1 \\ \bar{\rho}_2 &= -x \hat{f}_1 \end{aligned} \quad (2.33)$$

The constraint can be stated in the form

$$\int_0^l m \bar{\rho}_1 \dot{\rho}_1 \, dx + \int_0^{\frac{l}{\sqrt{2}}} 2m \bar{\rho}_2 \dot{\rho}_2 \, dx = 0 \quad (2.34)$$

Evaluating the derivatives from Equation (2.29) and performing the necessary algebra gives the constraint in the form

$$\cos(\alpha-\beta)(\dot{\alpha}-\dot{\beta}) - .7071 \cos\beta\dot{\beta} = 0 \quad (2.35)$$

For small deformations, the relationship between the angles will be

$$\dot{\beta} = .586 \dot{\alpha} \quad (2.36)$$

This is the same answer for small deformations that resulted from the Tisserand frame. This is to be expected since the Buckens frame is

simply a first-order Tisserand frame and they are identical for systems undergoing small deformations.

For the principal axis frame, the constraint will set the product of inertia to zero

$$I_{12} = \int_D \rho_x \rho_y \, dm = 0 \quad (2.37)$$

The constraint relationship for the example is then written

$$\int_0^{\ell} m \rho_{1x} \rho_{1y} \, dx + \int_0^{\frac{\ell}{\sqrt{2}}} 2m \rho_{2x} \rho_{2y} \, dx = 0 \quad (2.38)$$

Using the expressions found in Equation (2.29) which hold for any floating frame, and completing the necessary algebra yields

$$-.1367 \sin\beta \cos\beta + .0991 \sin(\alpha-2\beta) + .2341 \sin(\alpha-\beta) \cos(\alpha-\beta) = 0 \quad (2.39)$$

For small angles, the relationship between the coordinates is

$$\beta = .476 \alpha \quad (2.40)$$

The above constraint relationships are holonomic in form since they relate the coordinates. The Tisserand and Buckens constraints are of the Pfaffian form since they relate velocities. They may be integrated in this case and if both angles are zero initially, then they yield

$$\beta = .586 \alpha \quad (2.41)$$

This means that the principal axis frame is definitely distinct from the Tisserand frame for this example. The Tisserand frame will move more relative to the body fixed frame due to a deformation than will the principal axis frame for this specific case. The Tisserand frame will rotate 1.23 degrees for each degree that the principal axis frame rotates due to a deformation of the system. The rotation of the frames

discussed above is relative to the body fixed frame. One special case of the rotation of the Tisserand frame relative to inertial space should be mentioned. For a moment free body with zero net angular velocity, the angular momentum will remain zero due to conservation laws. For this case, by reference to Equation (2.9), the frame angular velocity must be zero since the inertia matrix is positive definite. Thus, the Tisserand frame in this special case will be inertially fixed, while the principal axis frame moves.

2.5 Historical Perspective

The principal axis and Tisserand frames both had applications to problems in the physical sciences during the late nineteenth century. The question that was addressed was posed by George Darwin:

"The subject of the fixidity or mobility of the earth's axis of rotation in that body... [has] from time to time attracted the notice of mathematicians and geologists. The latter look anxiously for some grand cause capable of producing such an enormous effect as the glacial period. Impressed by the magnitude of the phenomenon, several geologists have postulated... a wide variability in the position of the poles on the earth; and this, again, they have sought to refer back to the upheaval and subsidence of continents."¹

Very minor movement of the poles of perhaps 50 feet is measured by modern astronomers and is referred to as the variation of latitude. This variation is thought to be due to seasonal changes in the distribution of the air masses over the earth.

¹G.H. Darwin, Scientific Papers, (Cambridge, 1910), Volume 3, p. 1.

The use of floating frames was introduced in order to formulate equations of motion for a body undergoing small deformations due to elevation and subsidence of continents and sea beds. The researches of George Darwin were the most detailed in the evaluation of specific results. He introduced a principal axis frame and derived equations of motion for this frame. By adopting a system consisting of a rigid earth and a deformable thin shell, he studied the effects of deformation. The shell was deformed in such a way as to give the maximum movement of the poles consistent with geological evidence. He was able to show that a movement of the poles of 8 degrees would require one half of the earth's surface to be deflected by nearly two miles. This would effectively make continents out of oceans and vice versa. Darwin then concludes:

"If the geologists are right in supposing that where the continents now stand they have always stood, would it not be almost necessary to give up any hypothesis which involved a very wide excursion of the poles?"²

The mean axes which were popularized by Tisserand and which bear his name were introduced by Gylden in his study of the rotation of the earth. This is stated by Tisserand in Sections 214 and 216 of his *Traité de Mécanique Céleste*. Tisserand derives the equations of motion for what we call the Tisserand frame by setting the internal angular momentum to zero. He reports then on the work of Glyden in using this frame in deriving an expression for the deviation of the mean axes from the principal axes of the system. The application of

²Ibid., p. 39.

the floating reference frame was similar in intent to that of Darwin, but his conclusions regarding the motion of the poles was more analytical in nature and not as concrete.

CHAPTER 3

THE TISSERAND FRAME FOR A DEFORMABLE BODY

3.1 Chapter Summary

This chapter focuses in detail on the use of the Tisserand frame for vibration analysis of unconstrained systems. The choice of mode shapes to be used for expansion of the deformations relative to the floating frame is crucial. With an unwise choice of mode shapes, the constraint relationship may depend on all of the coordinates and may be difficult to deal with. The simplest constraint relationships result from the use of the free-free modes of an unconstrained system. The orthogonality of the rigid body modes (zero natural frequency) to the deformational modes allows for a rather elegant a priori evaluation of the constraint relationships. The constraint relationships then involve only the rigid body modal coordinates, which must be zero. This result may then be interpreted as a requirement that the rigid body mode is fixed relative to the Tisserand frame. The remaining coordinates are then independent, a condition which can greatly simplify the formulation of equations of motion. This special case of the Tisserand constraint that uses the free-free modes of an unconstrained system is termed the Mode Shape Constraint. An example is worked out in order to demonstrate the properties of the Mode Shape Constraint.

The classical Tisserand constraint cannot be employed for systems with rotating internal members. This class of systems represents spacecraft with momentum exchange controllers. These represent reaction wheel, momentum wheel and control moment gyro control systems. Several alternate extensions to the Tisserand frame are discussed and a Modified

Tisserand Constraint is introduced. The properties of this constraint relationship are discussed and the applicability of the Mode Shape Constraint is demonstrated.

3.2 Mode Shape Constraint

There were two requirements made in order to define the Tisserand frame for a deformable body. The first was that the center of mass be fixed in the frame. This would then insure that the system possessed no linear momentum relative to the frame. But by introducing this constraint, three additional variables were required to specify the location of the point of the frame occupied by the mass center, which point may be referred to as the frame origin. The second defining requirement was that the system had no angular momentum relative to the frame. This constraint then introduced an additional three coordinates to specify the angular orientation of the frame. The net result of injecting the Tisserand frame into the problem for a deformable body is to expand the dimension of the problem by six and to interrelate the coordinates by six scalar equations (two vector equations). It is the interrelation of the coordinates, and the resulting fact that they are no longer linearly independent, which can prove troublesome in the formulation of the equations of motion. Constraint relationships require the use of Lagrange multipliers when Lagrange's equations are used. It would be extremely advantageous to evaluate the constraint relationships and reduce the order of the system before the equations of motion are formulated.

There exists a very intimate relationship between the Tisserand frame and the free-free modes of an unconstrained system; this special

relationship we call the Mode Shape Constraint. This relationship employs the orthogonality conditions that exist between the rigid body modes and the deformational modes (which have nonzero natural frequencies) to allow a rather elegant a priori evaluation of the Tisserand constraint. This is accomplished by setting all rigid body modal coordinates to zero. This effectively reduces the order of the system to the original value and the remaining coordinates are all independent.

The constraint relationships that define a Tisserand constraint for a deformable body (which by virtue of small deformations are also the Buckens constraints) are given by

$$\int_D \underline{\rho} \, dm = 0 \quad (3.1)$$

and

$$\int_D \underline{\bar{\rho}} \times \underline{\dot{u}} \, dm = 0 \quad (3.2)$$

where $\underline{\rho}$ and $\underline{\bar{\rho}}$ are now measured from the frame origin to the generic mass element. A separation of variables is introduced using the free-free mode shapes of an unconstrained system

$$\underline{u} = \sum_{j=0}^n \underline{\phi}^j \eta_j \quad (3.3)$$

where the mode shapes for distinct eigenvalues are orthogonal

$$\int_D \underline{\phi}^i \cdot \underline{\phi}^j \, dm = 0 \quad i \neq j. \quad (3.4)$$

The constraint relationships are then written as

$$\sum_{j=0}^n \int_D \underline{\phi}^j \, dm \, \eta_j = 0 \quad (3.5)$$

and

$$\sum_{j=0}^n \int_D \bar{\rho} \times \underline{\phi}^j \, dm \, \dot{\eta}_j = 0 \quad (3.6)$$

where $\bar{\rho}$ is the undeformed location of the generic mass element. In the above, the zero subscript has been used to refer to all of the rigid body modes. These consist of a total of six modes. The three translational rigid body modes are taken as uniform translation along each of the axes. They may be written as

$$\begin{aligned} \underline{\phi}_1^0 &= C \hat{\underline{f}}_1 \\ \underline{\phi}_2^0 &= C \hat{\underline{f}}_2 \\ \underline{\phi}_3^0 &= C \hat{\underline{f}}_3 \end{aligned} \quad (3.7)$$

where C is a constant. The three rotational rigid body modes are taken as small rotations about each of the axes. They are pictured in Figure 3.1 and are written as

$$\begin{aligned} \underline{\phi}_4^0 &= \frac{y}{l} \hat{\underline{f}}_3 - \frac{z}{l} \hat{\underline{f}}_2 \\ \underline{\phi}_5^0 &= \frac{z}{l} \hat{\underline{f}}_1 - \frac{x}{l} \hat{\underline{f}}_3 \\ \underline{\phi}_6^0 &= \frac{x}{l} \hat{\underline{f}}_2 - \frac{y}{l} \hat{\underline{f}}_1 \end{aligned} \quad (3.8)$$

The translational rigid body modes are orthogonal to the rotational rigid body modes since the undeformed position has its origin at the center of mass and

$$\int_D \bar{\rho} \, dm = 0 \quad (3.9)$$

It will be most fruitful in the evaluation of the constraint relationships to investigate the orthogonality properties of the free-free

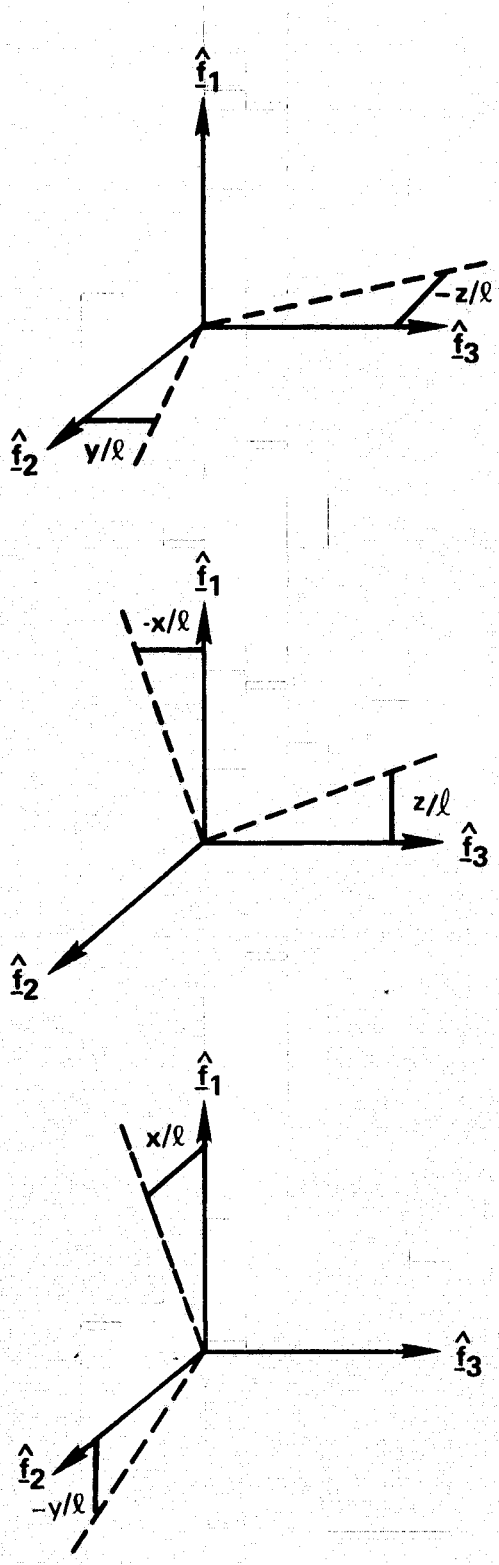


Figure 3.1. Rotational Rigid Body Modes.

modes further. Let $\underline{\phi}^j$ be a deformational mode corresponding to a nonzero natural frequency.

$$\underline{\phi}^j = \{\hat{\underline{f}}\}^T \begin{Bmatrix} \phi_1^j \\ \phi_2^j \\ \phi_3^j \end{Bmatrix} \quad (3.10)$$

This mode will be orthogonal to the translational modes, yielding the relationships

$$\begin{aligned} \int_D \underline{\phi}_1^0 \cdot \underline{\phi}_j \, dm &= C \int_D \phi_1^j \, dm = 0 \\ \int_D \underline{\phi}_2^0 \cdot \underline{\phi}_j \, dm &= C \int_D \phi_2^j \, dm = 0 \\ \int_D \underline{\phi}_3^0 \cdot \underline{\phi}_j \, dm &= C \int_D \phi_3^j \, dm = 0 \end{aligned} \quad (3.11)$$

This may be written in the vector form as

$$\int_D \underline{\phi}^j \, dm = 0 \quad (3.12)$$

This is recognized as the coefficient in the center of mass constraint of η . Coupled with the orthogonality of the rigid body translational modes to the rotational modes shown in Equation (3.9), the center of mass constraint can be rewritten as a relationship involving only the translational rigid body modal coordinates

$$\int_D \underline{\phi}_1^0 \, dm \, \eta_{01} + \int_D \underline{\phi}_2^0 \, dm \, \eta_{02} + \int_D \underline{\phi}_3^0 \, dm \, \eta_{03} = 0 \quad (3.13)$$

Evaluating the integrals will yield the three scalar equations

$$\begin{aligned}
M \eta_{01} &= 0 \\
M \eta_{02} &= 0 \\
M \eta_{03} &= 0
\end{aligned}
\tag{3.14}$$

where M is the total system mass. It is now quite clear that the center of mass constraint requires that the translational rigid body modal coordinates be zero

$$\begin{aligned}
\eta_{01} &= 0 \\
\eta_{02} &= 0 \\
\eta_{03} &= 0
\end{aligned}
\tag{3.15}$$

Now we shall turn to the constraint setting the internal angular momentum to zero by studying the orthogonality of a deformational mode, $\underline{\phi}^j$, to the rotational rigid body modes. The following orthogonality conditions hold

$$\begin{aligned}
\int_D \underline{\phi}_4^0 \cdot \underline{\phi}^j \, dm &= 0 \\
\int_D \underline{\phi}_5^0 \cdot \underline{\phi}^j \, dm &= 0 \\
\int_D \underline{\phi}_6^0 \cdot \underline{\phi}^j \, dm &= 0
\end{aligned}
\tag{3.16}$$

When the expression for the rigid body modes (Equation (3.8)) are substituted into the above, we have

$$\begin{aligned}
\int_D (y\phi_3^j - z\phi_2^j) \, dm &= 0 \\
\int_D (z\phi_1^j - x\phi_3^j) \, dm &= 0 \\
\int_D (x\phi_2^j - y\phi_1^j) \, dm &= 0
\end{aligned}
\tag{3.17}$$

where the factor of ℓ inverse has been eliminated. If the three scalar equations are considered as components of the vector bases of the floating frame, then one vector cross product relationship results from Equation (3.16)

$$\int_D \bar{\rho} \times \underline{\phi}^j \, dm = 0 \quad (3.18)$$

where $\bar{\rho}$ is the position of the undeformed generic mass element

$$\bar{\rho} = \{\hat{f}\}^T \begin{Bmatrix} x \\ y \\ z \end{Bmatrix} \quad (3.19)$$

This vector cross product expression (Equation (3.18)) is recognized as the coefficient of the modal coordinate velocity $\dot{\eta}_j$ in the constraint relationship (Equation (3.6)). The constraint relationship can then be written without the deformational modal velocities and also without the translational rigid body modal velocities. These latter are set to zero as a result of the center of mass constraint (Equation (3.15)). Writing the simplified expression for the constraint gives

$$\int_D \bar{\rho} \times \underline{\phi}_4^0 \, dm \, \dot{\eta}_{04} + \int_D \bar{\rho} \times \underline{\phi}_5^0 \, dm \, \dot{\eta}_{05} + \int_D \bar{\rho} \times \underline{\phi}_6^0 \, dm \, \dot{\eta}_{06} = 0 \quad (3.20)$$

Substituting the expression for the rigid body modes into the above yields

$$\{\hat{f}\}^T \left\{ \begin{array}{l} \left(\int_D (y^2+z^2) \, dm \right) \\ \left(\int_D -y \, x \, dm \right) \\ \left(\int_D -z \, x \, dm \right) \end{array} \right\} \dot{\eta}_{04} + \left\{ \begin{array}{l} \left(\int_D -x \, y \, dm \right) \\ \left(\int_D (x^2+z^2) \, dm \right) \\ \left(\int_D -z \, y \, dm \right) \end{array} \right\} \dot{\eta}_{05} + \left\{ \begin{array}{l} \left(\int_D -x \, z \, dm \right) \\ \left(\int_D -y \, z \, dm \right) \\ \left(\int_D (x^2+y^2) \, dm \right) \end{array} \right\} \dot{\eta}_{06} = 0 \quad (3.21)$$

The moments and products of inertia of the undeformed system are readily identified in the above. Writing the resultant scalar equations in matrix form yields

$$\begin{bmatrix} I_{11} & I_{12} & I_{13} \\ I_{21} & I_{22} & I_{23} \\ I_{31} & I_{32} & I_{33} \end{bmatrix} \begin{Bmatrix} \dot{\eta}_{04} \\ \dot{\eta}_{05} \\ \dot{\eta}_{06} \end{Bmatrix} = 0 \quad (3.22)$$

Since the inertia matrix is positive definite, the only solution of this constraint equation is

$$\begin{aligned} \dot{\eta}_{04} &= 0 \\ \dot{\eta}_{05} &= 0 \\ \dot{\eta}_{06} &= 0 \end{aligned} \quad (3.23)$$

This evaluation of the constraint relationship using free-free modes states definitively that the rigid body mode frame is fixed relative to the Tisserand frame. If initially aligned, the two frames will remain coincident. This is the prime advantage of the Mode Shape Constraint and is the connection between the rigid body mode and the Tisserand frame that was mentioned at the end of Section 2.3. Thus the Mode Shape Constraint, which involves a Tisserand frame, can be used to define a rigid body mode frame. This result has been discussed by Likins,¹ but has been expanded upon here. The mention of the connection between the orthogonality of the rigid body and deformational modes and the momentum expression was made by Buckens. He used it only to set

¹Peter W. Likins, "Analytical Dynamics and Nonrigid Spacecraft Simulation" (JPL TR 32-1593) p. 22.

total momentum to zero. Although the frame introduced by Buckens is crucial in the above arguments since it neglects second order terms, Buckens did not use the orthogonality properties in order to evaluate the constraint relationship for a floating frame.²

3.3 Discussion and Example of the Mode Shape Constraint

The development of the Mode Shape Constraint in the previous section has been quite detailed and may seem complex. A discussion and summary of the pertinent results are in order. The example problem from Section 2.4 will be expanded in order to demonstrate the Mode Shape Constraint in a concrete manner.

The Mode Shape Constraint is defined as a specific case of the Tisserand constraint where the deformations are expanded in terms of free-free modes of the unconstrained system. The main property of the Mode Shape Constraint is that it eliminates the rigid body modal coordinates from the problem and leaves the remaining coordinates independent. If an arbitrary choice of mode shapes is made, then the Tisserand constraint will render the modal coordinates dependent on each other. The specific structure of the interrelation of the modal coordinates depends on the choice of mode shapes. This may be determined from examining Equation (2.21).

The procedure that results from applying the Mode Shape Constraint is to expand the deformations in terms of the deformational modes only, ignoring the rigid body modes, which have zero natural frequency. The constraint relationship is fulfilled because each coefficient in

²F. Buckens "The Influence of Elastic Components on the Attitude Stability of a Satellite," Proceedings of the Fifth International Symposium on Space Technology and Science (Tokyo, 1964), p. 196.

Equation (2.21) is set to zero. The coordinates are then independent because of the specific choice of mode shapes. This interpretation gives rise to the name "Mode Shape" Constraint. The Mode Shape Constraint may also be viewed as a straightforward way of working with the rigid body mode frame. As noted before, the constraint relationship requires that the rigid body modes do not move relative to the Tisserand frame. Thus, the mode shape constraint may be used to locate both frames. This is a much easier method to locate the rigid body mode frame than a requirement involving zero strain energy.

The discussion will now take up the example problem first introduced in Section 2.4. This is a case of planar motion of a long slender member, so the constraint relationship will simplify to the scalar form

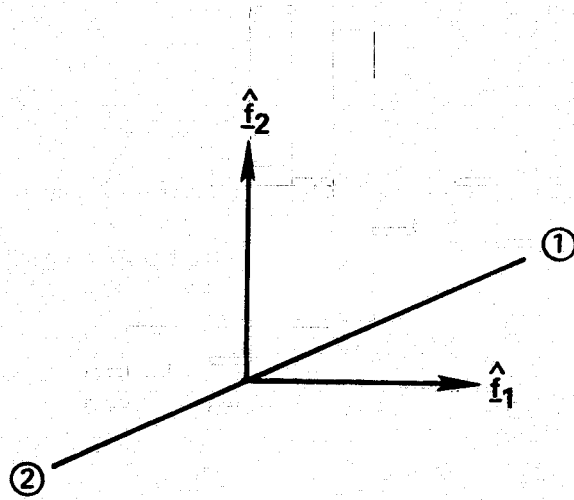
$$\int_D x \dot{u} \, dm = 0 . \quad (3.24)$$

If the velocity is expanded in terms of mode shapes, then

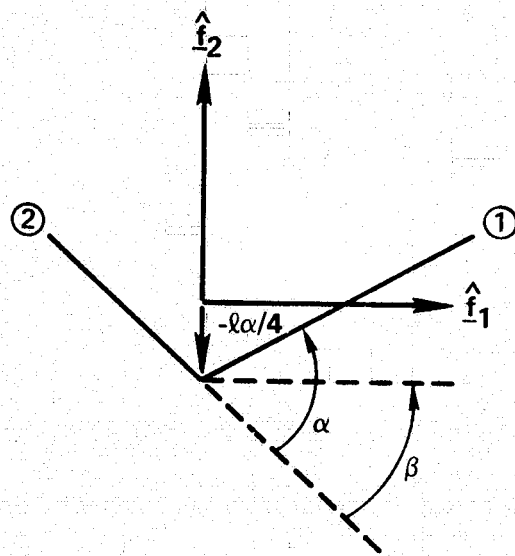
$$\sum_{j=0}^n \left(\int_D x \phi^j \, dm \right) \dot{\eta}_j = 0 \quad (3.25)$$

The mode shapes for the system shown in Figures 2.1 and 2.2 are the rigid body mode and one deformational mode relative to the Tisserand frame. They are shown in Figure 3.2. The mode shapes are

$$\begin{aligned} \phi^0 &= \frac{x}{\ell} & -\frac{\ell}{\sqrt{2}} \leq x \leq \ell \\ \phi^1 &= -\frac{\ell}{4} - .586 x & -\frac{\ell}{\sqrt{2}} \leq x \leq 0 \\ & -\frac{\ell}{4} + .414 x & 0 < x \leq \ell \end{aligned} \quad (3.26)$$



(a) RIGID BODY MODE



(b) DEFORMATIONAL MODE

Figure 3.2. Example Problem Mode Shapes.

Several characteristics of the mode shapes must be mentioned. They represent only small deformations and always place the origin at the center of mass (Equation (2.24)). The deformational mode resulted from setting the relative deformation, α , to one. The rotation of the body fixed frame relative to the Tisserand frame, β , would then be .586 (Equation (2.41)). The resultant movement of the center of mass would be $-\frac{\ell}{4}$. The essential property of these two modes is that they are orthogonal.

$$\int_D \phi^0 \phi^1 dm = \int_D \frac{x}{\ell} \phi^1 dm = 0 \quad (3.27)$$

Thus the mass matrix is diagonal. Since the relative deformations of the system result from only the second mode shape, the stiffness matrix is zero except for k_{22} . The modes chosen therefore are the natural modes of the unconstrained system which we call the free-free modes. The system is unconstrained as the singular stiffness matrix would indicate.

Now let us use the free-free modes in order to evaluate the coefficients of the Tisserand constraint relationship shown in Equation (3.25).

$$\begin{aligned} \int_D x \phi^0 dm &= \int_{-\frac{\ell}{\sqrt{2}}}^0 2m \frac{x^2}{\ell} dx + \int_0^{\ell} m \frac{x^2}{\ell} dx \\ &= 2.218 m \ell^2 \\ \int_D x \phi^1 dm &= 0 \end{aligned} \quad (3.28)$$

The last coefficient is set to zero because of the orthogonality condition. The Tisserand constraint for this system may be written

$$\left(\int_D \mathbf{x} \phi^0 dm \right) \dot{\eta}_0 + \left(\int_D \mathbf{x} \phi^1 dm \right) \dot{\eta}_1 = 0$$

$$(2.218 \text{ m } \ell^2) \dot{\eta}_0 = 0 \quad (3.29)$$

The constraint requires that the rigid body modal velocity be zero. Thus the rigid body mode does not move relative to the Tisserand frame. Since the original choice of axes is arbitrary, the modal coordinate may be set to zero and will remain zero because of the constraint.

3.4 Modified Tisserand Constraint

This section will deal with an extension of the Tisserand frame for deformable bodies to cover a new class of systems. Consider a deformable body with small relative displacements to which is added a spinning rigid rotor. The new system will no longer be a strictly deformable body, since the movement of the rotor will involve large relative displacements. If the classical Tisserand constraint is applied to this system, the frame itself must rotate relative to the system. The system angular momentum will consist of a component from the deformable body and a component from the rotor. The frame must rotate in such a way as to carry the total system angular momentum and thereby set internal angular momentum to zero. The frame motion cannot coincide with deformable body component of the system and large deformations result.

Two methods of modifying the Tisserand constraint present themselves. The first is to define a Tisserand frame for the deformable body only. This approach ignores the rotor altogether when the internal angular momentum relative to the deformable body center of mass is set to zero. The constraint relationship is then written

$$\int_D \underline{\rho}_C \times \dot{\underline{u}} \, dm = 0 \quad (3.30)$$

when $\underline{\rho}_C$ is the undeformed location relative to the center of mass of the deformable body. This approach is not used because it does not achieve the greatest simplification.

The second method to be considered is to examine the expression for the system angular momentum. The constraint relationship can then be made to simplify the structure of the angular momentum as much as possible while still assuring small deformations.

Before we write the expression for the system angular momentum, let us define several vector bases:

- $\{\hat{i}\}$: Inertially fixed reference axes
- $\{\hat{f}\}$: Axes fixed in the floating frame
- $\{\hat{b}\}$: Axes fixed in the mass element at the rotor mounting point
- $\{\hat{v}\}$: Axes fixed in the rotor

The angular momentum of the system about its center of mass is

$$\underline{H} = \int_S \underline{\rho} \times \dot{\underline{\rho}} \, dm \quad (3.31)$$

where S represents integration over the entire system, both the rotor and the deformable body. Evaluating the angular momentum for the deformable body will give

$$\int_D \underline{\rho} \times \dot{\underline{\rho}} \, dm = \underline{\square}_D \cdot \underline{\omega}^{fi} + \int_D \underline{\rho} \times \dot{\underline{u}} \, dm \quad (3.32)$$

where $\underline{\square}_D$ is the deformable body dyadic about the system center of mass. For the rotor, static balance has been assumed. The similar expression integrated over the rotor, R, is

$$\int_R \underline{\rho} \times \dot{\underline{\rho}} \, dm = \underline{\square}_R^S \cdot \underline{\omega}^{fi} + \underline{\square}_R \cdot \underline{\omega}^{vf} + M_R \underline{\rho}_R \times \dot{\underline{\rho}}_R \quad (3.33)$$

where

$\underline{\square}_R^S$: Rotor inertia dyadic about the system center of mass

$\underline{\square}_R$: Rotor inertia dyadic about its own center of mass

M_R : Rotor mass

$\underline{\rho}_R$: Location of rotor center of mass relative to system center of mass.

By combining these two quantities, the system angular momentum is found to be

$$\underline{H} = \underline{\square} \cdot \underline{\omega}^{fi} + \underline{\square}_R \cdot \underline{\omega}^{vf} + \int_D \underline{\rho} \times \dot{\underline{\rho}} \, dm + M_R \underline{\rho}_R \times \dot{\underline{\rho}}_R \quad (3.34)$$

The total system inertia dyadic is given by

$$\underline{\square} = \underline{\square}_D + \underline{\square}_R^S \quad (3.35)$$

The total angular momentum expression can be significantly simplified.

In order to do this, we introduce a Modified Tisserand Constraint.

$$\int_D \underline{\rho} \times \dot{\underline{\rho}} \, dm + M_R \underline{\rho}_R \times \dot{\underline{\rho}}_R + \underline{\square}_R \cdot \underline{\omega}^{bf} = 0 \quad (3.36)$$

Here we have made use of the chain rule for angular velocities

$$\underline{\omega}^{vf} = \underline{\omega}^{vb} + \underline{\omega}^{bf} \quad (3.37)$$

The system angular momentum then becomes

$$\underline{H} = \underline{\square} \cdot \underline{\omega}^{fi} + \underline{\square}_R \cdot \underline{\omega}^{vb} \quad (3.38)$$

The above has the same structure as a rigid body with an attached rotor.

The essential difference is that the inertia dyadic is not constant and

that the relative angular momentum of the rotor (the second term) is affected by the deformations. It is important to understand that rotations of the axes at the mounting point will reorient the rotor axes.

The internal angular momentum of the system relative to the frame is no longer zero,

$$\int_S \underline{\rho} \times \underline{\dot{u}} \, dm = \underline{\square}_R \cdot \underline{\omega}^{vb} . \quad (3.39)$$

This is a very simple result and may be verified by direct computation. Alternatively, a quick comparison of the above angular momentum expression (Equation (3.38)) and the general angular momentum expression (Equation (2.3)) will give the same result. The one term evaluation of the internal angular momentum will facilitate the evaluation of the equations of motion. In order to demonstrate this, let us evaluate the kinetic energy. We start with the general result given above (Equation (2.6)) which is now evaluated over the entire system

$$T = \frac{1}{2} \int_S \underline{\dot{\rho}} \cdot \underline{\dot{\rho}} \, dm + \frac{1}{2} \underline{\omega}^{fi} \cdot \underline{\square} \cdot \underline{\omega}^{fi} + \underline{\omega}^{fi} \cdot \int_S \underline{\rho} \times \underline{\dot{\rho}} \, dm \quad (3.40)$$

The first term must be evaluated over the deformable body and the rotor.

$$\begin{aligned} \frac{1}{2} \int_D \underline{\dot{\rho}} \cdot \underline{\dot{\rho}} \, dm &= \frac{1}{2} \int_D \underline{\dot{u}} \cdot \underline{\dot{u}} \, dm \\ \frac{1}{2} \int_R \underline{\dot{\rho}} \cdot \underline{\dot{\rho}} \, dm &= \frac{1}{2} M_R \underline{\dot{\rho}}_R \cdot \underline{\dot{\rho}}_R + \frac{1}{2} \underline{\omega}^{vb} \cdot \underline{\square}_R \cdot \underline{\omega}^{vb} \\ &\quad + \underline{\omega}^{bf} \cdot \underline{\square}_R \cdot \underline{\omega}^{vb} + \frac{1}{2} \underline{\omega}^{bf} \cdot \underline{\square}_R \cdot \underline{\omega}^{bf} \end{aligned} \quad (3.41)$$

Making the substitutions indicated will yield the kinetic energy for a deformable body and attached rigid rotor with static balance when the Modified Tisserand Constraint is employed.

$$\begin{aligned}
T = & \frac{1}{2} \int_D \dot{\underline{u}} \cdot \dot{\underline{u}} \, dm + \frac{1}{2} \underline{\omega}^{fi} \cdot \underline{\square} \cdot \underline{\omega}^{fi} + \underline{\omega}^{fi} \cdot \underline{\square}_R \cdot \underline{\omega}^{vb} \\
& + \frac{1}{2} M_R \dot{\underline{\rho}}_R \cdot \dot{\underline{\rho}}_R + \frac{1}{2} \underline{\omega}^{vb} \cdot \underline{\square}_R \cdot \underline{\omega}^{vb} + \underline{\omega}^{vb} \cdot \underline{\square}_R \cdot \underline{\omega}^{bf} + \frac{1}{2} \underline{\omega}^{bf} \cdot \underline{\square}_R \cdot \underline{\omega}^{bf}
\end{aligned} \tag{3.42}$$

Even with the simplification that comes from the Modified Tisserand Constraint, this system has a complicated structure for the kinetic energy.

The Modified Tisserand frame is distinct from the frame created by applying the classical Tisserand constraint to the deformable body only (Equation (3.30)). In order to demonstrate this, the internal angular momentum of the deformable body relative to its own center of mass will be calculated for the Modified Tisserand Constraint. Starting with Equation (3.39) we may write

$$\int_D \underline{\rho} \times \dot{\underline{\rho}} \, dm + \int_R \underline{\rho} \times \dot{\underline{\rho}} \, dm = \underline{\square}_R \cdot \underline{\omega}^{vb} \tag{3.43}$$

Each component of internal angular momentum may be evaluated by rewriting the expression relative to its own center of mass rather than the system center of mass.

$$\begin{aligned}
\int_D \underline{\rho} \times \dot{\underline{\rho}} \, dm &= \int_D \underline{\rho}_C \times \dot{\underline{u}} \, dm + (\mathcal{M} - M_R) \underline{r}_C \times \dot{\underline{r}}_C \\
\int_R \underline{\rho} \times \dot{\underline{\rho}} \, dm &= \underline{\square}_R \cdot \underline{\omega}^{vb} + \underline{\square}_R \cdot \underline{\omega}^{bf} + M_R \underline{\rho}_C \times \dot{\underline{\rho}}_R
\end{aligned} \tag{3.44}$$

where \mathcal{M} is the system mass and \underline{r}_C is the location of deformable body center of mass relative to the system center of mass. By using the center of mass expression

$$(\mathcal{M} - M_R) \underline{r}_C + M_R \underline{\rho}_R = 0 \tag{3.45}$$

we may evaluate the internal angular momentum of the deformable body relative to its own center of mass

$$\int_D \underline{\rho}_C \times \underline{\dot{u}} \, dm = - \underline{\square}_R \cdot \underline{\omega}^{bf} - \left(\frac{M_R \mathcal{M}}{\mathcal{M} - M_R} \right) \underline{\rho}_R \times \underline{\dot{\rho}}_R \quad (3.46)$$

This quantity will not generally be zero, and the deformable body will have a net internal angular momentum relative to its own center of mass when the Modified Tisserand Constraint is employed. This result also shows that the Modified Tisserand Constraint involves an extension of the classical Tisserand constraint for deformable bodies.

Going back to total system angular momentum (Equation (3.38)) it will be interesting to examine the frame motion. For the case where the system has zero net angular momentum and is free of external moments, the relationship will hold whereby

$$\underline{\square} \cdot \underline{\omega}^{fi} + \underline{\square}_R \cdot \underline{\omega}^{vb} = 0 \quad (3.47)$$

This relationship does not require that the frame be inertially fixed. Instead, the frame will move when the internal angular momentum (the second term) is altered in value. This is the process of momentum exchange that is employed by control systems.

The most important aspect of the Modified Tisserand Constraint has been left till now. We shall now attempt to tie together the advantages of the Mode Shape Constraint with the extended systems covered by the Modified Tisserand Constraint. The crux of this endeavor lies with the physical interpretation of the Modified Tisserand Constraint (Equation (3.36)). Let us start by discussing the terms present in the expression. The first term is the internal angular momentum of

the deformable body. It is the last two terms which involve the rotor. But neither term involves the rotor spin rate. Rather, these two terms represent the internal angular momentum of the rotor if it were indeed not spinning relative to the axes fixed at the mounting point. That is, the rotor would be fixed in the reference frame b . The constraint relationship may now be interpreted as a classical Tisserand constraint for a system with a "frozen" rotor. Once this interpretation has been made, the Mode Shape Constraint associated with a classical Tisserand frame may be applied to a deformable body with an attached rotor. The mode shapes used to expand the deformations are found from the free-free analysis of the system where the rotors have been frozen. Thus the rotor mass and inertia properties contribute to the free-free modes. The Modified Tisserand constraint will now require only that the rigid-body modal velocities be zero. This allows them to be ignored, and the analysis proceeds with the frame variables and the modal coordinates associated with nonzero natural frequencies. All of these coordinates are independent since the constraint relationship was evaluated by suppressing the rigid body modes.

All of the relationships given above for a system with one rotor with static balance will hold if additional rotors are added. The only change is that expressions involving rotor quantities are summed for all rotors.

CHAPTER 4

FINITE ELEMENT EQUATIONS OF MOTION

4.1 Chapter Summary

This chapter deals with the derivation of a generalized set of equations of motion for the class of spacecraft with distributed flexibility and momentum exchange controllers. The Finite Element Model adopted for this discussion consists of a finite number of rigid bodies interconnected by massless, elastic elements. This model allows the equations of motion of a continuum to be represented as a finite number of ordinary differential equations instead of a partial differential equation. The Finite Element approach is particularly powerful for dealing with systems characterized by nonuniform mass and stiffness properties. The Finite Element Model introduces six coordinates for each rigid body in the model, three coordinates for translation and three for rotation. The total number of discrete coordinates is then seen to be large even for a system of modest complexity. This suggests the adoption of distributed coordinates obtained by a modal analysis and the truncation to a smaller number of modes. The process of truncation is complicated and will be discussed in Chapter 6.

The equations of motion developed here deal with a system which has small, first order displacements and rotations, relative to an inertially fixed coordinate system. This requires that the variation of the rotor angular momentum is also a small, first order quantity. Although the equations of motion for this system can be written using an inertially fixed coordinate system, a Modified Tisserand Frame will be introduced. This derivation will demonstrate the process of

formulating equations of motion when this floating frame is employed, as may be necessary for the case of large system rotations. Particular attention will be paid to the impact of the constraint relation.

The equations of motion will be formulated using Lagrange's equations. The first step consists of the calculation of the system kinetic energy. In order to arrive at equations of motion containing first order quantities, care must be taken to include all second order quantities in the kinetic energy. Because the rotor angular velocity is a large quantity, not all terms can be represented by their first order approximation. The generalized forces for the system are conservative and the strain energy is a simple quadratic form involving the stiffness matrix.

The use of the Modified Tisserand Frame will involve a constraint relationship. Because the generalized coordinates are not independent, Lagrange multipliers are introduced in the equations of motion. The modal analysis is performed for the free-free system with the rotors frozen and the transformation from discrete to distributed coordinates does not include the rigid body modes. Thus, the Mode Shape Constraint is introduced to the problem and the result is the elimination of the Lagrange multipliers. The final set of equations of motion involves coupling between vibration and the Tisserand Frame motion. Gyroscopic coupling between the vibration coordinates is also present. If damping is desired in the system, a term may be added in the final set of equations to represent modal damping.

This set of equations could then be truncated to the frame variables and a smaller number of necessary modal coordinates. These

equations would be representative of the system motion of a spacecraft with small displacements from inertially fixed axes. They could then be incorporated in a control system design to attain precise pointing.

4.2 System Kinetic Energy

The first step in the process of formulating the equations of motion using Lagrange's equations is the derivation of the expression representing the system kinetic energy. Several assumptions have been made to facilitate this endeavor. The system is assumed to be free of external forces and the system center of mass then represents an inertial reference point. The resulting equations of motion will therefore not include any expression representing accelerations of the system center of mass. The equations of motion representing translation of the system center of mass will not appear in the derivation since in effect they have been solved a priori. The assumption is made that the rotor center of mass is located at the center of mass of the attached body. This assumption simplifies the structure of the resulting equations, but could be abandoned easily if it were judged inadequate for analysis of the system at hand. The rotor is assumed to be statically balanced. The angular momentum of the rotor is also assumed to undergo only small, first order variations. This would correspond to a requirement that the rotor produces only small, first order torques. This implies only first order changes in rotor speed for a momentum wheel or only first order changes in gimbal angles for a control moment gyro (CMG). A Modified Tisserand Frame is introduced for the system. This results in a significant simplification of the internal angular momentum expression which appears in the kinetic energy.

As shown before (Section 3.4), the expression for the kinetic energy for a deformable body containing a spinning rotor is

$$T = \frac{1}{2} \int_S \underline{\dot{\rho}} \cdot \underline{\dot{\rho}} \, dm + \underline{\omega}^{fi} \cdot \int_S \underline{\rho} \times \underline{\dot{\rho}} \, dm + \frac{1}{2} \underline{\omega}^{fi} \cdot \underline{\square} \cdot \underline{\omega}^{fi} \quad (4.1)$$

If a Modified Tisserand Constraint is introduced to define the floating frame, then the constraint is written as follows for a rotor with static balance.

$$\int_D \underline{\rho} \times \underline{\dot{\rho}} \, dm + M_R \underline{\rho}_R \times \underline{\dot{\rho}}_R + \underline{\square}_R \cdot \underline{\omega}^{bRf} = 0 \quad (4.2)$$

The resulting expression for the internal angular momentum is

$$\int_S \underline{\rho} \times \underline{\dot{\rho}} \, dm = \underline{\square}_R \cdot \underline{\omega}^{vbR} \quad (4.3)$$

The kinetic energy can now be put in the form

$$T = \frac{1}{2} \int_S \underline{\dot{\rho}} \cdot \underline{\dot{\rho}} \, dm + \underline{\omega}^{fi} \cdot \underline{\square}_R \cdot \underline{\omega}^{vbR} + \frac{1}{2} \underline{\omega}^{fi} \cdot \underline{\square} \cdot \underline{\omega}^{fi} \quad (4.4)$$

In order to analyze the first expression in the kinetic energy, the location of the generic mass element relative to the system mass center, $\underline{\rho}$, is defined for each body as in Figure 4.1

$$\underline{\rho} = \underline{\bar{\rho}}^i + \underline{u}^i + \underline{r}^i \quad (4.5)$$

where $\underline{\bar{\rho}}^i$ is the undeformed position of center of mass of body i and is fixed in the frame f .

$$\underline{\dot{\bar{\rho}}}^i = 0 \quad (4.6)$$

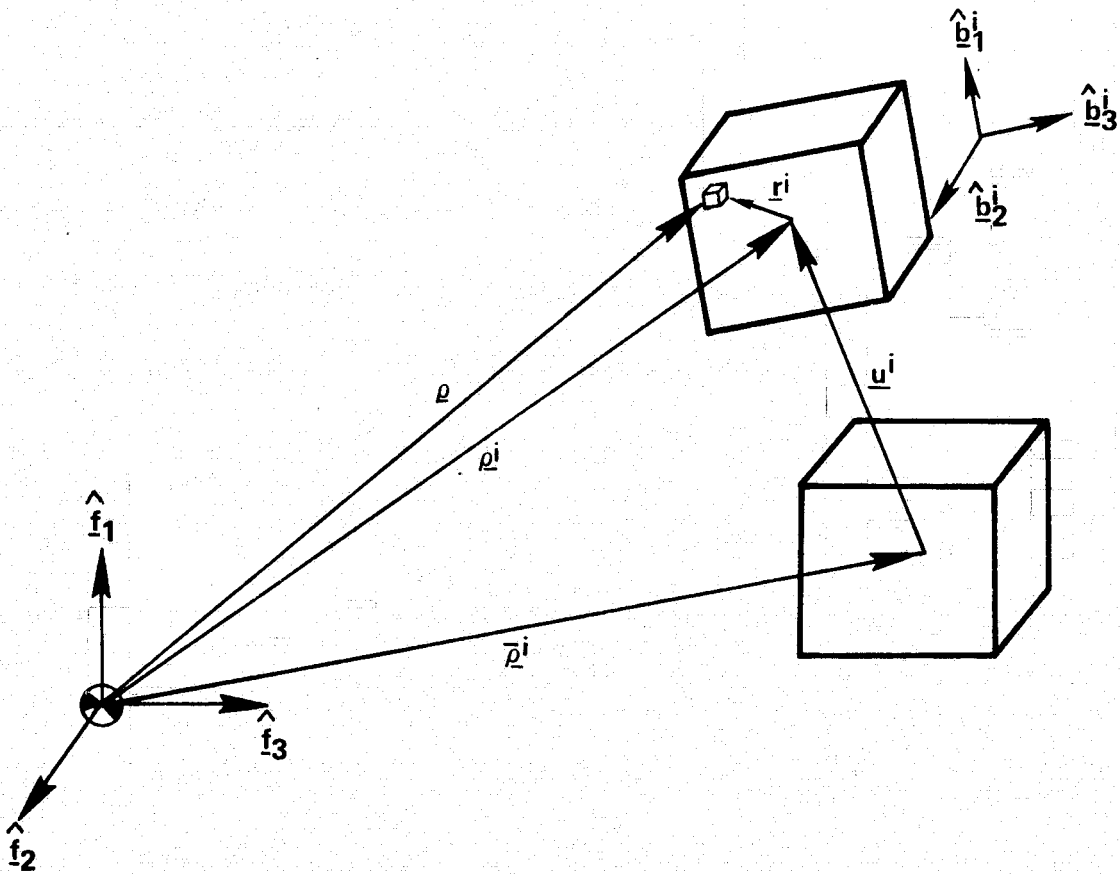


Figure 4.1. Location of Generic Mass Element.

The displacement in frame f of the center of mass of body i is represented by the vector, \underline{u}^i . The location of a generic mass element of body i relative to the body center of mass is \underline{r}^i and therefore obeys the constraint

$$\int_{B^i} \underline{r}^i dm = 0 \quad (4.7)$$

where the integration is taken over body i . A similar expression results for the location of a generic mass element of the rotor

$$\underline{\rho} = \underline{\rho}^R + \underline{u}^R + \underline{r}^R \quad (4.8)$$

where the superscript R refers to the rotor. The derivatives of the mass element expressions relative to the floating frame give

$$\begin{aligned} \dot{\underline{\rho}}^i &= \dot{\underline{u}}^i + \underline{\omega}^{b^i f} \times \underline{r}^i \\ \dot{\underline{\rho}}^R &= \dot{\underline{u}}^R + \underline{\omega}^{vf} \times \underline{r}^R \end{aligned} \quad (4.9)$$

where the reference frame b^i is fixed in the body i , the reference frame v is fixed in the rotor and f is fixed in the modified Tisserand frame. Remembering the center of mass constraint (Equation (4.7)) and the chain rule for angular velocities

$$\underline{\omega}^{vf} = \underline{\omega}^{vb^R} + \underline{\omega}^{b^R f} \quad (4.10)$$

we may now write the vector-dyadic expression for the system kinetic energy

$$\begin{aligned}
T = & \sum_{i=1}^n \left(\frac{1}{2} m_i \underline{\dot{u}}^i \cdot \underline{\dot{u}}^i + \frac{1}{2} \underline{\omega}^{b^i f} \cdot \underline{\square}^i \cdot \underline{\omega}^{b^i f} \right) \\
& + \frac{1}{2} M_R \underline{\dot{u}}^R \cdot \underline{\dot{u}}^R + \frac{1}{2} \underline{\omega}^{v b^R} \cdot \underline{\square}^R \cdot \underline{\omega}^{v b^R} \\
& + \frac{1}{2} \underline{\omega}^{b^R f} \cdot \underline{\square}^R \cdot \underline{\omega}^{b^R f} + \underline{\omega}^{b^R f} \cdot \underline{\square}^R \cdot \underline{\omega}^{v b^R} \\
& + \underline{\omega}^{f i} \cdot \underline{\square}^R \cdot \underline{\omega}^{v b^R} + \frac{1}{2} \underline{\omega}^{f i} \cdot \underline{\square}^i \cdot \underline{\omega}^{f i} \quad (4.11)
\end{aligned}$$

In the above expression, the reference frame b^R is fixed in the body to which the rotor is attached and the inertia dyadics $\underline{\square}^i$ and $\underline{\square}^R$ are for body i and the rotor, respectively, about their individual centers of mass. The body i and rotor masses are m_i and M_R respectively. The number of bodies in the model is n , not counting the rotor.

The next step in the evaluation of the system kinetic energy is to adopt a set of vector bases and express the kinetic energy in matrix form. The following set of vector bases are adopted:

- $\{\underline{\hat{i}}\}$: Fixed orientation relative to the inertially fixed reference frame.
- $\{\underline{\hat{f}}\}$: Fixed orientation relative to the Modified Tisserand frame.
- $\{\underline{\hat{b}}^i\}$: Fixed orientation relative to the locally attached frame in body i . Superscript R refers to the body to which the rotor is attached.
- $\{\underline{\hat{v}}\}$: Fixed orientation relative to the rotor attached frame.

Care must be taken in representing the vectors present in Equation (4.11) in terms of first order approximations. This cannot be done for the following terms since $\omega^{v b^R}$ is not a first order quantity

$$\underline{\omega}^{b^R f} \cdot \underline{\square}^R \cdot \underline{\omega}^{v b^R} + \underline{\omega}^{f i} \cdot \underline{\square}^R \cdot \underline{\omega}^{v b^R} \quad (4.12)$$

The angular velocities, $\omega^{b^R f}$ and ω^{fi} , present here must include second order terms in order to keep all the second order terms present in the kinetic energy. Referring to Appendix B, these terms may be written

$$\begin{aligned}\underline{\omega}^{b^R f} &= \{\underline{\hat{b}}^R\}^T (\{\dot{\beta}^R\} + [\beta_A^R] \{\dot{\beta}^R\}) \\ \underline{\omega}^{fi} &= \{\underline{\hat{f}}\}^T (\{\dot{\theta}\} + [\theta_A] \{\dot{\theta}\})\end{aligned}\quad (4.13)$$

The other vectors in the kinetic energy may be represented by their first order forms

$$\begin{aligned}\underline{\dot{u}}^i &= \{\underline{\hat{f}}\}^T \{\dot{u}^i\} \\ \underline{\omega}^{b^i f} &= \{\underline{\hat{b}}^i\}^T \{\dot{\beta}^i\} \\ \underline{\square}^i &= \{\underline{\hat{b}}^i\}^T [I^i] \{\underline{\hat{b}}^i\} \\ \underline{\dot{u}}^R &= \{\underline{\hat{f}}\}^T \{\dot{u}^R\} \\ \underline{\omega}^{vb^R} &= \{\underline{\hat{b}}^R\}^T \{\dot{s}\} \\ \underline{\square}^R &= \{\underline{\hat{b}}^R\}^T [I_R] \{\underline{\hat{b}}^R\} \\ \underline{\square} &= \{\underline{\hat{f}}\}^T [I] \{\underline{\hat{f}}\}\end{aligned}\quad (4.14)$$

The matrix expression for the system kinetic energy may now be written in a form which includes all second order terms

$$\begin{aligned}T &= \sum_{i=1}^n \left(\frac{1}{2} m_i \{\dot{u}^i\}^T \{\dot{u}^i\} + \frac{1}{2} \{\dot{\beta}^i\}^T [I^i] \{\dot{\beta}^i\} \right) \\ &+ \frac{1}{2} M_R \{\dot{u}^R\}^T \{\dot{u}^R\} + \frac{1}{2} \{\dot{\beta}^R\}^T [I_R] \{\dot{\beta}^R\} + \frac{1}{2} \{\dot{s}\}^T [I_R] \{\dot{s}\} \\ &+ \{\dot{\beta}^R\}^T [I_R] \{\dot{s}\} + \{\dot{\beta}^R\}^T [\beta_A^R]^T [I_R] \{\dot{s}\} + \{\dot{\theta}\}^T [\tilde{\beta}^R] [I_R] \{\dot{s}\} \\ &+ \{\dot{\theta}\}^T [I_R] \{\dot{s}\} + \{\dot{\theta}\}^T [\theta_A] [I_R] \{\dot{s}\} + \frac{1}{2} \{\dot{\theta}\}^T [I] \{\dot{\theta}\}\end{aligned}\quad (4.15)$$

In the above expression the "tilde" operator represents a skew symmetric matrix as typified by

$$[\tilde{\beta}^R] = \begin{bmatrix} 0 & -\beta_3^R & \beta_2^R \\ \beta_3^R & 0 & -\beta_1^R \\ -\beta_2^R & \beta_1^R & 0 \end{bmatrix} \quad (4.16)$$

The requirement that the variation of the rotor angular momentum be a small, first order quantity may now be applied to the components represented in Equation (4.14). The rotor angular momentum is written

$$\underline{H}_R = \underline{I}_R \cdot \underline{\omega}^{vi} \quad (4.17)$$

Since the angular velocity relative to inertial space includes the first order terms $\underline{\omega}^{bRf}$ and $\underline{\omega}^{fi}$, they can only contribute first order quantities to the rotor angular momentum. The variation of the rotor angular momentum which must be kept first order is:

$${}^b R \frac{d}{dt} \left(\underline{I}_R \cdot \underline{\omega}^{vbR} \right) = \{ \hat{b}^R \} \frac{d}{dt} \left([I_R] \{ \dot{s} \} \right) \quad (4.18)$$

For a reaction wheel or momentum wheel, the inertia matrix will be constant and the first order requirement will be

$$\{ \ddot{s} \} = 0^1 \quad (4.19)$$

For a control moment gyro (CMG), the rotor speed will be constant.

Then the first order requirement will be

$$[\dot{I}_R] = 0^1 \quad (4.20)$$

These first order requirements will prove important when the equations of motion are derived using the kinetic energy.

4.3 Constraint Equations

Since the kinetic energy was evaluated in terms of a Modified Tisserand Frame, the next step in the formulation of equations of motion is the evaluation of the associated constraint relationship. As given before (Equation (4.2)), the Modified Tisserand Constraint for a deformable body and a rotor with static balance is

$$\int_D \underline{\rho} \times \dot{\underline{\rho}} \, dm + M_R \underline{\rho}_R \times \dot{\underline{\rho}}_R + \underline{\square}_R \cdot \underline{\omega}^{b^R f} = 0 \quad (4.21)$$

If the same conventions are adopted as in the previous section (Figure 5.1), the first term may be evaluated by using Equations (4.5) and (4.9). The resulting first order expression is then

$$\sum_{i=1}^n \left(m_i \underline{\rho}^i \times \dot{\underline{u}}^i + \underline{\square}^i \cdot \underline{\omega}^{b^i f} \right) + M_R \underline{\rho}_R \times \dot{\underline{u}}_R + \underline{\square}_R \cdot \underline{\omega}^{b^R f} = 0 \quad (4.22)$$

The vectors and dyadics may be expressed in the same manner as before (Equations (4.13) and (4.14)) when a system of vector bases is adopted. To this representation we must add

$$\begin{aligned} \underline{\rho}^i &= \{\underline{\hat{f}}\}^T \{x^i\} \\ \underline{\rho}^R &= \{\underline{\hat{f}}\}^T \{x^R\} \end{aligned} \quad (4.23)$$

A common vector basis may be adopted, because to the first order

$$\{\underline{\hat{b}}^i\}^T = \{\underline{\hat{f}}\}^T ([E] + [\tilde{\beta}^i]) \quad (4.24)$$

where $[E]$ is an identity matrix and the "tilde" is the skew-symmetric representation shown in Equation (4.16). The resulting three scalar constraint equations can be written in the form

$$\sum_{i=1}^n \left(m_i [\tilde{x}^i] \{\dot{u}^i\} + [I^i] \{\dot{\beta}^i\} \right) + M_R [\tilde{x}^R] \{\dot{u}^R\} + [I_R] \{\dot{\beta}^R\} = 0 \quad (4.25)$$

Here the "tilde" skew-symmetric operator is a representation of the cross product.

4.4 Equations of Motion-Discrete Coordinates

The equations of motion may now be formulated using Lagrange's equations. For this discussion, the generalized coordinates are not independent and Lagrange multipliers must be introduced. The form of Lagrange's equations to be used here is

$$\frac{d}{dt} \left(\frac{\partial T}{\partial \dot{q}_k} \right) - \frac{\partial T}{\partial q_k} = Q_k - \sum_{s=1}^m \lambda_s A_{Sk}$$

$$k = 1, \dots, \nu \quad (4.26)$$

where ν is the number of generalized coordinates. There are m constraint relationships of the form

$$\sum_{k=1}^{\nu} A_{Sk} \dot{q}_k + B_S = 0$$

$$S = 1, \dots, m \quad (4.27)$$

For our problem, ν is equal to $6n + 3$, and m is equal to 3. The resultant equations of motion are first order only. It is important to realize that the application of Lagrange's equations to the system kinetic energy (Equation (4.15)) yields some second order terms. A crucial part of the equation derivation process is the identification and elimination of all second order terms; the requirement that the variation of the rotor angular momentum be first order will identify many second order terms to be eliminated by recognizing as first order quantities the terms in Equations (4.19) and (4.20).

The equations will be derived in groups of three. The first set of equations is for the Tisserand frame variables, $\{\theta\}$. As shown in Appendix B, the second order term in the angular velocity, $\underline{\omega}^{fi}$, can be written in two forms to facilitate the taking of derivatives

$$\{\dot{\theta}\}^T [\theta_A]^T = \{\theta\}^T [\dot{\theta}_B]^T \quad (4.28)$$

The second order terms have a very interesting structure which will be used here

$$[\ddot{\theta}_A]^T - [\ddot{\theta}_B]^T = [\ddot{\theta}] \quad (4.29)$$

Once the above are recognized and all second order terms are eliminated, the system rotation equations (for rotation of the Modified Tisserand Frame) are written

$$\begin{aligned} [I] \{\ddot{\theta}\} - \left([I_R] \{\dot{s}\} \right) \{\dot{\theta}\} - \left([I_R] \{\dot{s}\} \right) \{\dot{\beta}^R\} \\ + [I_R] \{\ddot{s}\} + [\dot{I}_R] \{\dot{s}\} = \{T_E\} \end{aligned} \quad (4.30)$$

where $\{T_E\}$ represents externally applied torques.

The next sets of equations will deal with the translation and rotation of body i . This body represents all bodies in the model which do not have attached rotors. The translation equations are

$$m_i \{\ddot{u}^i\} = \{Q^i\} + m_i [\tilde{x}^i] \{\lambda\} \quad (4.31)$$

Here the coordinates are present in the constraint relationship and the three Lagrange multipliers are introduced in a column matrix $\{\lambda\}$. The generalized forces are represented in a column matrix $\{Q^i\}$. The rotation equations for body i are

$$[I^i] \{\ddot{\beta}^i\} = \{Q_i\} - [I^i]^T \{\lambda\} \quad (4.32)$$

Equations will now be written for body R , which does have an attached rotor. The translation equations are

$$(m_R + M_R) \{\ddot{u}^R\} = \{Q^R\} + (m_R + M_R) [\tilde{x}^R] \{\lambda\} \quad (4.33)$$

The rotation equations for body R are more complicated. Use must be made of equations similar to Equations (4.28) and (4.29). When all second order terms have been eliminated, these equations can be written

$$\begin{aligned}
 & ([I^R] + [I_R])\{\ddot{\beta}^R\} - (\widetilde{[I_R]\{\dot{s}\}})\{\dot{\beta}^R\} + [I_R]\{\ddot{s}\} + [\dot{I}_R]\{\dot{s}\} \\
 & - (\widetilde{[I_R]\{\dot{s}\}})\{\dot{\theta}\} = \{Q_R\} - ([I^R]^T + [I_R]^T)\{\lambda\}
 \end{aligned} \tag{4.34}$$

The inertia matrix of body R about its own center of mass is $[I^R]$ and the rotor inertia matrix about the same point is $[I_R]$.

The derivation of the equations of motion is now complete. In order to examine their structure, a column matrix $\{q\}$ will be introduced. This represents the translation and rotation displacements for all bodies.

$$\{q\} = \begin{pmatrix} \{u^1\} \\ \{\beta^1\} \\ \{u^2\} \\ \{\beta^2\} \\ \vdots \\ \{u^R\} \\ \{\beta^R\} \\ \vdots \\ \{u^n\} \\ \{\beta^n\} \end{pmatrix} \tag{4.35}$$

The generalized forces for all the bodies may be rewritten in terms of a stiffness matrix, $[K]$.

$$\{Q\} = \begin{pmatrix} \{Q^1\} \\ \{Q_1\} \\ \vdots \\ \{Q^n\} \\ \{Q_n\} \end{pmatrix} = - [K]\{q\} . \tag{4.36}$$

$$[R] = \begin{bmatrix} 0 \\ \vdots \\ 0 \\ \widetilde{[I_R]\{\dot{s}\}} \\ 0 \\ \vdots \\ 0 \end{bmatrix} \quad (4.41)$$

$$[L] = \begin{bmatrix} m_1[\tilde{x}^1] \\ -[I^1]^T \\ \vdots \\ (m_R + M_R)[\tilde{x}^R] \\ -([I^R]^T + [I_R]^T) \\ \vdots \\ m_n[\tilde{x}^n] \\ -[I^n]^T \end{bmatrix} \quad (4.42)$$

The system rotation equation may be rewritten using equations (4.35) and (4.41).

$$[I]\{\ddot{\theta}\} - (\widetilde{[I_R]\{\dot{s}\}})\{\dot{\theta}\} = -[R]^T\{\dot{q}\} - [I_R]\{\ddot{s}\} - [\dot{I}_R]\{\dot{s}\} \quad (4.43)$$

Here the external torques have been set to zero. The term involving the derivative of the rotor inertia matrix in the above equation and in Equation (4.40) can be expressed in an alternate way.

$$[\dot{I}_R]\{\dot{s}\} = [\tilde{s}][\dot{I}_R]\{\dot{s}\} \quad (4.44)$$

The complete equations of motion for the system have now been found. The next step is to attempt to introduce distributed coordinates into the analysis.

4.5 Modal Analysis

The system equations of motion have now been formulated using discrete coordinates and consist of the system rotation Equations (4.43), the system vibration Equations (4.37) and the constraint Equations (4.25). The modal analysis will be introduced in order to substitute distributed coordinates for discrete coordinates in the vibration equations. The objective is to reduce the order of the system (number of degrees of freedom) while still being able to represent system behavior adequately. This process is generally termed "truncation".

The first decision is the choice of the eigenvalue problem to be solved. If the eigenvalue analysis is performed on the homogeneous vibration equation

$$[M]\{\ddot{q}\} + [G]\{\dot{q}\} + [K]\{q\} = 0 \quad (4.45)$$

the result will yield complex modes, or eigenvectors represented by complex numbers. A major drawback of this course of action is that these modes depend on the spin rate. From a numerical standpoint, working with complex numbers may also prove cumbersome.

Real modes would result from an eigenvalue analysis of the equations

$$[M]\{\ddot{q}\} + [K]\{q\} = 0 . \quad (4.46)$$

since $[M]$ and $[K]$ are real and symmetric. This represents a modal analysis of the free-free system where the rotor has been "frozen" (spin rate set to zero). Besides the numerical ease of working with real numbers only, the major advantage of this choice of eigenvalue problem is that the Modified Tisserand Frame may be defined by the Mode

Shape Constraint. This will eliminate the Lagrange multipliers from the vibration equations.

Let $[\phi]$ be a rectangular modal matrix corresponding to Equation (4.46) where the six rigid body modes have been eliminated. The deformational modes included in $[\phi]$ have nonzero natural frequencies and are normalized so that

$$\begin{aligned} [\phi]^T [M] [\phi] &= [E] \\ [\phi]^T [K] [\phi] &= \begin{bmatrix} \omega_n^2 \end{bmatrix} \end{aligned} \quad (4.47)$$

where $[E]$ is the identity matrix and $\begin{bmatrix} \omega_n^2 \end{bmatrix}$ is a diagonal matrix of natural frequencies squared. The substitution is made that

$$\{q\} = [\phi] \{\eta\} \quad (4.48)$$

where $\{\eta\}$ depends on time only and the vibration equations are pre-multiplied by $[\phi]$ transpose. The resulting vibration equations are

$$\begin{aligned} \{\ddot{\eta}\} + \begin{bmatrix} \omega_n^2 \end{bmatrix} \{\eta\} &= - [\phi]^T [G] [\phi] \{\dot{\eta}\} \\ &+ [\phi]^T [R] \{\dot{\theta}\} + [\phi]^T \{F\} + [\phi]^T [L] \{\lambda\} \end{aligned} \quad (4.49)$$

An examination of the constraint relationship Equation (4.25), shows that it can be written in the matrix form

$$- [L]^T \{\dot{q}\} = 0 \quad (4.50)$$

With the modal coordinates defined in Equation (4.48), the constraint relationship becomes

$$- [L]^T [\phi] \{\dot{\eta}\} = 0 \quad (4.51)$$

But with the Mode Shape Constraint, the coordinates $\{\eta\}$ are independent as a consequence of the orthogonality of the nonzero frequency modes to the rigid body modes. Thus the constraint relationship must be

fulfilled by setting all coefficients of the modal coordinates to zero in the constraint equation

$$- [L]^T [\phi] = 0 \quad (4.52)$$

It is an easy step from the above to eliminate the Lagrange multipliers from the problem by realizing

$$[\phi]^T [L] = 0 . \quad (4.53)$$

When the modal matrix is introduced into the system rotation equation, the resulting equations for system behavior become

$$[I]\{\ddot{\theta}\} - (\widetilde{[I_R]}\{\dot{s}\})\{\dot{\theta}\} = - [\Delta]^T\{\dot{\eta}\} - [I_R]\{\ddot{s}\} - [\dot{I}_R]\{\dot{s}\} \quad (4.54)$$

$$\{\ddot{\eta}\} + 2[\zeta][\omega_n]\{\dot{\eta}\} + [\omega_n^2]\{\eta\} = - [\phi]^T[G][\phi]\{\dot{\eta}\} + [\Delta]\{\dot{\theta}\} + [\phi]^T\{F\}$$

where the coupling between system rotation and vibration depends on

$$[\Delta] = [\phi]^T [R] \quad (4.55)$$

Modal damping is also added for this set of equations. The quantity $[\zeta]$ is a diagonal matrix containing the percent of critical damping for each mode. This final set of equations describes the motion of a system which is free of external forces and torques and for which changes in the rotor angular momentum are first order.

The structure of the system equations of motion has several important aspects. First, the rotation of the Modified Tisserand Frame (rigid body mode) is coupled to the vibration and vice-versa. The second aspect is that the vibration modal coordinates are coupled to each other by the gyroscopic term. This complicates the truncation process. An examination of this gyroscopic term will have to be made in order to successfully truncate the number of modal coordinates. The

last point is that the "inertial coupling" present in the hybrid coordinate technique for analyzing flexible appendages is not present here. That is, the coupling is not between the second derivatives of the frame coordinates and modal coordinates. The use of the Modified Tisserand Frame has permitted the elimination of this "inertial coupling" from the final equations.

CHAPTER 5

CONTINUUM ANALYSIS

5.1 Chapter Summary

In this chapter we define a very simple physical system for an analysis as a continuum. The continuum analysis uses Hamilton's Principle to derive governing partial differential equations with boundary conditions. The physical system consists of a long slender beam with an axisymmetric rotor mounted at the tip of the beam with the axis of symmetry normal to the beam and parallel to a principal axis of the beam cross section, when the beam is undeformed. The rotor is symmetric with static and dynamic balance. The center of mass of the rotor lies on the beam centroid in order to simplify the presentation. The rotor spins with a constant rate plus a small, first order speed variation. The beam is uniform and inextensible and is modeled as a Bernoulli-Euler beam. The beam is allowed to vibrate in the plane defined by the beam and the rotor axis, in the orthogonal plane containing the beam, and about the centroidal axis (torsional vibration). No damping is assumed and the system is free of external moments and forces.

The governing partial differential equations have a very simple structure. Three separate equations result for the system. They represent in-plane bending, out-of-plane bending and twist. All of the equations are homogeneous and are the familiar forms associated with the bending and torsion of a uniform bar. On the other hand, the boundary conditions for the equations have a very complicated structure. Because of the gyroscopic coupling provided by the rotor, the in-plane bending and torsion are coupled through the boundary

conditions. In addition to this coupling, the boundary conditions depend on the eigenvalues of the system. The out-of-plane bending is not coupled to the other system motion, but the boundary conditions depend on the rotor speed changes and are therefore time dependent.

The solution of an equation with time dependent boundary conditions involves a special transformation which for some cases renders the boundary conditions time independent. For a modified system, this solution technique is presented for out-of-plane bending. If a traditional separation of variables is employed for the coupled bending and torsion, the independence of each coordinate will cause only one solution to be admitted; this is the trivial solution corresponding to zero displacements. This result forces the separation of variables to adopt a new structure. The spatially dependent coordinates are distinct for bending and torsion, but they both have the same natural frequency. A difference in phase is allowed between bending and torsion. The result of this solution form involves complex mode shapes. The interpretation of these modes leads to the physical solution where in-plane bending and torsion are ninety degrees out of phase. The rotor tip is then seen to trace out an ellipse where one axis represents pure bending and the other axis represents pure torsion.

The last section of the chapter provides numerical solutions for a particular choice of parameters. The solutions for different rotor speeds are presented to show the dependence of complex modes on the spin rate. The actual solution for the natural frequencies and mode shapes for specific systems allows greater physical insight into the dynamics of the system.

5.2 Governing Partial Differential Equations

In this section, Hamilton's Principle will be used to derive the equations of motion and boundary conditions which govern the behavior of a very simple physical system. This system consists of a long slender flexible beam with a rotor mounted at the tip. This system is shown in Figure 5.1. The system is free of externally applied forces and moments. Because of this, the system center of mass is an inertial reference point. A set of inertially fixed unit vectors, $\{\hat{i}\}$, have their origin at the center of mass. The system has no damping and the beam is uniform and inextensible. It is modeled as a Bernoulli-Euler beam with degrees of freedom for displacement in-plane, out-of-plane and torsional twist about the centroidal axis. The beam does not include the effects of rotary inertia and shear deformation and no degree of freedom is included to allow longitudinal vibration. The rotor is mounted on the tip of the beam with the center of mass of the rotor placed on the beam centroid. The rotor is symmetric and has static and dynamic balance. A locally attached vector basis, $\{\hat{b}\}$, is fixed at the tip of the beam, with one axis aligned along the rotor axis of symmetry and another axis aligned along the beam. The origin of these axes is placed on the beam centroid. This set of axes is representative of a general set of axes fixed in each beam cross-section. A frame v is fixed relative to the rotor. The rotor speed consists of a constant rate plus a small, first order variation that is time dependent. It is not necessary to employ a Tisserand frame, since the requirement that the speed variation be small will ensure that the inertial displacements of the beam are small (first order quantities).

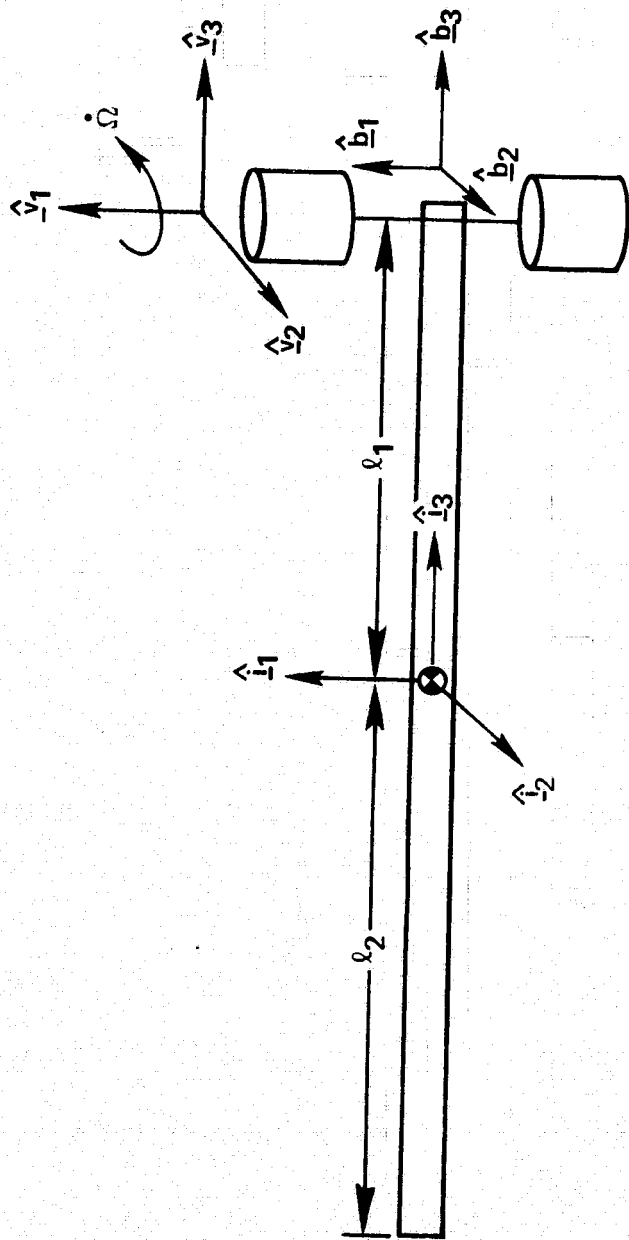


Figure 5.1. Uniform Beam with Tip Mounted Rotor.

A first order analysis is used when we apply Hamilton's Principle. For conservative, homonomic systems, Hamilton's Principle is written

$$\delta \int_{t_1}^{t_2} \mathcal{L} dt = 0 \quad (5.1)$$

where \mathcal{L} is the Lagrangian of the system. The Lagrangian is the difference between the system kinetic energy and the system potential energy.

$$\mathcal{L} = T - U. \quad (5.2)$$

Hamilton's Principle requires that the actual path (Newtonian path) of the system in configuration space renders the value of the definite integral of Equation (5.1) stationary with respect to all arbitrary variations of the path between the two time points. The arbitrary variations from the true path create what is called the varied path. It must be understood in Hamilton's Principle that the varied path coincides with the true path at the endpoints of the integration; that is at time points t_1 and t_2 the variations are zero. The advantage of Hamilton's Principle is that it provides in a formal manner both the partial differential equations of the system and the associated boundary conditions.

In order to keep first order terms in the equations of motion and the boundary conditions, second order terms must be preserved in the kinetic and strain energies. The kinetic energy for the system is first written as

$$T = \frac{1}{2} \int_S \dot{\underline{\rho}} \cdot \dot{\underline{\rho}} dm \quad (5.3)$$

For the beam component of our system, the vector $\underline{\rho}$ from the system mass center to the generic mass element may be written

$$\underline{\rho} = \underline{r} + \underline{p} = \bar{\underline{\rho}} + \underline{u} + \underline{p} \quad (5.4)$$

The geometry of the beam is shown in Figure 5.2. The beam centroid is defined by the relationship for each cross-section dA

$$\int_{dA} \underline{p} \, dm = 0 \quad (5.5)$$

The vector \underline{p} is normal to the centroidal axis and locates the mass element relative to the beam centroid. This vector is fixed in the locally attached vector basis $\{\hat{\underline{b}}\}$ and has no component in the $\hat{\underline{b}}_3$ direction. The vector is written

$$\underline{p} = \{\hat{\underline{b}}\}^T \begin{pmatrix} p_1 \\ p_2 \\ 0 \end{pmatrix} \quad (5.6)$$

The torsional twist, ψ , is assumed to be about the centroid. If rotary inertia effects are to be ignored, then the only component of angular velocity of the locally attached frame, $\{\hat{\underline{b}}\}$ that needs to be considered is that associated with torsion, $\dot{\psi}\hat{\underline{b}}_3$. Thus the derivative of the vector \underline{p} with respect to inertial space is

$$\dot{\underline{p}} = \underline{\omega}^{bi} \times \underline{p} \cong \{\hat{\underline{b}}\}^T \begin{pmatrix} -\dot{\psi}p_2 \\ \dot{\psi}p_1 \\ 0 \end{pmatrix} \quad (5.7)$$

The displacement of the beam centroid is represented by the vector \underline{r} . This vector may be broken into two components: a vector, $\bar{\underline{\rho}}$, which locates the position of the undeformed centroid and is fixed relative to the inertial axes, and a vector \underline{u} which represents the displacement of the centroid. If the undeformed centroidal axis is aligned along the $\hat{\underline{i}}_3$ direction as shown in Figure 5.2, then $\bar{\underline{\rho}}$ is simply $z \hat{\underline{i}}_3$ and \underline{u} has

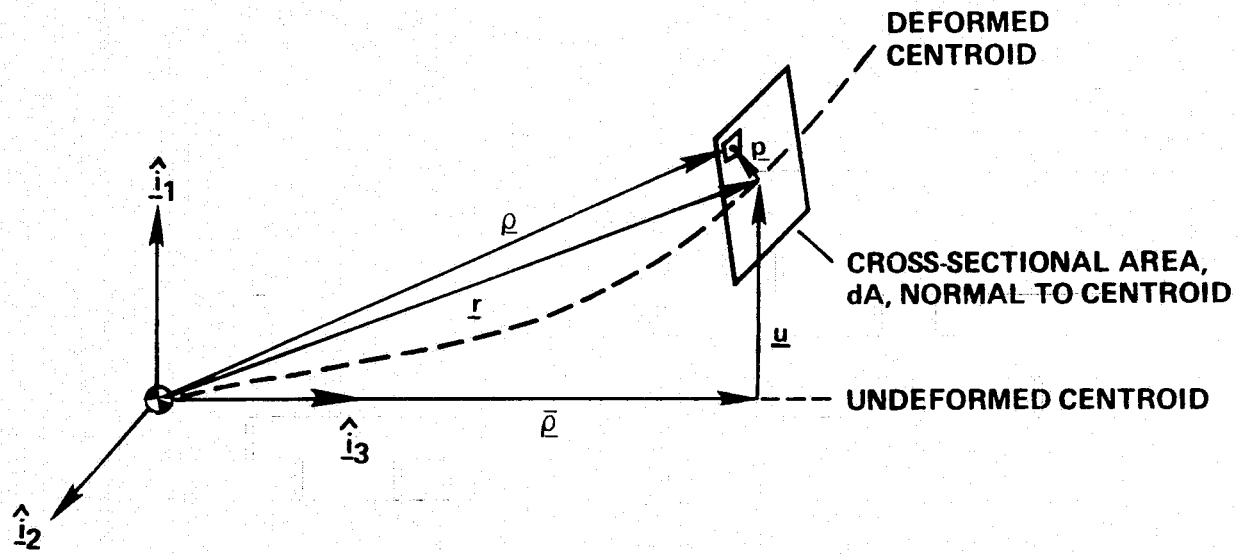


Figure 5.2. Geometry of the Beam Element.

no component in the \hat{i}_3 direction. The derivative of the vector \underline{r} may then be written

$$\dot{\underline{r}} = \{\hat{i}\}^T \begin{pmatrix} \dot{u}_1 \\ \dot{u}_2 \\ 0 \end{pmatrix} \quad (5.8)$$

Remember that the vector $\bar{\rho}$ is fixed relative to the inertial axes and thus the location of the undeformed centroid, z , has a zero derivative. The kinetic energy of the beam may now be written in greater detail

$$\frac{1}{2} \int_B \dot{\underline{p}} \cdot \dot{\underline{p}} \, dm = \frac{1}{2} \int_B m(\dot{u}_1^2 + \dot{u}_2^2) dz + \frac{1}{2} \int_B I_P \dot{\psi}^2 dz \quad (5.9)$$

This relationship has been simplified by eliminating terms made zero by the centroid definition (Equation (5.5)) and by recognizing the mass per unit length, m , and the mass moment of inertia per unit length

$$I_P = \int_{dA} (p_1^2 + p_2^2) \, dm. \quad (5.10)$$

For the rotor, the center of mass lies on the centroid and is located relative to the system center of mass by the vector $\underline{\rho}_R$. The derivative relative to inertial space of $\underline{\rho}_R$ is $\dot{\underline{\rho}}_R$. The kinetic energy of the rotor is simplified because of terms set to zero by the definition of the rotor center of mass. The kinetic energy of the rotor is written

$$\frac{1}{2} \int_R \dot{\underline{p}} \cdot \dot{\underline{p}} \, dm = \frac{1}{2} M_R \dot{\underline{u}}_R \cdot \dot{\underline{u}}_R + \frac{1}{2} \underline{\omega}^{vi} \cdot \underline{\square}_R \cdot \underline{\omega}^{vi} \quad (5.11)$$

where M_R and $\underline{\square}_R$ are the rotor mass and inertia dyadic respectively and $\underline{\omega}^{vi}$ is the angular velocity of the rotor-fixed axes relative to inertial space. Care must be taken in the evaluation of $\underline{\omega}^{vi}$ since it is not a

first order term and since all second order terms must be retained in Equation (5.11). The rotor angular velocity is

$$\underline{\omega}^{vi} = \underline{\omega}^{vb} + \underline{\omega}^{bi} \quad (5.12)$$

In this expression, the angular velocity of the rotor relative to the mounting frame, $\underline{\omega}^{vb}$, is not a first order quantity. It has a magnitude, $\dot{\Omega}$, which is an arbitrary constant plus a first order variation and it has direction \hat{b}_1 :

$$\underline{\omega}^{vb} = \dot{\Omega} \hat{b}_1 . \quad (5.13)$$

The angular velocity of the beam tip with respect to inertial space is $\underline{\omega}_R^{bi}$. The detailed derivation of the components of $\underline{\omega}_R^{bi}$ is given in Appendix B. The second order terms must be included in the analysis.

$$\underline{\omega}_R^{bi} = \{\hat{b}\}^T \left(\begin{Bmatrix} -\dot{u}'_{R_2} \\ \dot{u}'_{R_1} \\ \dot{\psi}_R \end{Bmatrix} + \begin{Bmatrix} \psi_R \dot{u}'_{R_1} \\ \psi_R \dot{u}'_{R_2} \\ -u'_{R_1} \dot{u}'_{R_2} \end{Bmatrix} \right) \quad (5.14)$$

The components of \underline{u}_R in inertial axes are $(u_{R_1}, u_{R_2}, 0)$. The primes indicate spatial derivatives and the dots represent time derivatives, so that

$$\begin{aligned} \dot{u}'_{R_1} &= \frac{\partial^2 u_{R_1}}{\partial z \partial t} \\ \dot{u}'_{R_2} &= \frac{\partial^2 u_{R_2}}{\partial z \partial t} \end{aligned} \quad (5.15)$$

As noted above, the twist due to torsion is the angle ψ and the subscript R denotes evaluation at the rotor mounting point. The rotor

has a symmetric moment of inertia I_S and transverse moments of inertia I_T . The inertia dyadic may be written as

$$\underline{\underline{\square}}_R = \{\hat{\underline{b}}\}^T \begin{bmatrix} I_S & 0 & 0 \\ 0 & I_T & 0 \\ 0 & 0 & I_T \end{bmatrix} \{\hat{\underline{b}}\} \quad (5.16)$$

Keeping all second order terms, the last quantity in Equation (5.11) is written

$$\begin{aligned} \frac{1}{2} \underline{\omega}^{vi} \cdot \underline{\underline{\square}}_R \cdot \underline{\omega}^{vi} = & \frac{1}{2} I_S \dot{\Omega}^2 + I_S \ddot{\Omega} (-\dot{u}'_{R_2} + \psi_R \dot{u}'_{R_1}) \\ & + \frac{1}{2} I_S (\dot{u}'_{R_2})^2 + \frac{1}{2} I_T (\dot{u}'_{R_1})^2 + \frac{1}{2} I_T (\dot{\psi}_R)^2 \end{aligned} \quad (5.17)$$

It is now possible to write the system kinetic energy

$$\begin{aligned} T = & \frac{1}{2} \int_B m(\dot{u}_1^2 + \dot{u}_2^2) dz + \frac{1}{2} \int_B I_P \dot{\psi}^2 dz \\ & + \frac{1}{2} M_R \left[(\dot{u}'_{R_1})^2 + (\dot{u}'_{R_2})^2 \right] + \frac{1}{2} I_S \dot{\Omega}^2 \\ & - I_S \dot{\Omega} \dot{u}'_{R_2} + I_S \dot{\Omega} \psi_R \dot{u}'_{R_1} \\ & + \frac{1}{2} I_S (\dot{u}'_{R_2})^2 + \frac{1}{2} I_T (\dot{u}'_{R_1})^2 + \frac{1}{2} I_T (\dot{\psi}_R)^2 \end{aligned} \quad (5.18)$$

The kinetic energy includes all second order terms. The subscript R represents evaluation of the quantity at the rotor mounting point, where z equals l_1 .

The strain energy of the system comes from three types of deformation: in-plane bending, out-of-plane bending and torsion about the centroidal axis. The strain energy may be written

$$U = \frac{1}{2} \int_B \left[EI_1 \left(\frac{\partial^2 u_1}{\partial z^2} \right)^2 + EI_2 \left(\frac{\partial^2 u_2}{\partial z^2} \right)^2 \right] dz + \frac{1}{2} \int_B GJ \left(\frac{\partial \psi}{\partial z} \right)^2 dz \quad (5.19)$$

where EI is flexural rigidity and GJ is torsional stiffness.

It is now possible to write the Lagrangian in terms of the scalar functions $u_1(z,t)$, $u_2(z,t)$ and $\psi(z,t)$. By taking the first variations of the kinetic energy in Equation (5.18) and of the strain energy in Equation (5.19) it is now possible to write Hamilton's principle in the form.

$$\begin{aligned} \delta \int_{t_1}^{t_2} \mathcal{L} dt = & \int_{t_1}^{t_2} \left\{ \int_{-l_2}^{l_1} m(\dot{u}_1 \delta \dot{u}_1 + \dot{u}_2 \delta \dot{u}_2) dz + \int_{-l_2}^{l_1} I_P \dot{\psi} \delta \dot{\psi} dz \right. \\ & + M_R \dot{u}_1(l_1) \delta \dot{u}_1(l_1) + M_R \dot{u}_2(l_1) \delta \dot{u}_2(l_1) \\ & - I_S \dot{\Omega} \delta \dot{u}_2'(l_1) + I_S \dot{\Omega} \psi(l_1) \delta \dot{u}_1(l_1) \\ & + I_S \dot{\Omega} \dot{u}_1'(l_1) \delta \psi(l_1) + I_S \dot{u}_2'(l_1) \delta \dot{u}_2'(l_1) \\ & + I_T \dot{u}_1'(l_1) \delta \dot{u}_1'(l_1) + I_T \dot{\psi}(l_1) \delta \dot{\psi}(l_1) \\ & - \int_{-l_2}^{l_1} EI_1 u_1'' \delta u_1'' dz - \int_{-l_2}^{l_1} EI_2 u_2'' \delta u_2'' dz \\ & \left. - \int_{-l_2}^{l_1} GJ \psi' \delta \psi' dz \right\} dt = 0 \quad (5.20) \end{aligned}$$

In order to arrive at the final formulation of Hamilton's Principle it is necessary to integrate by parts. When variations of the coordinates at times t_1 and t_2 are set to zero, Hamilton's Principle has the form

$$\begin{aligned}
& \int_{t_1}^{t_2} \left\{ \int_{-\ell_2}^{\ell_1} [-m\ddot{u}_1 - EI_1 u_1''''] \delta u_1 dz + \int_{\ell_2}^{\ell_1} [-m\ddot{u}_2 - EI_2 u_2''''] \delta u_2 dz \right. \\
& + \int_{-\ell_2}^{\ell_1} [-I_P \ddot{\psi} + GJ\psi''] \delta \psi dz + [EI_1 u_1'''(\ell_1) - M_R \ddot{u}_1(\ell_1)] \delta u_1(\ell_1) \\
& + [-I_S \dot{\omega} \dot{\psi}(\ell_1) - I_T \ddot{u}_1'(\ell_1) - EI_1 u_1''(\ell_1)] \delta u_1'(\ell_1) \\
& + [EI_2 u_2'''(\ell_1) - M_R \ddot{u}_2(\ell_1)] \delta u_2(\ell_1) \\
& + [-I_S \ddot{u}_2'(\ell_1) - EI_2 u_2''(\ell_1) + I_S \ddot{\omega}] \delta u_2'(\ell_1) \\
& + [I_S \dot{\omega} \dot{u}_1'(\ell_1) - I_T \ddot{\psi}(\ell_1) - GJ\psi'(\ell_1)] \delta \psi(\ell_1) \\
& - [EI_1 u_1'''(-\ell_2)] \delta u_1(-\ell_2) + [EI_1 u_1''(-\ell_2)] \delta u_1'(-\ell_2) \\
& \left. - [EI_2 u_2'''(-\ell_2)] \delta u_2(-\ell_2) + [EI_2 u_2''(-\ell_2)] \delta u_2'(-\ell_2) - [GJ\psi'(-\ell_2)] \delta \psi(-\ell_2) \right\} dt = 0
\end{aligned} \tag{5.21}$$

Since the variations are independent and arbitrary, all quantities in square brackets must be set to zero. For in-plane bending, u_1 , the partial differential equation is

$$m\ddot{u}_1 + EI_1 u_1'''' = 0 \tag{5.22}$$

with the boundary conditions

$$\begin{aligned}
u_1''(0) &= 0 \\
u_1'''(0) &= 0 \\
EI_1 u_1''(L) &= -I_T \ddot{u}_1'(L) - I_S \dot{\omega} \dot{\psi}(L) \\
EI_1 u_1'''(L) &= M_R \ddot{u}_1(L)
\end{aligned} \tag{5.23}$$

A shift of origin was made in the spatial coordinate so that $-\ell_2$ became zero and ℓ_1 became L , the beam length. The boundary conditions for in-plane bending depend on the torsion ψ . The partial differential equation for torsion is

$$I_p \ddot{\psi} - GJ\psi'' = 0 \quad (5.24)$$

with the boundary conditions

$$\begin{aligned} \psi'(0) &= 0 \\ GJ\psi'(L) &= -I_T \ddot{\psi}(L) + I_S \dot{\Omega} u_1'(L) \end{aligned} \quad (5.25)$$

Again there is coupling between torsion, ψ , and in-plane bending, u_1 , in the boundary conditions. This represents the gyroscopic coupling present in the system. Both coupling terms in the boundary conditions are seen to depend on the rotor spin rate, $\dot{\Omega}$. The partial differential equation for out-of-plane bending is

$$m\ddot{u}_2 + EI_2 u_2'''' = 0 \quad (5.26)$$

with the boundary conditions

$$\begin{aligned} u_2''(0) &= 0 \\ u_2'''(0) &= 0 \\ EI_2 u_2''(L) &= -I_S \ddot{u}_2'(L) + I_S \ddot{\Omega} \\ EI_2 u_2'''(L) &= M_R \ddot{u}_2(L) \end{aligned} \quad (5.27)$$

The out-of-plane bending is not coupled to other system behavior, but the boundary conditions are time dependent. The term $\ddot{\Omega}$ in Equation (5.27) represents a small acceleration in rotor speed which is a first order function of time.

Hamilton's Principle has been used to formulate the partial differential equations and the boundary conditions which govern system behavior. The boundary conditions represent moment and shear forces applied to the beam ends. The structure of the system equations demonstrates gyroscopic coupling between in-plane and torsional motion. The next section will deal with the solution of these equations by using separation of variables.

5.3 Solution of the Partial Differential Equations

In this section, the technique of separation of variables is employed to solve the partial differential equations which govern the system behavior. The first approach is to choose independent coordinates for the separation of variables. The out-of-plane motion is independent but the boundary conditions include time dependent terms and mixed spatial and time derivatives (Equation (5.27)). The separation of variables method cannot be applied to this equation and boundary conditions because of their structure. Solution techniques involving integral transform methods such as Laplace transforms may be applicable, but they will be hampered by the complexity of the system and are not investigated here. Instead, a modified system of greater simplicity is introduced for out-of-plane bending. A generalized separation of variables method is applied and the problem is transformed into one containing a nonhomogeneous differential equation with homogeneous boundary conditions. This system of equations is solved using the normal mode method.

Investigation of the coupled solution for in-plane bending and torsion shows that the choice of independent coordinates will allow

only the translational rigid body mode and the trivial solution to be admitted. The system motion is found by using a separation of variables with distinct spatial functions (mode shapes) but with the same time dependent function (modal coordinate). The in-plane bending and torsion then have the same natural frequency. Solution of the partial differential equation and boundary conditions yields "complex" mode shapes. This means that the modes, or eigenfunctions of the system, are functions with values which are complex numbers. The physical interpretation of these complex mode shapes is that in-plane bending is ninety degrees out of phase in the time domain with torsional bending. With both motions harmonic, the system normal modes oscillate back and forth between pure in-plane bending and pure torsion. The tip of the rotor shaft mounted on the beam can then be seen to travel in an ellipse with one axis representing in-plane bending and the other axis representing torsion. This represents a coning of the rotor shaft about the vertical where the cone angle varies sinusoidally. This motion is shown in greater detail in the next section.

Addressing the out-of-plane bending motion, the structure of the boundary conditions (Equation (5.29)) presents two degrees of complexity. The first property of the boundary conditions is that they involve both spatial and time derivatives. The presence of time derivatives normally causes the boundary conditions to depend on the eigenvalues of the system. The second property is that the boundary conditions involve the accelerations of the rotor and are therefore time dependent. Each of these complexities could be dealt with separately by known methods involving separation of variables, but these methods do not work for

the problem at hand. The methods for transforming time dependent boundary conditions into homogeneous boundary conditions require that the system does not have time derivatives in the boundary conditions. In order to proceed to a solution for out-of-plane bending, the physical system is further simplified and the time derivatives are eliminated from the boundary conditions. The system for out-of-plane bending is one where the rotor and beam, taken together, have the mass and inertia properties of a uniform beam. This eliminates the moment and shear forces applied to the beam tip by the "nonspinning" rotor. The equation describing the system is

$$\mu_2 u_2'' + EI_2 u_2'''' = 0 \quad (5.28)$$

with the simplified boundary conditions

$$\begin{aligned} u_2''(0) &= 0 \\ u_2''''(0) &= 0 \\ EI_2 u_2''(L) &= I_S \ddot{\Omega} \\ u_2''''(L) &= 0 \end{aligned} \quad (5.29)$$

These boundary conditions are now free of time derivatives and may be transformed to homogeneous boundary conditions by

$$u_2(z, t) = w(z, t) + S(z) I_S \ddot{\Omega} \quad (5.30)$$

where the step function $S(z)$ is

$$\begin{aligned} S(z) &= 0_2 & 0 \leq z < L - \epsilon \\ S(z) &= \frac{z^2}{2EI} & L - \epsilon \leq z \leq L \end{aligned} \quad (5.31)$$

The choice of S is not unique but it must satisfy the constraints

$$\begin{aligned}
S''(0) &= 0 \\
S'''(0) &= 0 \\
EIS''(L) &= 1 \\
S'''(L) &= 0
\end{aligned}
\tag{5.32}$$

The transposed partial differential equation is then

$$w'''' + \frac{m}{EI_2} \ddot{w} = - S'''' I_S \ddot{\Omega} - \frac{m}{EI} S I_S \ddot{\Omega}
\tag{5.33}$$

with the homogeneous boundary conditions

$$\begin{aligned}
w''(0) &= 0 \\
w'''(0) &= 0 \\
w''(L) &= 0 \\
w'''(L) &= 0
\end{aligned}
\tag{5.34}$$

The homogeneous solution is then found using the separation of variables

$$w(z,t) = g(z)\mu(t)
\tag{5.35}$$

This yields the natural frequencies, ω_n , and mode shapes, $g(z)$, of a free-free uniform beam. The nonhomogeneous solution is then found by modal analysis

$$\ddot{\mu}_n(t) + \omega_n^2 \mu_n(t) = N_n(t)
\tag{5.36}$$

where

$$N_n(t) = - H_n^* I_S \ddot{\Omega} - H_n I_S \ddot{\Omega}$$

and

$$\begin{aligned}
H_n &= \int_0^L g_n \left(\frac{m}{EI} \right) S dz \\
&= \frac{m}{2(EI)^2} \int_{L-\epsilon}^L g_n z^2 dz
\end{aligned}$$

$$\begin{aligned}
H_n^* &= \int_0^L g_n S'''' dz \\
&= -\frac{4}{EI} g_n'(L-\epsilon) - \frac{2}{EI}(L-\epsilon) g_n''(L-\epsilon) - \frac{1}{EI} (L-\epsilon)^2 g_n'''(L-\epsilon) \quad (5.37)
\end{aligned}$$

The last expression involves the derivatives of S across the discontinuity. The resultant derivatives of Dirac "delta" functions must be integrated by parts, but this allows easy evaluation of the remaining integrals. The solution of Equation (5.36) for zero initial conditions is given by the convolution integral

$$\mu_n(t) = \frac{1}{\omega_n} \int_0^t N_n(\tau) \sin \omega_n(t-\tau) d\tau \quad (5.38)$$

The final out-of-plane bending for our simplified model is then described by

$$u_2(z,t) = \sum_{i=1}^n g_n(z) \eta_n(t) + I_S \ddot{\Omega} S(z) \quad (5.39)$$

The use of a step function for S raises questions concerning the spatial continuity of the solution and invariance of the solution to the location of the step. For physical reasons, the value of ϵ would be kept small due to the fact that the moment is applied at the beam tip.

The coupled in-plane bending and torsional motions are described by the following partial differential equations and boundary conditions

$$\begin{aligned}
m\ddot{u}_1 + EI_1 u_1'''' &= 0 \\
u_1''(0) &= 0 \\
u_1'''(0) &= 0 \\
EI u_1''(L) &= -I_T \ddot{u}_1'(L) - I_S \ddot{\Omega} \psi(L) \\
EI u_1'''(L) &= M_R \ddot{u}_1(L)
\end{aligned}$$

(Continued)

$$I_P \ddot{\psi} - GJ\psi'' = 0$$

$$\psi'(0) = 0$$

$$GJ\psi'(L) = - I_T \ddot{\psi}(L) + I_S \dot{\omega}_1'(L) \quad (5.40)$$

If independent coordinates are chosen, then the separation of variables has the form

$$u_1(z, t) = f(z) \lambda(t)$$

$$\psi(z, t) = h(z) \nu(t) \quad (5.41)$$

The first motion to be investigated is the rigid body mode corresponding to zero natural frequency. If zero initial displacements are assumed, then the general solutions are given by

$$u_1 = (D_1 + D_2 x + D_3 x^2 + D_4 x^3) t$$

$$\psi = (D_5 + D_6 x) t \quad (5.42)$$

Substituting these expressions into the boundary conditions will set all constants to zero except D_1 . The rigid body motion allowed by the system is in-plane translation. Rotational rigid body modes are not permitted.

Proceeding with the separation of variables using independent coordinates, the equation for the in-plane bending modal coordinate is

$$\ddot{\lambda} + \omega_1^2 \lambda = 0 \quad (5.43)$$

where ω_1 is the natural frequency. The equation for the mode shape is

$$f'''' - \frac{EI_1}{m} \omega_1^2 f = 0 \quad (5.44)$$

with the boundary conditions

$$f''(0) = 0$$

$$f'''(0) = 0$$

$$EI_1 f''(L)\lambda = \omega_1^2 I_T f'(L)\lambda - i\omega_3 I_S \dot{\omega} h(L)v$$

$$EI_1 f'''(L) = -\omega_1^2 M_R f(L). \quad (5.45)$$

The boundary conditions depend on the eigenvalue, ω_1 , because of Equation (5.43). The introduction of the imaginary number, i , comes from the equation for the modal coordinate for torsion

$$\ddot{v} + \omega_3^2 v = 0 \quad (5.46)$$

where ω_3 is the natural frequency. The solution for this equation is

$$v = ce^{i\omega_3 t} \quad (5.47)$$

The time derivative of ψ found in the boundary conditions (Equation (5.40)) can then be eliminated using

$$\dot{\psi}(L) = i\omega_3 h(L)v \quad (5.48)$$

By employing a similar substitution for the time derivative of the in-plane bending variable based on Equation (5.43), we have

$$\dot{u}'_1(L) = i\omega_1 f'(L)\lambda \quad (5.49)$$

The differential equation for torsion becomes

$$h'' + \frac{I_P}{GJ} \omega_3^2 h = 0 \quad (5.50)$$

with the boundary conditions

$$h'(0) = 0$$

$$GJh'(L)v = \omega_3^2 I_T h(L)v + i\omega_1 I_S \dot{\omega} f'(L)\lambda. \quad (5.51)$$

Let us look in detail at the boundary conditions given by Equations (5.45) and (5.51). It has not been possible to eliminate the time dependent variables from the boundary conditions. These time dependent variables have distinct natural frequencies. The boundary conditions containing the time dependent coordinates are

$$\begin{aligned} \left[EI_1 f''(L) - \omega_1^2 I_T f'(L) \right] \lambda(t) + \left[i\omega_3 I_S \dot{\omega} h(L) \right] v(t) &= 0 \\ \left[GJh'(L) - \omega_3^2 I_T h(L) \right] v(t) - \left[i\omega_1 I_S \dot{\omega} f'(L) \right] \lambda(t) &= 0 \end{aligned} \quad (5.52)$$

The only manner that these equations may be satisfied when $\lambda(t)$ and $v(t)$ have distinct, nonzero, natural frequencies is to set the terms within square brackets to zero. As a consequence of this, the boundary conditions in Equation (5.52) become

$$\begin{aligned} f'(L) &= 0 \\ f''(L) &= 0 \\ h(L) &= 0 \\ h'(L) &= 0 \end{aligned} \quad (5.53)$$

The general solutions of Equations (5.44) and (5.50) are

$$\begin{aligned} f(z) &= C_1 \sin\beta_1 z + C_2 \cos\beta_1 z + C_3 \sinh\beta_1 z + C_4 \cosh\beta_1 z \\ h(z) &= C_5 \sin\beta_2 z + C_6 \cos\beta_2 z \end{aligned} \quad (5.54)$$

where

$$\begin{aligned} \beta_1^4 &= \frac{m}{EI_1} \omega_1^2 \\ \beta_2^2 &= \frac{I_P}{GJ} \omega_3^2 \end{aligned} \quad (5.55)$$

When these functions are substituted into the boundary conditions that come from Equations (5.45), (5.51) and (5.53), the solution for the constants becomes

$$C_1 = C_2 = C_3 = C_4 = C_5 = C_6 = 0 \quad (5.56)$$

This represents the trivial solution corresponding to zero movement.

In order to solve for the system behavior, a different separations of variables technique must be used. The modal coordinates for in-plane bending and torsion now are assumed to have the same natural frequency, ω . They are separated in time by a phase delay ϕ . The separation of variables has the new form where the coordinates are coupled

$$\begin{aligned} u_1(z,t) &= f(z) \lambda(t) \\ \psi(z,t) &= h(z) \lambda(t-\phi) \end{aligned} \quad (5.57)$$

The time dependent terms may now be eliminated from the boundary conditions given by Equation (5.52). The procedure is to replace $v(t)$ by $\lambda(t-\phi)$ in Equations (5.45) and (5.51). When dividing by $\lambda(t)$ we may use the relationship

$$\lambda(t) = ce^{i\omega t} \quad (5.58)$$

The boundary conditions for the coupled set of equations then have the form

$$\begin{aligned} f''(0) &= 0 \\ f'''(0) &= 0 \\ h'(0) &= 0 \\ EI_1 f''(L) &= \omega^2 I_T f'(L) - \omega I_S \dot{\Omega} h(L) e^{-i\omega\phi} \\ EI f'''(L) &= -\omega^2 M_R f(L) \\ GJ h'(L) &= \omega^2 I_T h(L) + i\omega I_S \dot{\Omega} f'(L) e^{i\omega\phi} \end{aligned} \quad (5.59)$$

Using the general solution forms given by Equations (5.54) and the first three equations given above will give the result

$$\begin{aligned}
C_3 &= C_1 \\
C_4 &= C_2 \\
C_5 &= 0
\end{aligned} \tag{5.60}$$

This result assumes that the natural frequency is not zero. Thus the rigid body mode is excluded from the solutions which use Equation (5.60). The last three boundary conditions of Equation (5.59) deal with the moments and shear forces applied to the beam by the rotor. Using the solution forms in Equation (5.54), the boundary conditions are written in matrix form.

$$\begin{bmatrix}
EI_1 \beta_1^2 (\sinh \beta_1 L - \sin \beta_1 L) & EI_1 \beta_1^2 (\cosh \beta_1 L - \cos \beta_1 L) & \omega I_2 \dot{\phi} \cos(\nu_2 L) e^{i(\frac{\pi}{2} - \phi)} \\
-\omega^2 I_1 \beta_1 (\cos \beta_1 L + \cosh \beta_1 L) & -\omega^2 I_1 \beta_1 (\sin \beta_1 L + \sinh \beta_1 L) & 0 \\
EI_1 \beta_1^3 (\cosh \beta_1 L - \cos \beta_1 L) & EI_1 \beta_1^3 (\sin \beta_1 L + \sinh \beta_1 L) & 0 \\
+\omega^2 I_2 \beta_1 (\sin \beta_1 L + \sinh \beta_1 L) & +\omega^2 I_2 (\cos \beta_1 L + \cosh \beta_1 L) & 0 \\
-\omega I_2 \beta_1 (\cos \beta_1 L + \cosh \beta_1 L) e^{i(\frac{\pi}{2} + \phi)} & -\omega I_2 \beta_1 (\sin \beta_1 L - \sinh \beta_1 L) e^{i(\frac{\pi}{2} + \phi)} & -GJ \beta_2 \sin \beta_2 L - \omega^2 I_2 \cos \beta_2 L
\end{bmatrix}
\begin{Bmatrix}
C_1 \\
C_2 \\
C_3 \\
C_4 \\
C_5 \\
C_6
\end{Bmatrix} = 0 \tag{5.61}$$

where

$$\begin{aligned}
\beta_1^4 &= \frac{m}{EI_1} \omega^2 \\
\beta_2^2 &= \frac{I_P}{GJ} \omega^2
\end{aligned} \tag{5.62}$$

The characteristic equation of the system is found by setting the determinant of the above matrix to zero. This will yield the equation for the nonzero system natural frequencies.

$$\begin{aligned}
& \left[\left(\sqrt{I_P G J} \sin \beta_2 L + I_T \omega \cos \beta_2 L \right) \right. \\
& \left[\left[m^5 (EI_1)^3 \right]^{1/4} \sqrt{\omega} (\cos \beta_1 L \cosh \beta_1 L - 1) \right. \\
& - m I_T \omega^2 \cos \beta_1 L (\sin \beta_1 L + \sinh \beta_1 L) \\
& + M_R (EI_1 m)^{1/2} \omega (\cos \beta_1 L \sinh \beta_1 L - \sin \beta_1 L \cosh \beta_1 L) \\
& \left. - M_R I_T \left(\frac{m}{EI_1} \right)^{1/4} \omega^{5/2} (\cos^2 \beta_1 L + \cos \beta_1 L \cosh \beta_1 L - \sin \beta_1 L \sinh \beta_1 L) \right\} \\
& + \omega (I_S \dot{\Omega})^2 \cos \beta_2 L \left[m (\sin \beta_1 L \cosh \beta_1 L + \cos \beta_1 L \sinh \beta_1 L) \right. \\
& \left. \left. + M_R \left(\frac{m}{EI} \right)^{1/4} \omega^{1/2} (\cos \beta_1 L \cosh \beta_1 L + 1) \right] \right] = 0 \quad (5.63)
\end{aligned}$$

The above equation for the natural frequency must be solved numerically. Once a natural frequency has been found, the corresponding mode shapes come from the solution of the matrix equations (5.61). The mode shapes are found to be

$$\begin{aligned}
f(z) &= C_1 [\sin \beta_1 z + \sinh \beta_1 z + R_1 (\cos \beta_1 z + \cosh \beta_1 z)] \\
g(z) &= C_1 R_2 e^{-i \left(\frac{\pi}{2} - \phi \right)} \cos \beta_2 z \quad (5.64)
\end{aligned}$$

where the real constants R_1 and R_2 are

$$R_1 = - \frac{(m^3 EI_1)^{1/4} (\cosh \beta_1 L - \cos \beta_1 L) + M_R (\sin \beta_1 L + \sinh \beta_1 L)}{(m^3 EI_1)^{1/4} (\sin \beta_1 L + \sinh \beta_1 L) + M_R (\cos \beta_1 L + \cosh \beta_1 L)}$$

$$R_2 = \frac{\left[\sqrt{EI_1 m} (\cosh\beta_1 L - \cos\beta_1 L) - I_T \left(\frac{m}{EI_1}\right)^{1/4} \omega^{3/2} (\sin\beta_1 L + \sinh\beta_1 L) \right]}{\left[(m^3 EI_1)^{1/4} (\cosh\beta_1 L - \cos\beta_1 L) + M_R \omega^{1/2} (\sin\beta_1 L + \sinh\beta_1 L) \right]} \frac{\left[\sqrt{EI_1 m} (\sinh\beta_1 L - \sin\beta_1 L) - I_T \left(\frac{m}{EI_1}\right)^{1/4} \omega^{3/2} (\cos\beta_1 L + \cosh\beta_1 L) \right]}{\left[(m^3 EI_1)^{1/4} (\sin\beta_1 L + \sinh\beta_1 L) + M_R \omega^{1/2} (\cos\beta_1 L + \cosh\beta_1 L) \right]} (I_S \dot{\Omega} \cos\beta_2 L)$$

$$I_S \dot{\Omega} \cos\beta_2 L \quad (5.65)$$

The above mode shape for torsion is a complex mode shape. In order to place the proper physical interpretation on the complex mode shape, it is necessary to examine the displacements.

$$u_1 = f_1(z) e^{i\omega t}$$

$$\phi = h(z) e^{i(\omega t - \phi)} \quad (5.66)$$

Since we know that the displacements are real, we shall take the real parts of the expressions in Equation (5.66) by using the relationship

$$e^{i\omega t} = \cos\omega t + i \sin\omega t \quad (5.67)$$

The displacements then become

$$u_1 = C_1 [\sin\beta_1 z + \sinh\beta_1 z + R_1 (\cos\beta_1 z + \cosh\beta_1 z)] \cos\omega t$$

$$\psi = C_1 [R_2 \cos\beta_2 z] \sin\omega t \quad (5.68)$$

The arbitrary time lag, ϕ , drops out of the equations. The equations for the displacement show that the in-plane bending is always ninety degrees out of phase with the torsional bending. This follows directly from the phase relationship of the sine and cosine functions. It is this phase relationship between in-plane bending and torsion which shows the system to have gyroscopic coupling. The system behavior may now be calculated by solving the frequency Equation (5.63) and then

calculating the mode shapes by (Equation (5.64)). This work must be accomplished numerically due to the complicated structure of the equations.

5.4 Numerical Solutions

In this section, we shall formulate an example problem and solve for the coupled in-plane and torsional motion. In this manner, we shall be able to examine the gyroscopic coupling exhibited by this system for a specific case. This should increase our understanding of the dynamic interactions involved for this class of systems.

We start by choosing physical parameters for the system. The beam will be 10 meters long with an in-plane bending fundamental frequency equal to 1 Hertz and a torsional fundamental frequency equal to 5 Hertz. The mass of the beam will be 150 kg. and it has a cross section which is one meter square. The relationships for the fundamental frequencies of a free-free uniform beam are

$$f_B = 3.563 \sqrt{\frac{EI}{mL^4}}$$

$$f_T = \frac{1}{2L} \sqrt{\frac{GJ}{I_P}} \quad (5.69)$$

These expressions are inverted in order to solve for the values of flexural rigidity and torsional stiffness

$$EI = 11820. \frac{\text{kg-m}^3}{\text{sec}^2}$$

$$GJ = 25000. \frac{\text{kg-m}^3}{\text{sec}^2} \quad (5.70)$$

The value for mass moment of inertia per unit length, I_P , is 2.5 kg-m.

The rotor has a mass of 5.236 kg, a symmetric moment of inertia of .2909 kg-m² and a transverse moment of inertia of .5818 kg-m². The rotor spin speed is fixed at values between 0 and 1000 radians per second. This value is varied parametrically.

The first result to be shown is the dependence of the system natural frequencies on the rotor spin speed. Solutions of the frequency equation (Equation (5.63)) were obtained numerically for rotor speeds between 0 and 1000 radians per second. The first two natural frequencies are plotted in Figures 5.3 and 5.4. In order to examine the mode shapes themselves, the rotor spin speed was fixed at 1000 radians per second and the mode shapes were calculated using Equation (5.64). These mode shapes are shown for the first five natural frequencies in Figures 5.5 to 5.9. The first mode (Figure 5.5) involves much more rotation than bending. It is related to the rotational rigid body mode that would result if the beam were rigid. This is confirmed by noting in Figure 5.3 that for zero spin speed this mode has zero natural frequency. The last aspect of the system behavior to be examined involves the rotor motion. For small in-plane displacements, the rotor shaft will rotate an angle equal to the slope of the in-plane mode shape evaluated at the beam tip. The tip of the rotor shaft will then rotate in an ellipse as shown in Figure 5.10. The rotor is spinning counter clockwise, but the rotor tip can cone in either direction. The direction of the coning motion is determined by the moment applied to the rotor (negative of the moment applied to the beam) and is thus a function of the curvature (second derivative) of the mode shape evaluated at the beam tip.

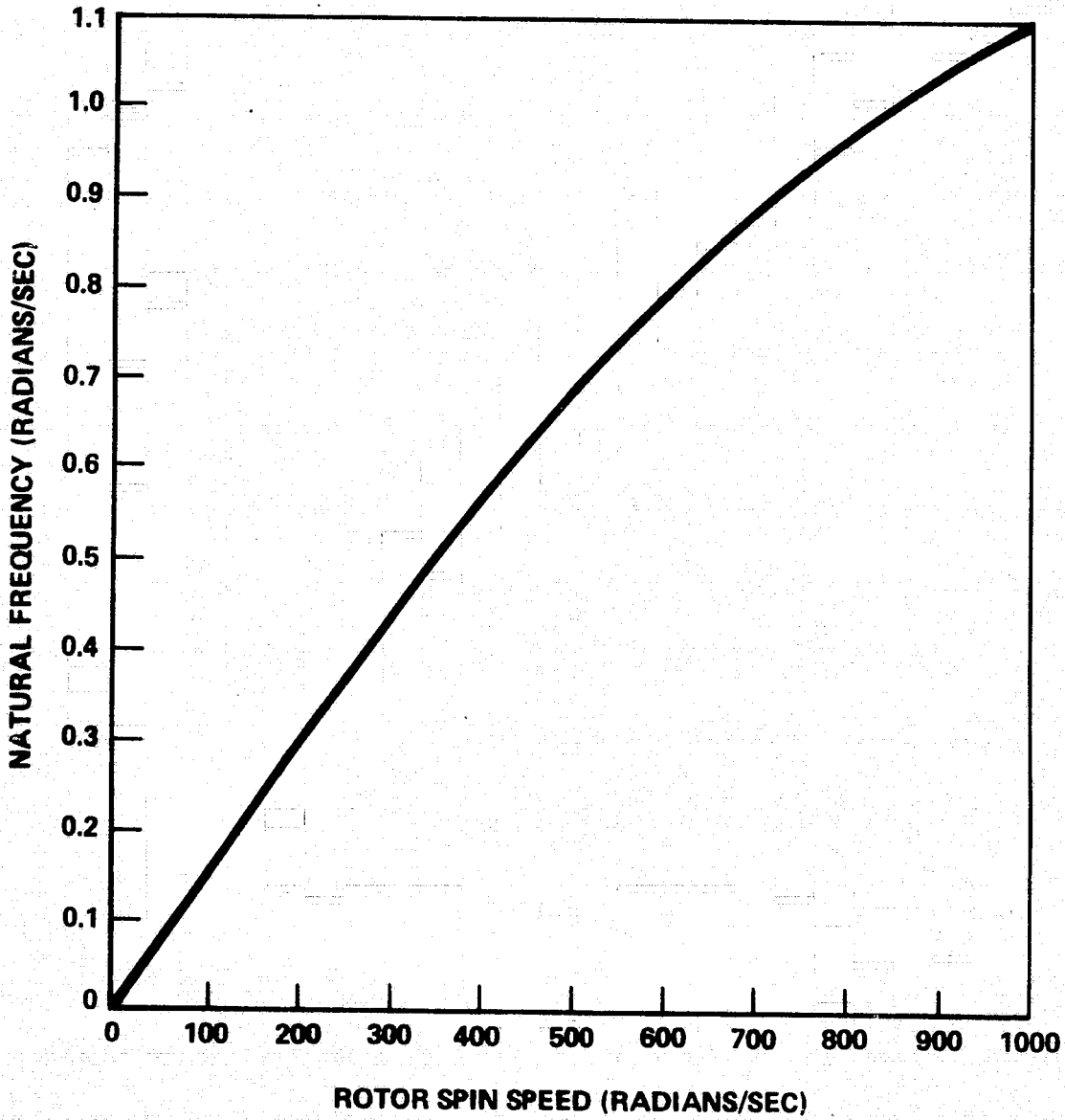


Figure 5.3. First Natural Frequency.

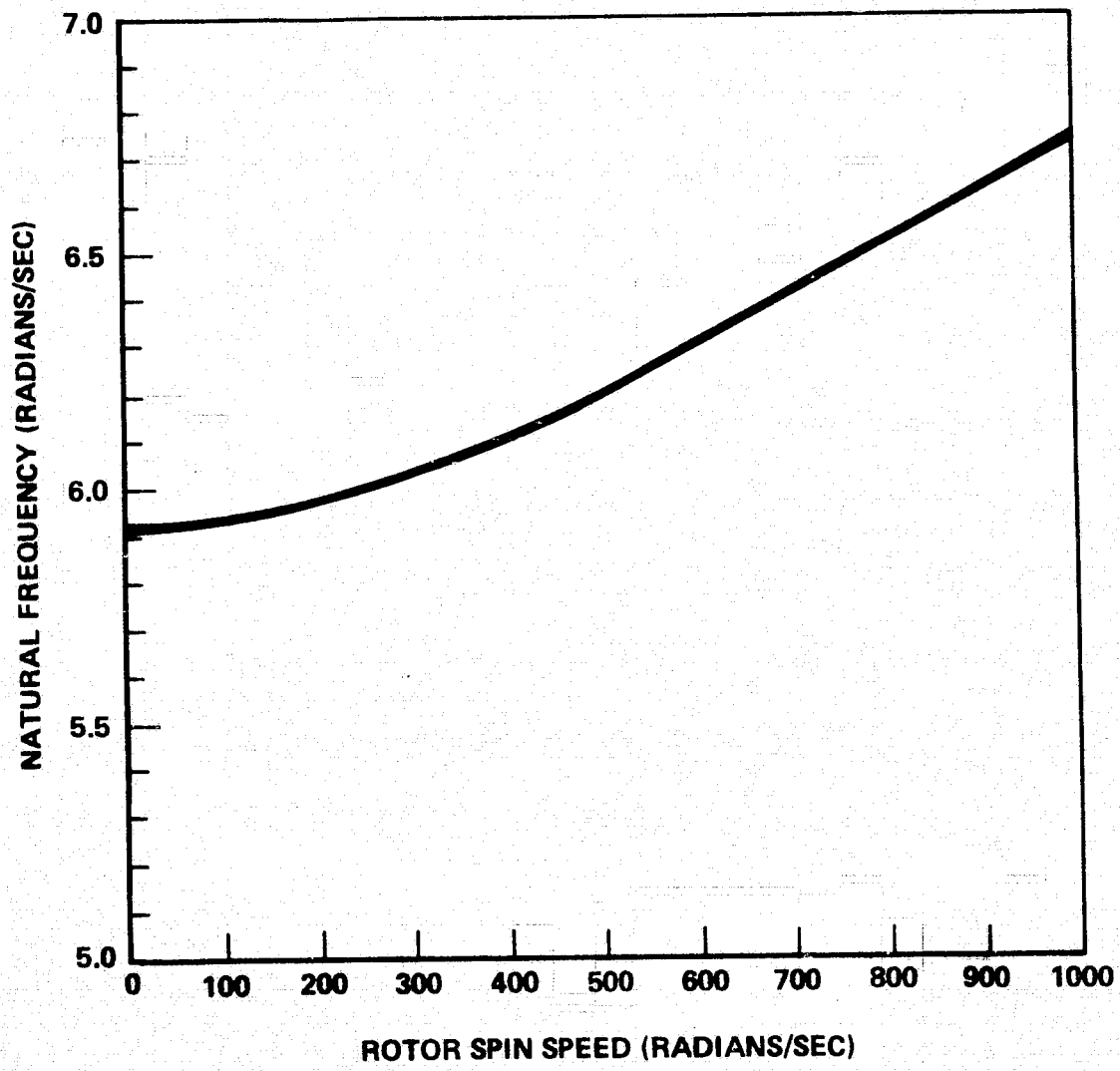


Figure 5.4. Second Natural Frequency.

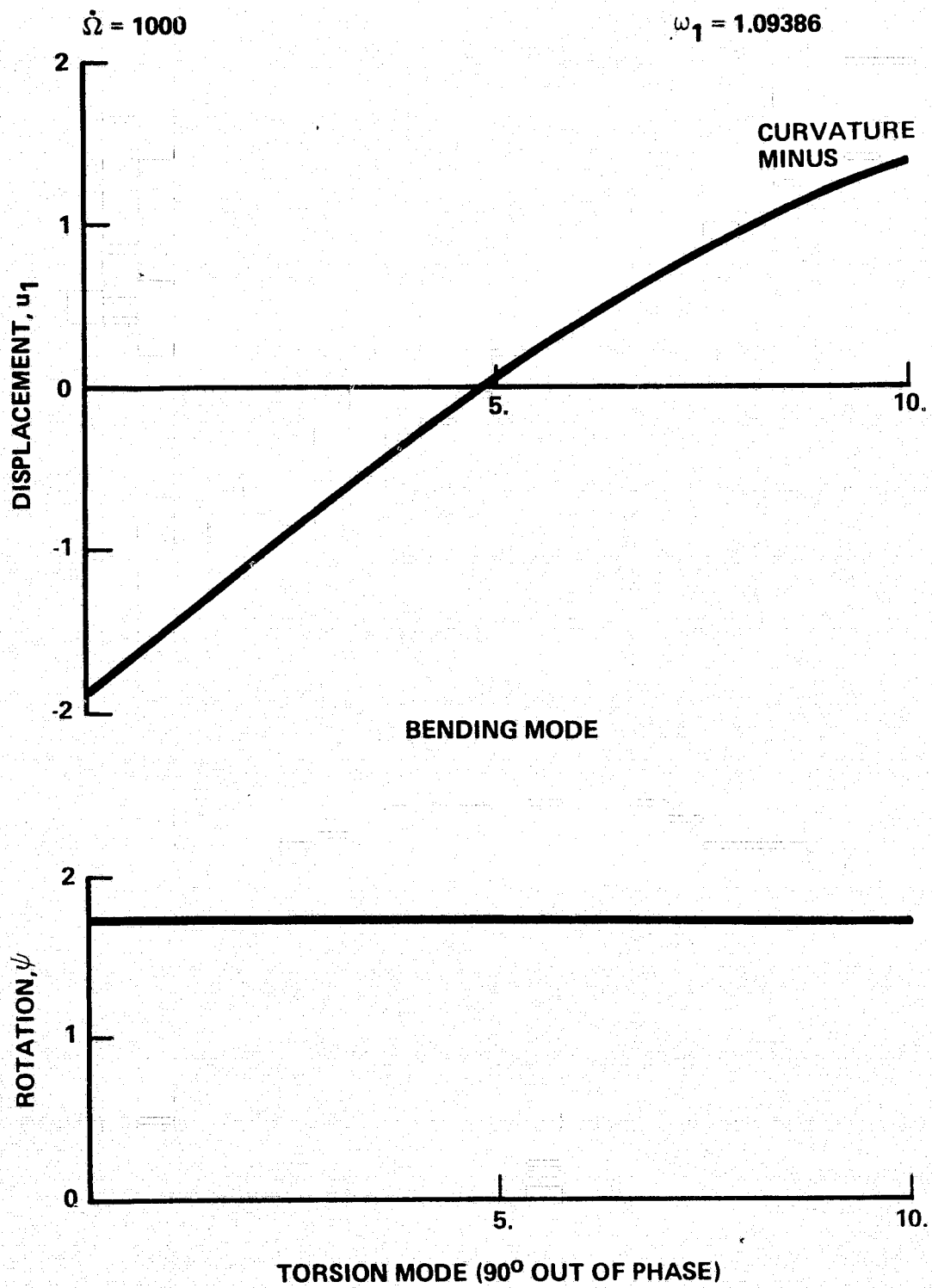


Figure 5.5. First Mode Shapes.

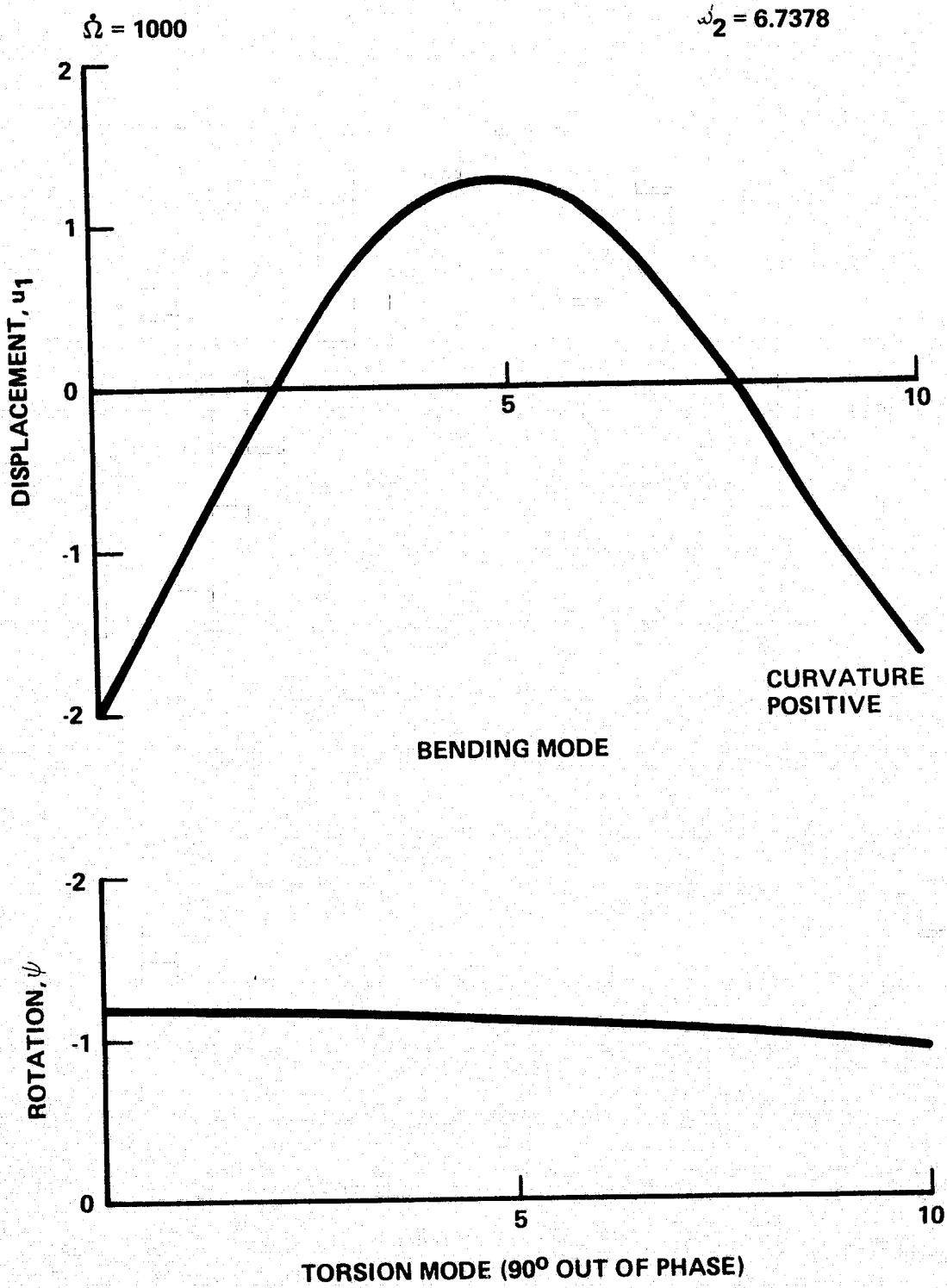


Figure 5.6. Second Mode Shapes.

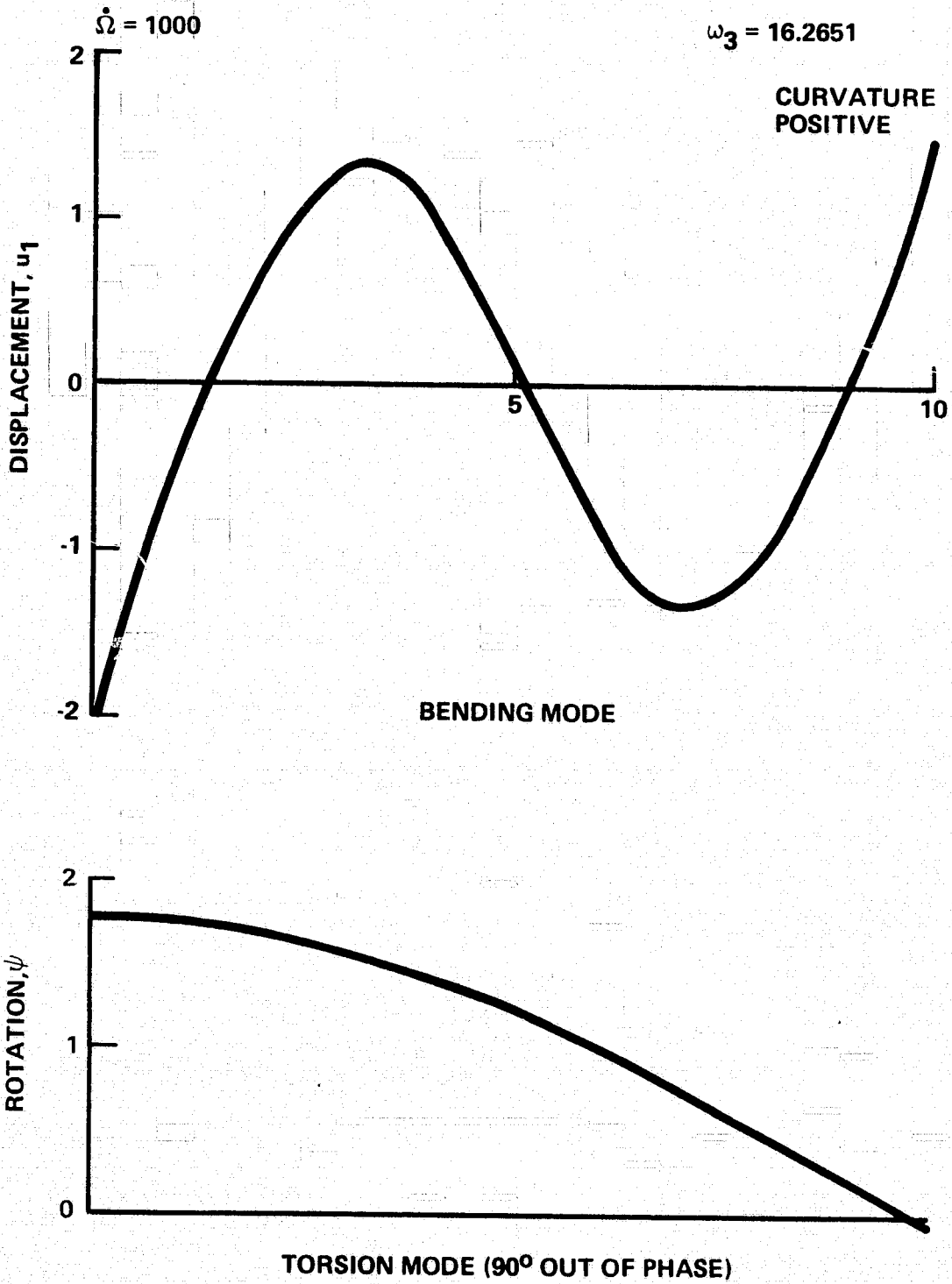


Figure 5.7. Third Mode Shapes.

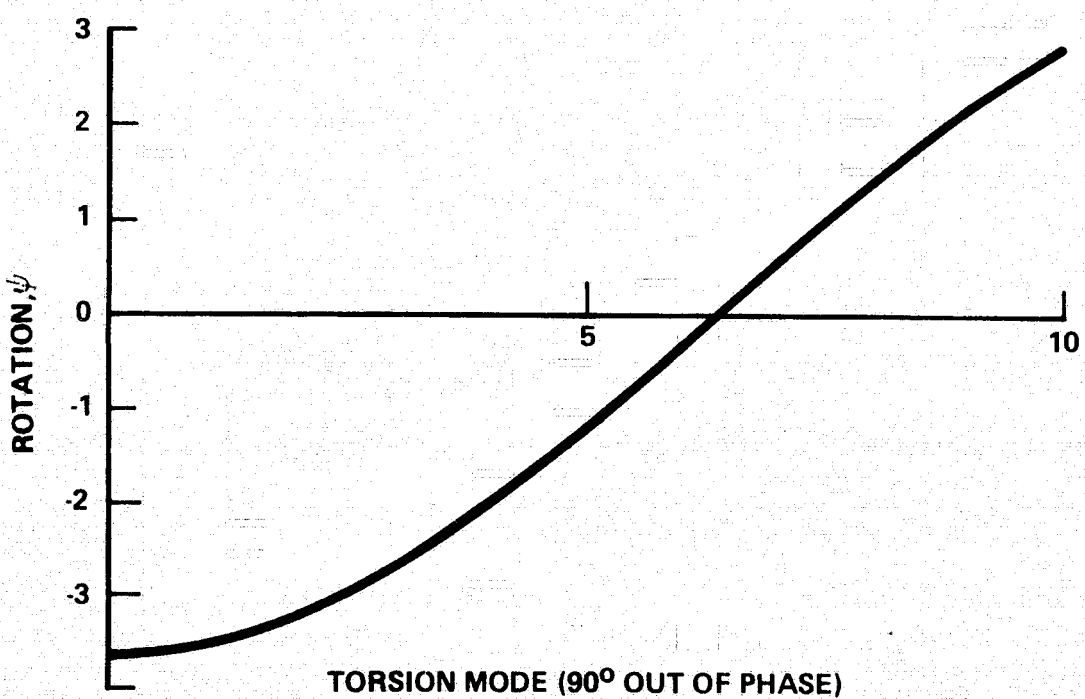
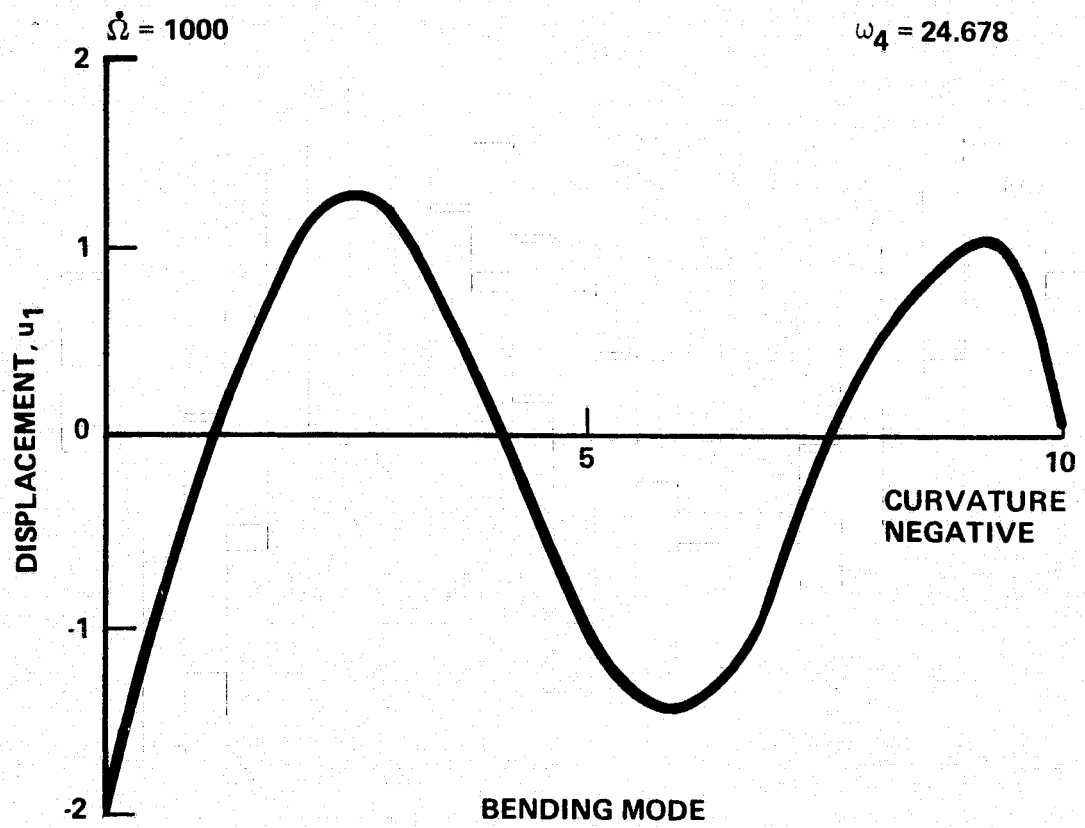


Figure 5.8. Fourth Mode Shapes.

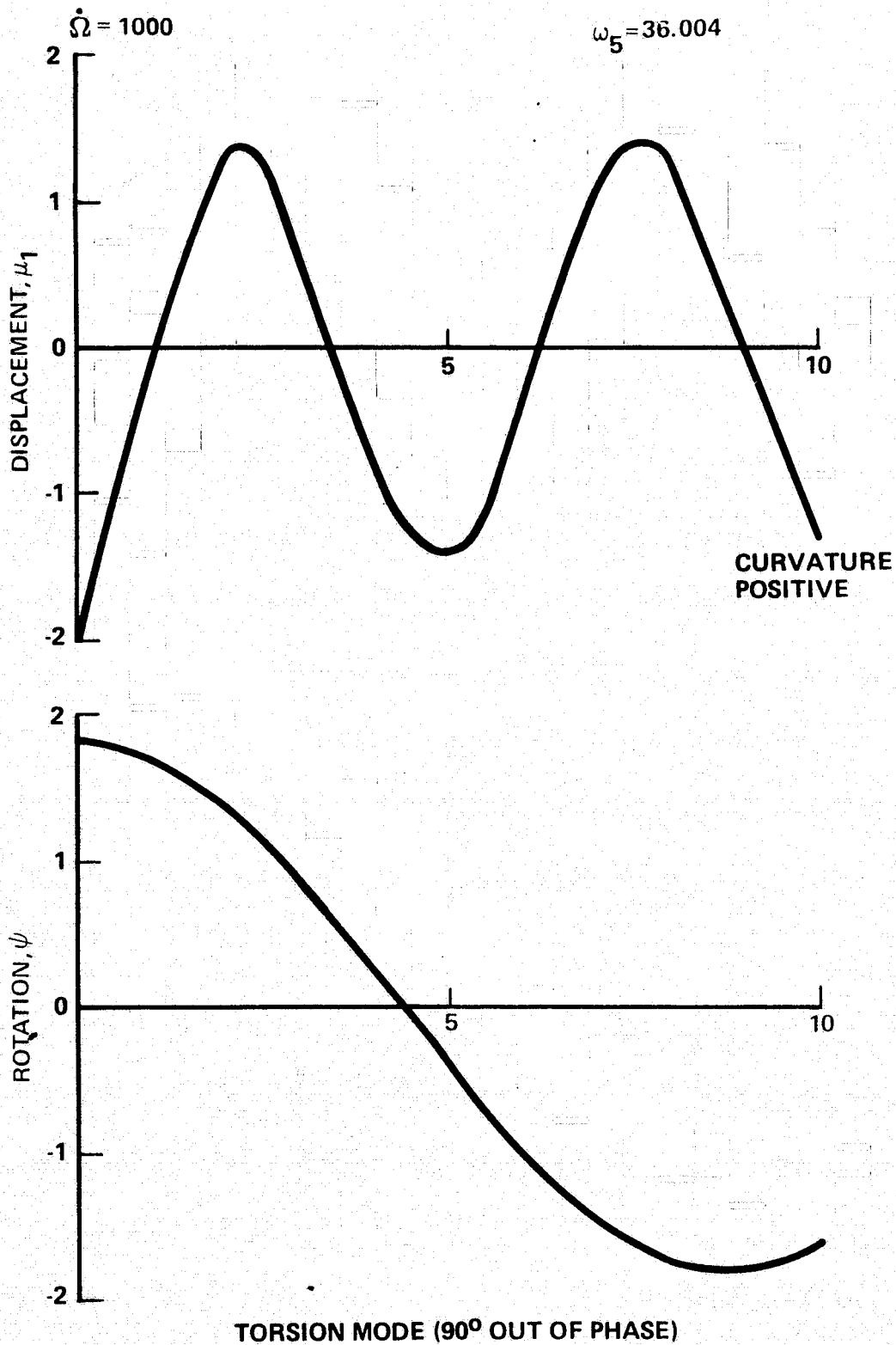


Figure 5.9. Fifth Mode Shapes.

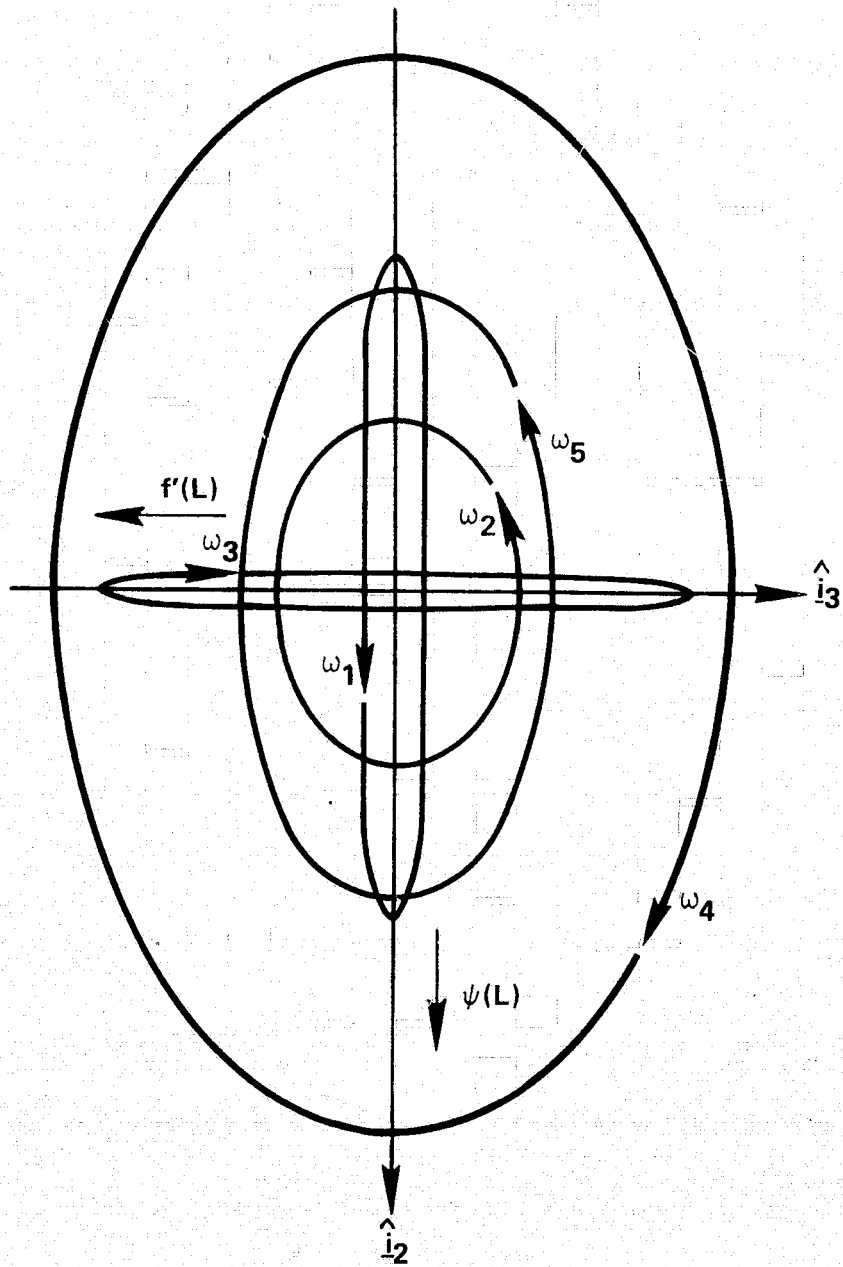


Figure 5.10. Motion of the Tip of the Rotor Shaft.

CHAPTER 6

NUMERICAL RESULTS FOR THE FINITE ELEMENT MODEL

6.1 Chapter Summary

This chapter presents a solution using numerical integration for the finite element model equations of motion. The physical system chosen for the example problem consists of a uniform beam with a constant speed, axisymmetric rotor mounted at the tip. This is the same system analyzed in the previous chapter which used a continuum approach that required the solution of the governing partial differential equations. The verification strategy consists of a comparison of the results of the numerical integration of the finite element equations of motion with the closed form solution attained by the continuum analysis. The initial conditions are calculated using the closed form solution and correspond to a system normal mode for the coupled in-plane bending and torsional motion.

The modal analysis is performed on the system with the rotor "frozen" (zero spin rate). In the construction of the mass and stiffness matrices, constraint relationships arise since each mass element of the beam has only three degrees of freedom. The constraint relationships are accommodated through the introduction of displacement compatibility matrices when the final matrices are assembled from their component parts. The stiffness matrix may also be calculated from the continuum strain energy expression by the adoption of finite differences. An eigenvalue analysis of the final mass and stiffness matrices produces a set of natural frequencies and real modes (eigenvectors).

The numerical integration is accomplished by a fourth-order Runge-Kutta algorithm. The only variables integrated are the Tisserand frame variables and the modal coordinates corresponding to the lowest nonzero frequencies for both in-plane bending and torsion. This represents a truncation of the number of coordinates from thirty to four (no out-of-plane motion is initiated). The results of the integration show good agreement with the closed form solutions. The chapter closes with a discussion of the truncation procedure. Emphasis is placed on the interrelation of the coordinates that results from gyroscopic coupling. Modes which are strongly coupled should be treated as a unit in the truncation procedure; that is, they should be kept as a group or truncated as a group.

6.2 Example Problem and Modal Analysis

This section will describe the physical system to be modeled and the constraint relationships involved. It will then construct the mass and stiffness matrices to be used in the modal analysis. The physical system is the same as the one described in Chapter 5. The difference here will be the method by which a mathematical model of the system is created. For the previous analysis, the system was modeled as a uniform continuum and partial differential equations with boundary conditions resulted. Ordinary differential equations were obtained by introducing a separation of variables. For the finite element model, ordinary differential equations are obtained directly by breaking the system into a number of discrete, finite elements.

To review the selection of parameters, the beam is 10 meters in length, 150 kg in mass and has a 1 meter square cross section. The

flexural rigidity, EI , is equal to $11820 \text{ kg-m}^3/\text{sec}^2$ and the torsional stiffness, GJ , is $25000 \text{ kg-m}^3/\text{sec}^2$. The rotor has a mass of 5.236 kg , a symmetric moment of inertia of $.2909 \text{ kg-m}^2$ and a transverse moment of inertia of $.5818 \text{ kg-m}^2$. The rotor spin speed is fixed at 10 radians per second.

The beam is divided into fifteen equal rigid bodies that are connected by massless beams as shown in Figure 6.1. Each rigid body has a mass of 10 kg and a moment of inertia about the third axis of 1.6667 kg-m^2 . The other moments of inertia are set to zero in order to eliminate rotary inertia effects. The system moments of inertia are 1262.8 , 1263.1 and 25.6 kg-m^2 about axes one, two and three respectively. Each massless beam has a length of two thirds of a meter.

We shall be concerned with the calculation of natural frequencies and mode shapes for in-plane bending and torsion. The plane mentioned here contains the rotor symmetric axis and the undeformed beam centroid. Torsion is about the beam centroid. If we consider in-plane motion first, we see that each rigid body will have three degrees of freedom; transverse displacement and longitudinal displacement of the center of mass and rotation about axis number two. The first constraint simply sets the longitudinal displacement to zero by assuming that the beam is inextensible. The second constraint relates the rotation to the transverse displacement. This is the same curvature constraint which was used in the continuum analysis (Equation (5.14)) and is derived in Appendix B.

$$\beta_2 = \frac{\partial u_1}{\partial z} \quad (6.1)$$

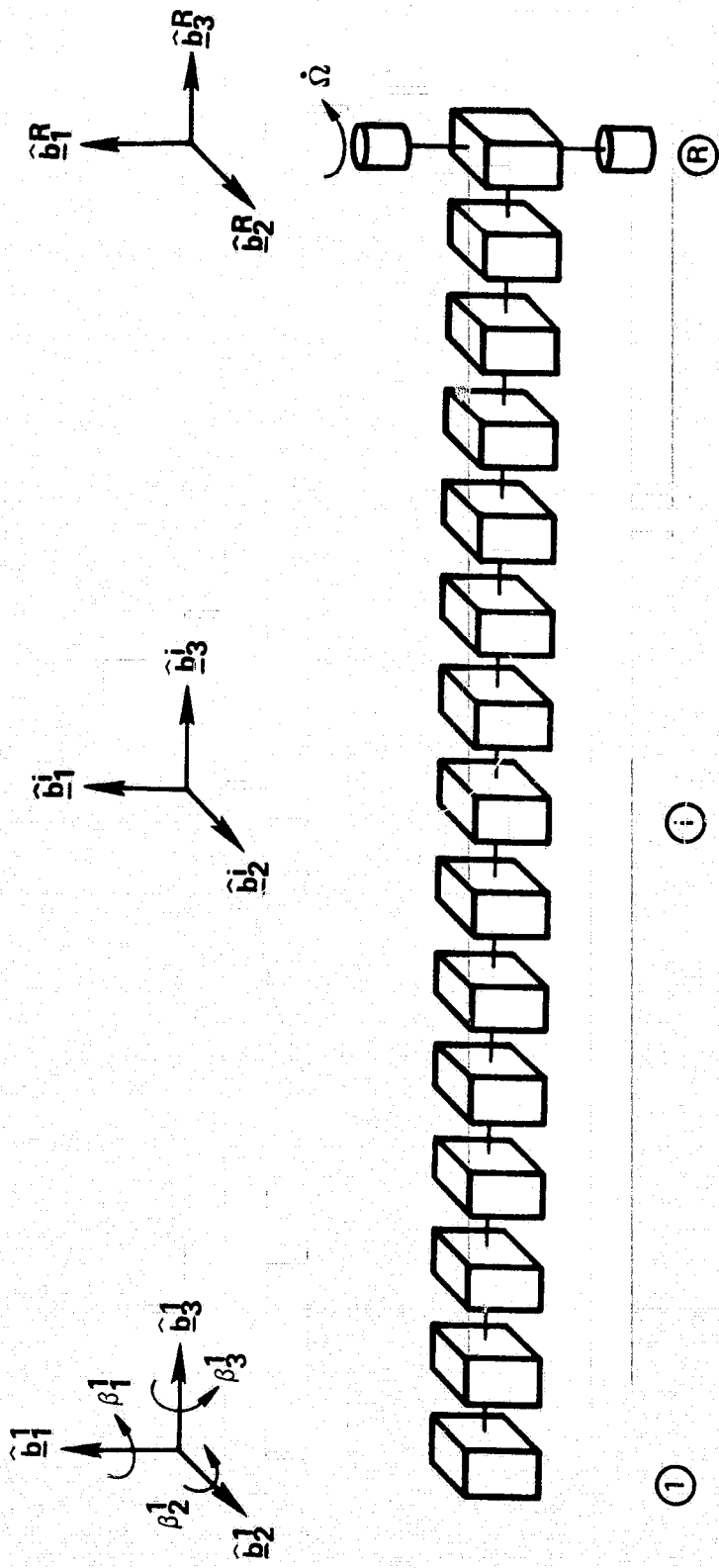


Figure 6.1. Finite Element Model

If this constraint is applied at the midpoint between rigid bodies and if the angle is taken to be the average value for the two neighboring bodies, the constraint relationships take the form

$$\frac{\beta_2^i + \beta_2^{i+1}}{2} = \frac{u_1^{i+1} - u_1^i}{\Delta z} \quad i = 1, \dots, n-1 \quad (6.2)$$

where Δz is the distance between body centers of mass and is here equal to two thirds of a meter. This relationship can be solved for u_1^{i+1} and yields

$$u_1^{i+1} = u_1^i + \frac{\Delta z}{2} (\beta_2^i + \beta_2^{i+1}) \quad i = 1, \dots, n-1 \quad (6.3)$$

This same result may be attained using a different perspective. Let the bodies be connected at the midpoints between them by a line hinge, then the requirement for compatible displacements at the hinge point will yield

$$u_1^i + \frac{\Delta z}{2} \beta_i = u_{i+1} - \frac{\Delta z}{2} \beta_{i+1} \quad i = 1, \dots, n-1 \quad (6.4)$$

where the rotations are assumed to be small. This will produce the same result (Equation (6.3)) as the curvature constraint. There are now (n-1) constraint relationships and they may be used to eliminate the variables u_1^2 through u_1^n . In matrix form, the constraint relationships may be expressed as

where guidance has been taken from Equation (4.38) and m_i is the mass of body i and I_T is the rotor transverse moment of inertia. The inertias of each body about axis number two have been set to zero in order to eliminate the rotary inertia effect. The final mass matrix has the form

$$[M'] = [C]^T [M] [C] \quad (6.8)$$

where $[M']$ is symmetric but is no longer diagonal. The stiffness matrix for in-plane bending is constructed from an assemblage of simple component matrices by using compatibility matrices. The simple component matrix is constructed for each massless beam by using assumed mode shapes. Each member of this matrix is found by evaluating the expression

$$k_{ij} = \int_0^{\ell} EI \phi_i'' \phi_j'' dx \quad (6.9)$$

The assumed mode shapes, ϕ_i , chosen here arise from a general third order polynomial that is forced in turn to represent unit displacements and rotations about each end of the beam. For unit displacement about the end at $x = 0$, the mode shape is

$$\phi_1(x) = 3\left(\frac{\ell-x}{\ell}\right)^2 - 2\left(\frac{\ell-x}{\ell}\right)^3 \quad (6.10)$$

For unit rotation about this end, the mode shape is

$$\phi_2(x) = x\left(\frac{\ell-x}{\ell}\right)^2 \quad (6.11)$$

For unit displacement about the end at $x = \ell$, the mode shape is

$$\phi_3 = 3\left(\frac{x}{\ell}\right)^2 - 2\left(\frac{x}{\ell}\right)^3 \quad (6.12)$$

Note that the structure of $[C']$ consists of $(n-1)$ four by four identity matrices with each one overlapping the last two columns of its predecessor. The final stiffness matrix may then be written in the form

$$[K'] = ([C'] [C])^T [K] [C'] [C] \quad (6.17)$$

A different perspective may be taken in order to derive the strain matrix. To do this, we start with the continuum expression for the strain energy

$$U = \frac{1}{2} \int_0^L EI \left(\frac{\partial^2 u_1}{\partial z^2} \right)^2 dz \quad (6.18)$$

where L is the length of the entire beam. Introducing the curvature constraint (Equation (6.1)) yields

$$U = \frac{1}{2} \int_0^L EI \left(\frac{\partial \beta_2}{\partial z} \right)^2 dz \quad (6.19)$$

This expression may now be evaluated using a finite difference approach. First the substitution is made

$$\frac{\partial \beta_2}{\partial z} = \frac{\beta_2^{i+1} - \beta_2^i}{\Delta z} \quad (6.20)$$

where Δz is the distance between mass centers. The strain energy may then be written

$$U = \frac{1}{2} \sum_{i=1}^{n-1} \frac{EI}{(\Delta z)^2} \left(\beta_2^{i+1} - \beta_2^i \right)^2 \quad (6.21)$$

Expressed in matrix form, the stiffness matrix, $[K_1]$, may be introduced

$$U = \frac{1}{2} \{\beta_2\}^T [K_1] \{\beta_2\} \quad (6.22)$$

where $\{\beta_2\}$ is the column matrix of rotations. In detail, the stiffness matrix has the structure

$$[K_1] = \frac{EI}{(\Delta z)^2} \begin{bmatrix} 1 & -1 & 0 & 0 & - & - & - & - & 0 \\ -1 & 2 & -1 & 0 & - & - & - & - & 0 \\ & & & - & - & - & & & \\ 0 & - & - & - & - & 0 & -1 & 2 & -1 \\ 0 & - & - & - & - & 0 & 0 & -1 & 1 \end{bmatrix} \quad (6.23)$$

An interesting result is that the strain energy does not involve the displacement u_1^1 . This means that the matrix $[K']$ found in Equation (6.17) must be singular; that is, it must possess a zero first row and column. The matrix multiplications indicated in Equation (6.17) were performed numerically and the stiffness matrix was found to be singular. The first row and column were found to be zero and the populated submatrix was equal to $[K_1]$ found in Equation (6.23). This zero row singularity will yield a zero eigenvalue which will correspond to the translational rigid body mode. Since the rank of $[K']$ is degenerate by 2 (two less than order of the matrix) another zero eigenvalue will be present and corresponds to the rotational rigid body mode.

The free-free modal analysis of the in-plane bending is performed by solving the eigenvalue problem

$$([K'] - \omega^2[M'])\{q'\} = \{0\} \quad (6.24)$$

The resulting eigenvectors $\{q_i^1\}$ for distinct natural frequencies are orthogonal since the mass and stiffness matrices are symmetric.

$$\{q_i^1\}^T [M'] \{q_j^1\} = 0 \quad \begin{array}{l} i \neq j \\ \omega_i \neq \omega_j \end{array} \quad (6.25)$$

If the eigenvectors are arranged by columns in a modal matrix $[\phi^1]$, and

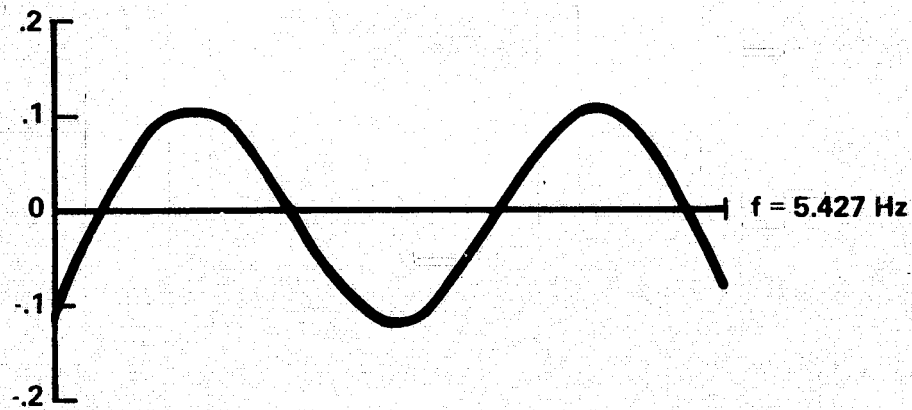
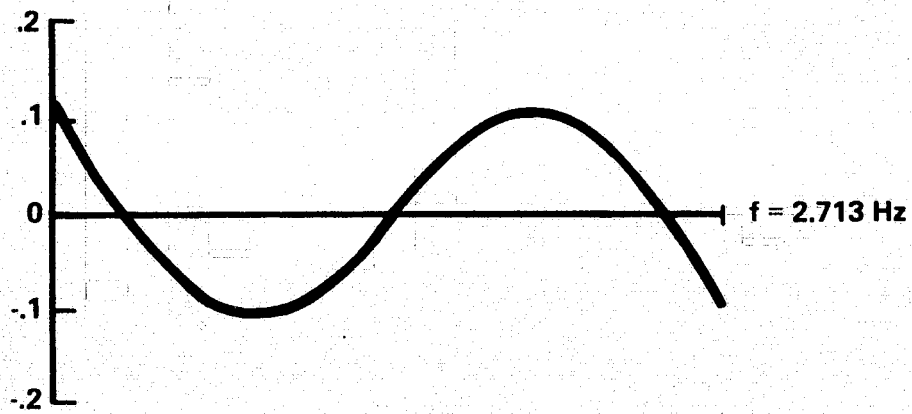
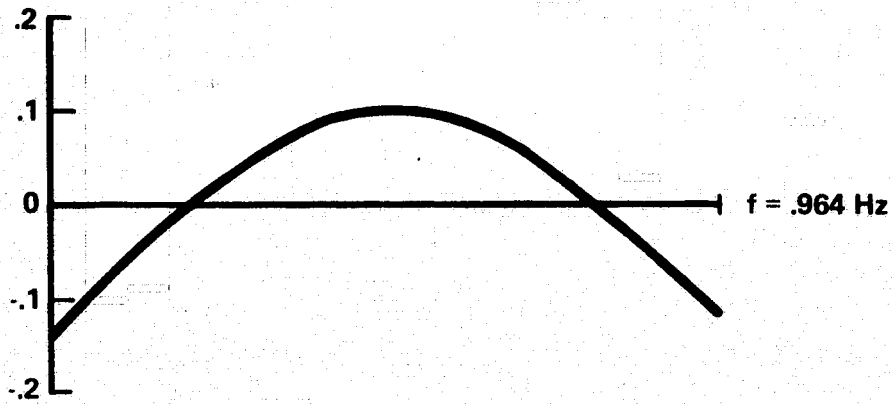


Figure 6.2. Bending Mode Shapes.

The strain energy may then be written

$$U = \frac{1}{2} \sum_{i=1}^{n-1} \frac{GJ}{(\Delta z)^2} \left(\beta_3^{i+1} - \beta_3^i \right)^2 \quad (6.31)$$

If we write the strain energy in matrix form, we introduce the stiffness matrix, $[K']$

$$U = \frac{1}{2} \{\beta_3\}^T [K'] \{\beta_3\} \quad (6.32)$$

where $\{\beta_3\}$ is the column matrix of rotations about axis three for all bodies. The structure of $[K']$ is

$$[K'] = \frac{GJ}{(\Delta z)^2} \begin{bmatrix} 1 & -1 & 0 & 0 & - & - & - & - & 0 \\ -1 & 2 & -1 & 0 & - & - & - & - & 0 \\ & & & \vdots & & & & & \\ 0 & - & - & - & 0 & -1 & 2 & -1 & \\ 0 & - & - & - & 0 & 0 & -1 & 1 & \end{bmatrix} \quad (6.33)$$

It is now possible to proceed with the free-free modal analysis of the torsional motion by solving the eigenvalue problem

$$([K'] - \omega^2 [M']) \{\beta_3\} = \{0\} \quad (6.34)$$

The modal matrix, $[\phi]$, is formed by the eigenvectors arranged in columns and is normalized to obey the relation

$$[\phi]^T [M'] [\phi] = [E] \quad (6.35)$$

The first three nonzero modes are shown in Figure 6.3. One rigid body mode corresponding to uniform rotation about axis three is present.

The modal analyses is now complete. The real mode shapes and natural frequencies for in-plane bending and torsion found here may be

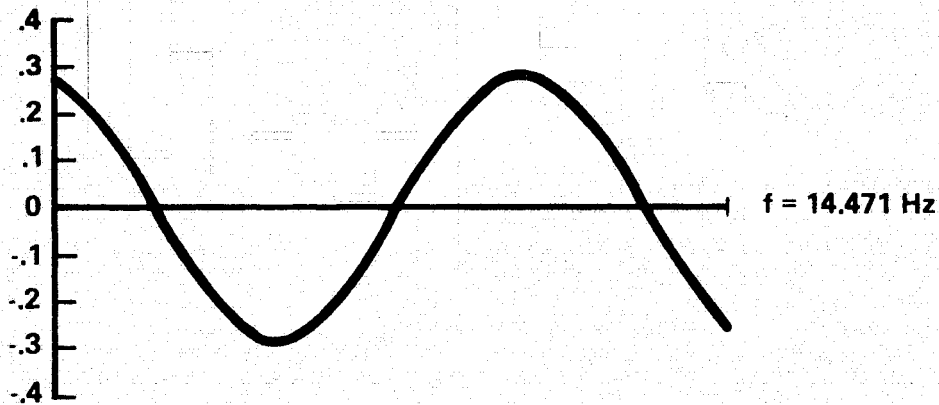
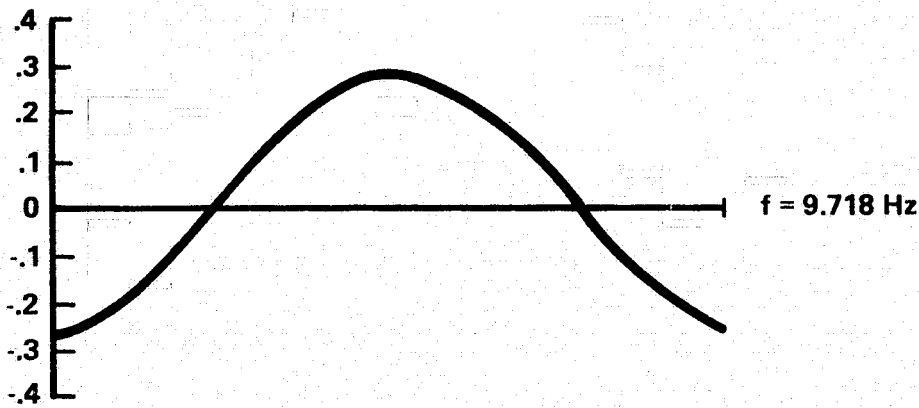
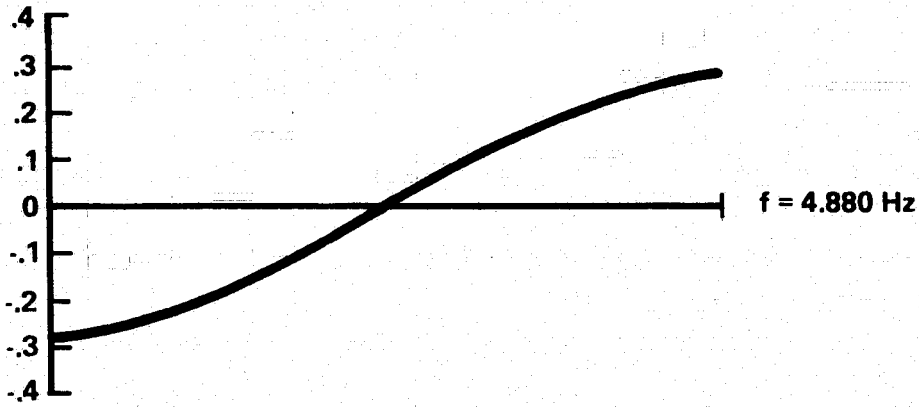


Figure 6.3. Torsion Mode Shapes.

used in the finite element model equations of motion. The next step is the actual integration of the equations of motion.

6.3 Numerical Integration and Truncation Procedure

This section presents the results of a numerical integration of the finite element model equations of motion for a system with a constant spin rate. The initial conditions chosen for the integration correspond to a system normal mode and should therefore produce periodic motion. The initial conditions (Figure 6.4) were calculated using the closed form solutions resulting from the continuum analysis of the previous chapter.

The initial modal coordinates and velocities are calculated using the inverse modal matrix. This may be represented in a very simple form due to the normalized orthogonality condition (Equation (4.47))

$$([\phi]^T[M])[\phi] = [E] \quad (6.36)$$

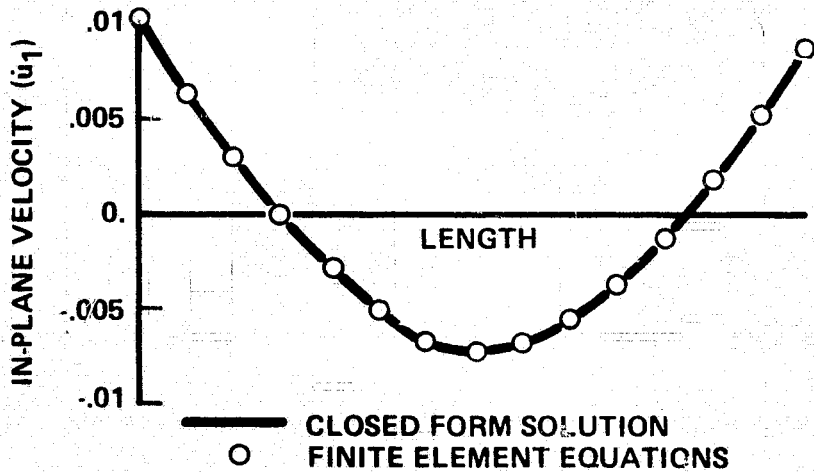
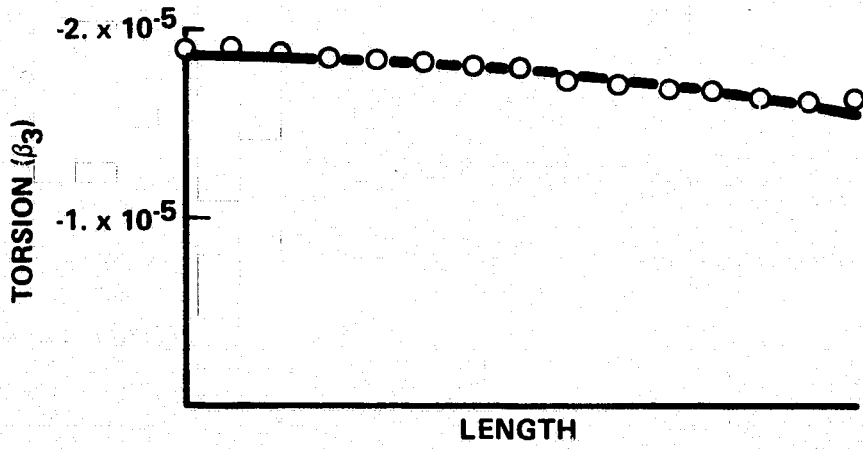
This then requires that the first two matrices in parentheses be equal to the inverse modal matrix

$$[\phi]^{-1} = [\phi]^T[M] \quad (6.37)$$

The initial modal coordinates are then

$$\begin{aligned} \{\eta\}_{t=0} &= [\phi]^T[M]\{q\}_{t=0} \\ \{\dot{\eta}\}_{t=0} &= [\phi]^T[M]\{\dot{q}\}_{t=0} \end{aligned} \quad (6.38)$$

The resulting initial modal coordinates and velocities corresponding to nonzero frequency modes are shown in Table 6.1. The initial Tisserand frame variables are simply the weighted mean values of the initial angular variables. The initial θ_3 value is $-.17515 \text{ E-}4$, the initial $\dot{\theta}_2$



$\dot{\beta}_3$ AND u_1 ARE ZERO

Figure 6.4. Initial Conditions.

TABLE 6.1

INITIAL MODAL COORDINATES AND VELOCITIES

Torsion		In Plane Bending	
Natural Frequency (Hz)	Modal Coordinate	Natural Frequency (Hz)	Modal Velocity
4.880	.47711837 E-5	0.964	-.72829664 E-1
9.718	-.11208203 E-5	2.713	-.36030891 E-3
14.471	-.47018966 E-6	5.427	-.15179138 E-3
19.091	-.24678593 E-6	9.165	.39719278 E-4
23.527	-.14601846 E-6	14.023	.32309908 E-4
27.727	-.92882146 E-7	20.138	.78941230 E-5
31.641	-.62197614 E-7	27.741	.14494639 E-4
35.218	.43088221 E-7	37.273	-.60349703 E-5
38.415	.30428964 E-7	49.649	.33760443 E-5
41.190	-.21900632 E-7	66.720	-.56705903 E-5
43.511	-.15267688 E-7	92.398	.44775661 E-5
45.346	.10585609 E-7	136.712	.23686443 E-5
46.673	-.64728738 E-8	236.365	-.69689122 E-7
47.477	-.31017748 E-8	723.839	-.13253566 E-5

value is $-.17337 \text{ E-3}$, the remaining Tisserand frame values are initially zero.

An examination of the initial modal coordinates and velocities will show that the mode shape represented in Figure 6.4 is dominated by the first in-plane bending mode (.964 Hz) and by the Tisserand frame variable, θ_3 , representing uniform rotation about axis number three (corresponding to the torsional rigid body modes). The first torsional mode (4.880 Hz) is also used in order to provide a variation of torsional rotation along the length of the beam. The numerical simulation will be performed for the Tisserand frame variables and the lowest frequency bending and torsion modes. This represents a truncation of the remaining twenty six coordinates.

The integration was performed by a fourth-order Runge-Kutta algorithm with a step size of .01 seconds. The integration time span was set equal to 1.06 seconds, the period of the normal mode used for the initial conditions.

The first aspect of the results of the numerical integration to be examined is the simulation of the natural frequency of the normal mode. The times corresponding to the quarter cycle points are shown in Table 6.2. For the closed form solution, the bending and torsion have equal natural frequencies, but for the numerical integration, u_1 and β_3 have unequal natural frequencies. The in-plane bending is well behaved and has a period of 1.04 seconds. The torsional motion, β_3 , follows the periodic motion less precisely. A comparison of the displacements is shown for the quarter cycle points in Figures 6.5 to 6.8. Again, the in-plane bending shows very excellent agreement, while the agreement for

TABLE 6.2

COMPARISON OF NATURAL FREQUENCIES

$\omega_n t$ (degrees)	Times of Occurrence (seconds)		
	Closed Form	Numerical Integration	
	Solution	u_1	β_3
0	0.0	0.0	0.0
90	0.27	0.26	0.27
180	0.53	0.52	0.50
270	0.80	0.78	0.72
360	1.06	1.04	> 1.06

torsion is not as precise. It is important to note, however, that the magnitude of the torsional motion is very small, and the imprecision does not result in a great error in the position of each finite element. The last aspect of the numerical integration to be examined is the motion of the tip of the rotor shaft. As shown in Figure 6.9, the rotor shaft follows the correct path as determined from the closed form solution with only a small imprecision.

The agreement of the numerical integration results with the closed form solution is good. The deviations which do exist are small and may be attributed to three sources. First there is the difference in the mathematical models used; a continuum analysis should agree with a finite element analysis only in the limit. For a small number of bodies, as chosen here, a difference in results will occur. The second source is the truncation procedure. The number of coordinates was reduced from thirty to four. The truncation alters the angular momentum of the

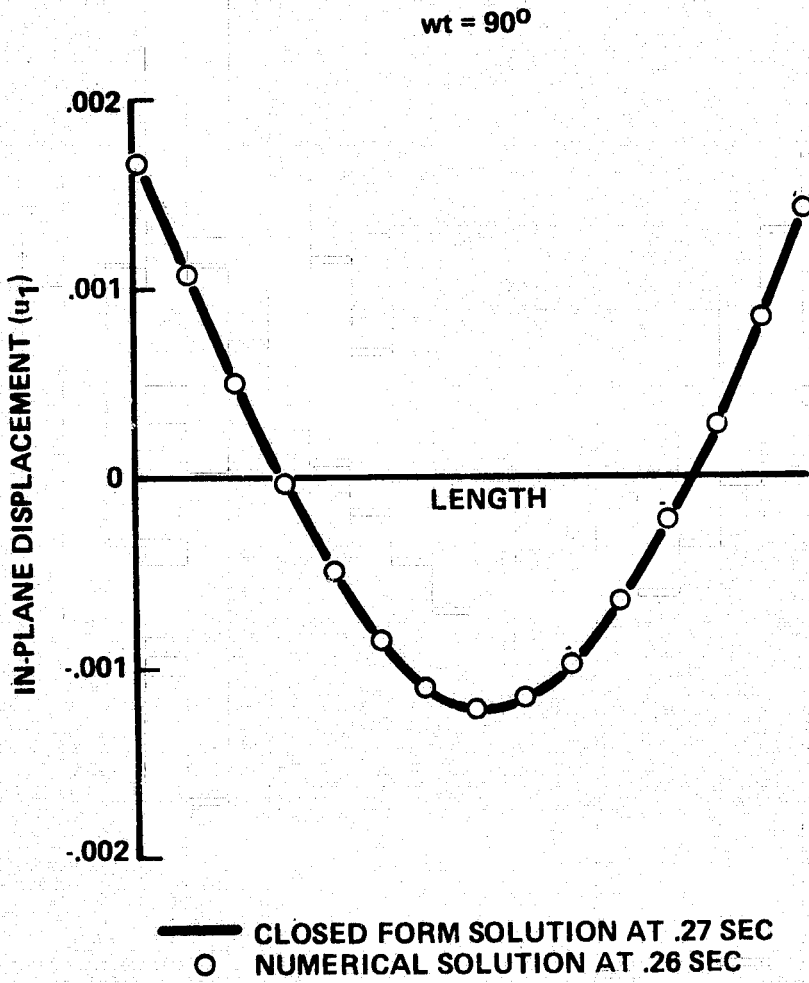


Figure 6.5. Numerical Results at Quarter Period Point

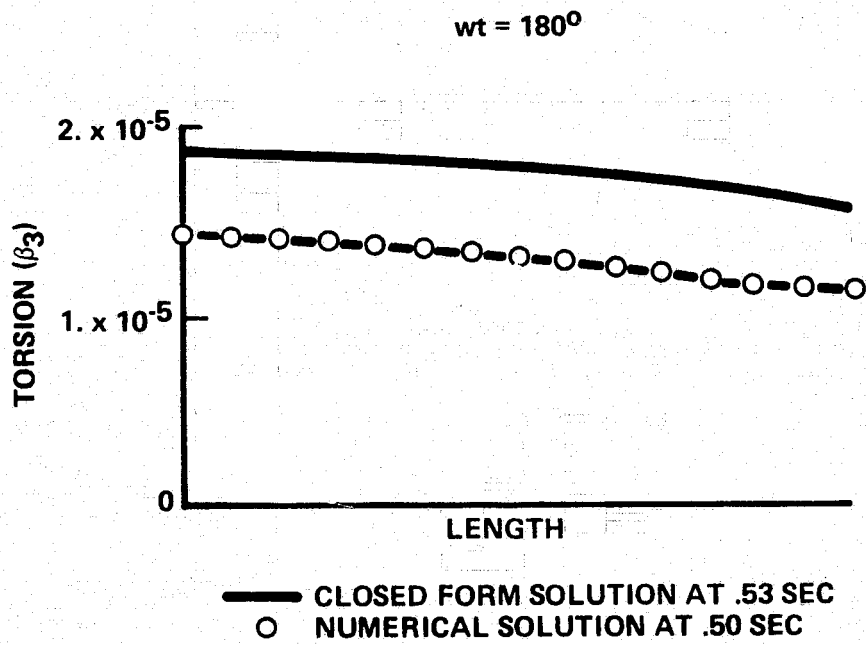


Figure 6.6. Numerical Results at Half Period Point.

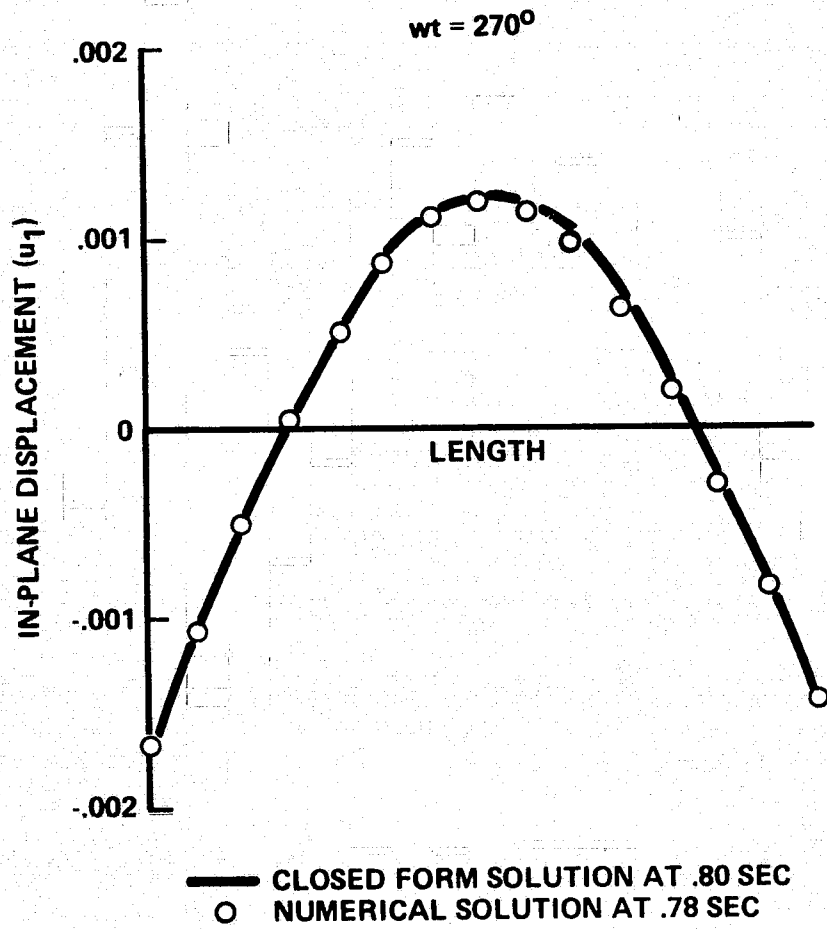


Figure 6.7. Numerical Results at Three Quarter Period Point.

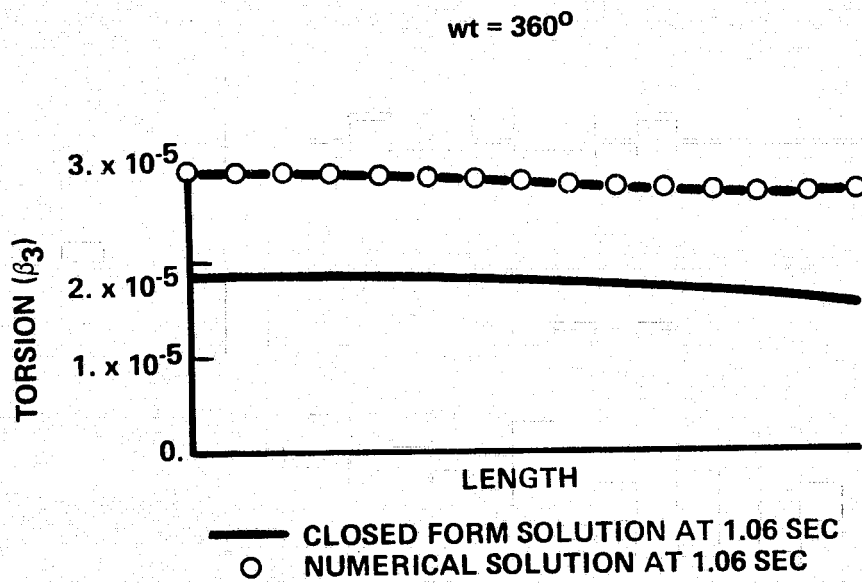


Figure 6.8. Numerical Results at One Period Point.

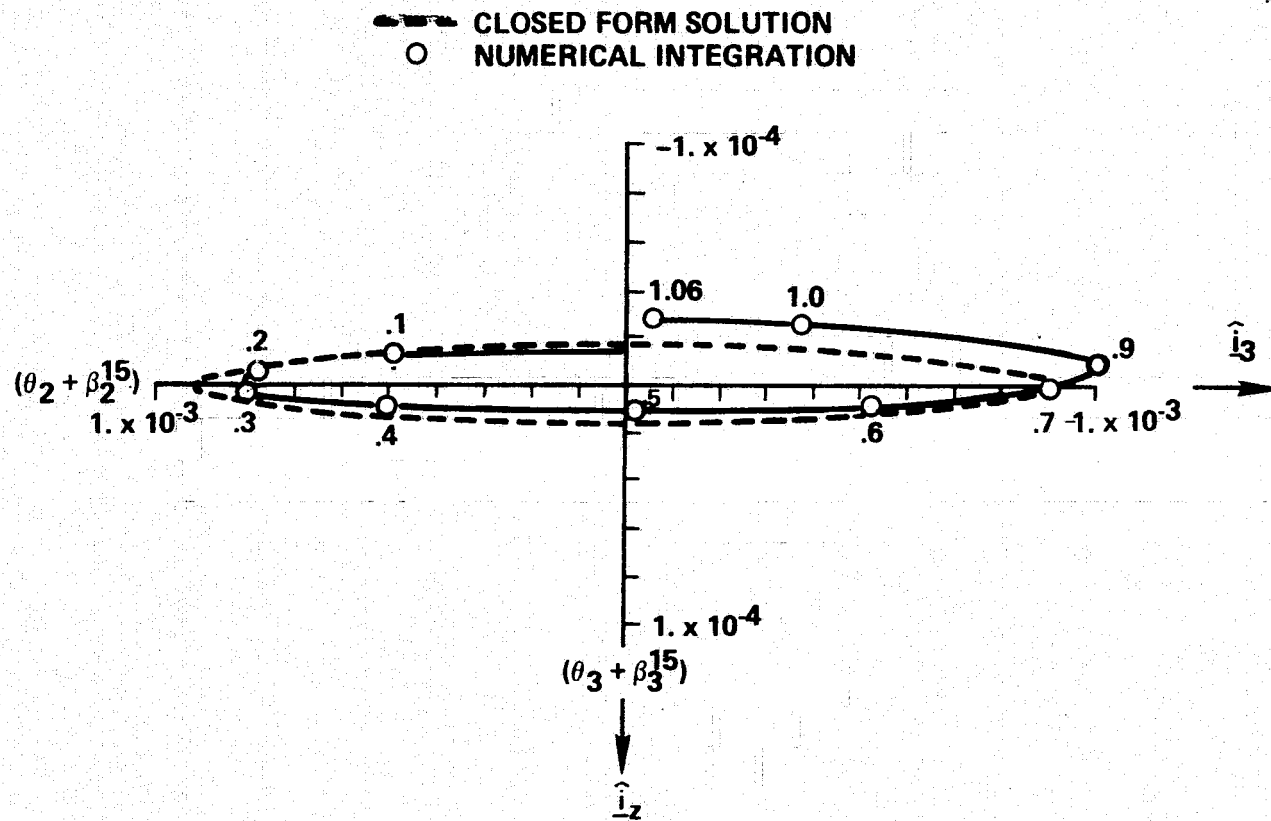


Figure 6.9. Motion of the Tip of the Rotor Shaft.

system, which probably causes the shift of the center of the locus of the tip of the rotor shaft seen in Figure 6.9. The computational ease of integrating the truncated set of finite element equations of motion is one of the main advantages of the formulation. In fact, if the number of modes is increased, not only do the computations become more numerous, but they also experience numerical difficulties arising from small differences of large numbers. The third source is a small difference in the mounting location of the rotor shaft. For the continuum analysis, the rotor is mounted at the tip, at $L = 10$ m. In order to collocate the centers of mass of the rotor and the last rigid body, the rotor shaft is mounted at $L = 9.333$ m, in the finite element model.

For this numerical example, the truncation was performed in an ad hoc manner by examining the initial modal coordinates. A more formal procedure would necessitate the examination of the modal gyroscopic coupling matrix, $\phi^T G \phi$. The structure of the coupling matrix would indicate which modes were strongly coupled for the case at hand. Strongly coupled modes correspond to components of a complex mode shape. They must be truncated or incorporated in the system of equations as a unit. Partial truncation of strongly coupled modes would introduce unnecessary truncation errors. A further point concerns the analysis of the sensitivity of vibrations to excitation sources. True natural frequencies of the system are to be avoided or somehow compensated for by the control system. It is important to realize that the natural frequencies present in the equations of motion are not the true system natural frequencies when the rotor spin rates are nonzero. For nearly constant spin rates, the true natural frequencies correspond to the

complex mode shapes. If the spin rates vary greatly, a range of natural frequencies would have to be included in the analysis of the effects of excitation sources. An example of this behavior was given in the previous chapter in Figures 5.3 and 5.4. The relationship between complex modes and real modes must then be made by identifying the dominant terms when the components of a complex mode are expressed as linear combinations of real modes. It is obvious that the truncation procedure for the finite element model equations of motion will be complicated for true spacecraft systems. The above must certainly be expanded upon by further investigation.

This completes the numerical investigation of the finite element equations of motion. The principal conclusion is that it is possible to represent the behavior of a complex normal mode by a set of real modes in a coupled set of equations of motion.

CHAPTER 7

SUMMARY, CONTRIBUTIONS AND FUTURE WORK

This chapter will tie together the results of the previous work and present conclusions. This dissertation attempted to deal with the problems presented by the next generation of spacecraft. We are entering a new period in the analysis of the effects of spacecraft flexibility. Until now, the effects of flexibility for real spacecraft systems have consisted mainly of those produced by flexible appendages attached to central rigid bodies. This research addresses the more general case where the structural flexibility is distributed throughout the body. The problem is significantly complicated by the presence in the system of momentum exchange controllers.

The first part of the dissertation consists of a detailed investigation of floating reference frames. These frames are defined in such a way that they somehow follow the overall motion of the body. When deformations are expanded relative to these frames, they are small. This makes a first order vibration analysis possible and thereby yields a significant advantage. One possible drawback to their use is the introduction of the constraint relationships which define their motion. An investigation is made of the constraint relationship which defines a floating frame by setting to zero the linear and angular momentum relative to the frame. This is the Tisserand frame, named after a nineteenth century French astronomer. A special case of this frame is found which uses the free-free modes of the unconstrained system, and which satisfies the constraint relationship if the rigid body modal coordinates are simply set to zero. Since the remaining modal

coordinates are independent due to properties of their mode shapes, it is called the Mode Shape Constraint. It is possible to expand these ideas to cover a deformable body containing spinning rigid rotors by defining a Modified Tisserand Constraint.

The main body of the dissertation deals with the formulation of equations of motion for spacecraft with distributed flexibility and momentum exchange controllers. We are interested in addressing the coupled structure-actuator dynamics. The control variables for these systems would be the rotor spin speeds. For the specific application studied, the rotor torques must formally be treated as small, first order quantities. For engineering systems, it may be possible to relax this requirement, and the rotor spin speeds will then vary greatly. If complex mode shapes, for which the eigenvectors are complex numbers, were used in the formal analysis, the resulting equations of motion would not include the spin speeds of the rotor as explicit functions. Any relaxation of the first-order torque requirement would probably require the staging of complex modes for different ranges of spin speeds.

The technique developed here uses the real modes of the unconstrained system where the rotors have been "frozen", that is, they have zero spin rates. The resulting derivation requires that the modal coordinates are coupled, but it is possible to truncate the system to a smaller number of coordinates and still achieve accurate results.

A main advantage of the final set of equations of motion is that the control variables, the rotor spin speeds, appear as explicit terms in the equations. The Modified Tisserand Constraint is used in the formulation in order to provide an example of its properties. The

Modified Tisserand frame may also make it easier to relax the constraint that rotor torques are small, first order quantities.

Considerable attention is paid to developing physical insight into system behavior and the numerical verification of results. A continuum analysis is used to formulate closed form solutions for a simple example system consisting of a uniform beam with a nearly constant speed, axisymmetric rotor mounted at the tip. The governing partial differential equations and boundary conditions are obtained in a unified, systematic fashion by the application of Hamilton's Principle. Closed form solutions are obtained through the use of generalized techniques for the separation of variables. For a specific choice of parameters and a constant spin speed, system normal modes are calculated. The rotor shaft is found to cone with a sinusoidally varying cone angle.

The numerical verification technique of the finite element equations of motion also uses this simple physical system. After the real mode shapes have been calculated for the system with a "frozen" rotor, the initial conditions are chosen with the aid of the closed form solutions so that they produce a periodic system normal mode. The truncated equations of motion are integrated numerically for one period and the results compare well with those predicted by the continuum analysis.

The research undertaken in the dissertation has contributed to the understanding and solution of an engineering problem of current interest. Specifically, the contributions of the dissertation are:

1. Formulated a set of finite element equations of motion suitable for the analysis of spacecraft with distributed flexibility and momentum exchange controllers. A significant advantage of this

formulation is that the control parameters (rotor spin speeds) appear explicitly in the equations, and that the coordinates can be truncated.

2. Gained insight into the physical behavior of this class of dynamical system by obtaining closed form solutions using a continuum analysis.
3. Expanded the understanding and usage of the floating Tisserand reference frame. Made it possible to bring the advantages of a rigorous first order vibration analysis to a system experiencing large rotations.

It seems appropriate that this dissertation should close with an enumeration of work still left to be done. It seems to be in the nature of things that each answer only necessitates further questions. The areas of future research connected with this dissertation are:

1. Control system analysis of the finite element equations of motion. This is a rich field for future work and involves the assessment of questions of stability, observability and controllability. Specifically, questions of where to put sensors and actuators, and how many are needed, will have to be answered. Transfer functions should also be developed.
2. A method of synthetic modes should be developed in order to compensate for the error in system angular momentum caused by truncation.
3. The finite element equations of motion could be formally extended to cover large rotor torques and large rotations of the Tisserand frame. This could aid in assessing the possibility of relaxing the first order torque requirement

for the simpler system of equations presented in Chapter four.

4. Further analysis of the truncation procedure. Formal procedures need to be developed by expanding on the ideas presented here. Sensitivity of the model accuracy to truncation needs to be assessed.
5. The class of dynamical systems covered could be expanded. One extension would involve the addition of an articulated member to the system.

BIBLIOGRAPHY

1. Abell, George O., Exploration of the Universe, 2nd ed., Holt, Rinehart and Winston, New York, 1969.
2. Ashley, Holt, "Observations on the Dynamic Behavior of Large Flexible Bodies in Orbit," AIAA J., Vol. 5, pp. 460-469, March 1967.
3. Buckens, F., "The Influence of Elastic Components on the Attitude Stability of a Satellite," Proceedings of the Fifth International Symposium on Space Technology and Science, Tokyo, 1963, AGNE Publishers, Inc., Tokyo, 1964, pp. 193-203.
4. Darwin, George H., Scientific Papers, Vol. 3, Cambridge University Press, Cambridge, England, 1910.
5. Grote, D.B., J.C. McMunn, and R. Gluck, "Equations of Motion of Flexible Spacecraft," J. Spacecraft and Rockets, Vol. 8, pp. 561-567, 1971.
6. Gylden, H., "Recherches sur Rotation de la Terre," Actes de la Société Royale des Sciences d' Upsal, 3^e série, Tome VIII, 1871.
7. Hooker, W.W., "A Set of r Dynamical Attitude Equations for an Arbitrary n-Body Satellite Having r Rotational Degrees of Freedom," AIAA J., Vol. 8, pp. 1205-1207, 1970.
8. Hooker, W.W. and G. Margulies, "The Dynamical Attitude Equations for an n-Body Satellite," J. Astronaut. Sci., Vol. 12, pp. 123-128, 1965.
9. Hurty, Walter C. and Moshe F. Rubinstein, Dynamics of Structures, Prentice-Hall, Englewood Cliffs, New Jersey, 1964.
10. Jeffreys, Harold, The Earth, 3rd ed., Cambridge University Press, Cambridge, England, 1952.
11. Likins, P.W., "Analytical Dynamics and Nonrigid Spacecraft Simulation," Jet Propulsion Laboratory, Pasadena, California, Technical Report 32-1593, July 15, 1974.
12. Likins, P.W., "Dynamics and Control of Flexible Space Vehicles, Revision 1," Jet Propulsion Laboratory, Pasadena, California, Technical Report 32-1329, January 15, 1970.
13. Likins, P.W., Elements of Engineering Mechanics, McGraw-Hill, New York, 1973.
14. Meirovitch, Leonard, Analytic Methods in Vibration, Macmillan, New York, 1967.

15. Meirovitch, Leonard, Methods of Analytic Dynamics, McGraw-Hill, New York, 1970.
16. Milne, R.D., "Some Remarks on the Dynamics of Deformable Bodies," AIAA J., Vol. 6, No. 3, pp. 556-558, March 1968.
17. Mindlin, R.D. and L.E. Goodman, "Beam Vibrations with Time-Dependent Boundary Conditions," Journal of Applied Mechanics, Vol. 75, pp. 377-380, December 1950.
18. Munk, W.H. and G.J.F. MacDonald, The Earth, a Geophysical Discussion, Cambridge University Press, Cambridge, England, 1960.
19. Thompson, William T., Vibration Theory and Applications, Prentice-Hall, Englewood Cliffs, New Jersey, 1965.
20. Tisserand, F., Traité de Mécanique Céleste, Vol. 2, Gauthier-Villars, Paris, 1889.
21. Whitaker, E.T., A Treatise on the Analytical Dynamics of Particles and Rigid Bodies, Fourth Ed., Cambridge University Press, Cambridge, England, 1970.

APPENDIX A
NOMENCLATURE

		<u>Ref. Eq.</u>
a_j	Constraint relationship coefficients for a Pfaffian constraint	(2.18)
B^i	Body i in the finite element model	(4.7)
$\{\hat{b}\}$	Vector basis fixed in the mass element locally attached frame. Commonly at the rotor mounting point	
[C]	Compatibility matrix	(6.6)
c_i	Constant	(5.54)
D_i	Constant	(5.42)
dA	Beam cross section normal to centroid	(5.5)
EI	Beam flexural rigidity	(5.19)
{F}	Forcing matrix	(4.37)
f	Spatial variable for in-plane bending	(5.41)
$\{\hat{f}\}$	Vector basis fixed in the system floating frame commonly the Tisserand frame	
f_B	Bending fundamental frequency	(5.69)
f_T	Torsion fundamental frequency	(5.69)
[G]	Gyroscopic matrix, skew symmetric	(4.37)
GJ	Beam torsional stiffness	(5.19)
g	Spatial variable for out-of-plane bending	(5.35)
\underline{H}	System angular momentum	(2.1)
\underline{H}_R	Rotor angular momentum	(4.17)
h	Spatial variable for torsion	(5.41)
\square	System inertia dyadic about system center of mass	(2.3)

		<u>Ref. Eq.</u>
\square_D	Deformable body inertia dyadic about the system center of mass	(3.32)
\square_R	Rotor inertia dyadic relative to rotor center of mass	(3.33)
\square_R^S	Rotor inertia dyadic about the system center of mass	(3.33)
I_P	Polar mass moment of inertia per unit length length	(5.9)
I_S	Rotor symmetric axis principal moment of inertia	(5.16)
I_T	Rotor transverse axis principal moment of inertia	(5.16)
I_{11}, I_{22}, I_{33}	Moments of inertia of the undeformed system	(3.22)
I_{12}, I_{13}, I_{23} I_{21}, I_{31}, I_{32}	Products of inertia of the undeformed system	(3.22)
$[I]$	System inertia matrix	(4.34)
$[I^i]$	Inertia matrix of body i	(4.14)
$[I^R]$	Inertia matrix of body to which the rotor is attached	(4.34)
$[I_R]$	Inertia matrix of the rotor	(4.14)
$\{\hat{i}\}$	Vector basis fixed in inertial reference system	
$[K]$	Stiffness matrix-symmetric	(4.36)
\mathcal{L}	Lagrangian of the system	(5.1)
L	Beam length	(5.23)
$\{L\}$	Lagrange multiplier coefficient matrix	(4.37)
l_1	Distance between beam free end and system center of mass	(5.20)
l_2	Distance between rotor mounting point and system center of mass	(5.20)
\mathcal{M}	System mass	(3.14)
$[M]$	Mass matrix-symmetric	(4.37)

		<u>Ref Eq.</u>
M_R	Rotor mass	(3.33)
m	Mass per unit length for a beam	(5.9)
\underline{p}	Location of a beam mass element in the plane normal to the centroid	(5.4)
$(p_1, p_2, 0)$	Scalar components of \underline{p} in the beams locally attached coordinate system with the origin at the centroid	(5.6)
$\{Q\}$	Matrix of generalized forces	(4.36)
Q_k	Generalized force corresponding to generalized coordinate k .	(4.26)
$\{q\}$	Matrix of displacement and rotation coordinates	(4.35)
$[R]$	Discrete coordinate coupling matrix	(4.37)
R_1, R_2	Constants	(5.68)
\underline{r}	Location of the beam centroid relative to the system center of mass	(5.4)
\underline{r}_c	Location of the deformable body center of mass relative to the system center of mass	(3.44)
\underline{r}^i	Location of generic mass element relative to body i center of mass	(4.5)
S	Spatial step function	(5.30)
$\{\dot{s}\}$	Components of $\underline{\omega}^{vbR}$ in the coordinate system of body R .	(4.14)
T	Kinetic Energy	(2.5)
$\{T_E\}$	System external torques	(4.30)
U	System potential energy	(5.2)
\underline{u}	Deformation of a generic mass element. For a beam, the deformation of the centroid.	(2.10)
\underline{u}^i	Displacement of body i center of mass due to deformations	(4.5)

		<u>Ref. Eq.</u>
$\{u^i\}$	Components of \underline{u}^i in the floating frame coordinate system	(4.14)
\underline{u}_R	Deformation of the rotor mounting point	(5.11)
$(u_{R1}, u_{R2}, 0)$	Components of \underline{u}_R in inertial coordinate system	(5.14)
(u_1, u_2, u_3)	Components of \underline{u} in the floating frame coordinate system	(2.13)
$\{\hat{v}\}$	Vector bases fixed in the rotor frame	
w	Component of out of plane bending	(5.30)
(x, y, z)	Components of $\bar{\rho}$ in the floating frame coordinate system	(2.13)
$\{x^i\}$	Components of $\bar{\rho}^i$ in floating frame coordinate system	(4.23)
$\{\beta^i\}$	Components of $\underline{\omega}^{b^i f}$ in body i coordinate system	(4.14)
β_1, β_2	Constants related to angular velocity	(5.55)
$[\Delta]$	Modal coordinate coupling matrix	(4.55)
ϵ	Small number used in step function	(5.31)
$[\zeta]$	Diagonal matrix of modal percent of critical damping terms	(4.54)
$\{\eta\}$	Matrix of modal coordinates	(4.48)
η_i	Modal coordinate	(2.14)
η_{oi}	Rigid body modal coordinate	(3.13)
$\{\theta\}$	Tisserand frame variables	(4.13)
λ	Time variable for in-plane bending (later for torsion also)	(5.41)
λ_s	Lagrange multiplier term corresponding to constraint relationship s.	(4.26)
$\{\lambda\}$	Lagrange multiplier matrix	(4.37)
μ	Time variable for out of plane bending	(5.35)

		<u>Ref. Eq.</u>
v	Time variable for torsion	(5.41)
$\underline{\rho}$	Location of the generic mass element relative to the center of mass	(2.1)
$\dot{\underline{\rho}}$	Time derivative of $\underline{\rho}$ relative to an inertial reference frame	(2.1)
$\dot{\underline{\rho}}^o$	Time derivative of $\underline{\rho}$ relative to floating reference frame f.	(2.2)
$\underline{\rho}^i$	Location of the generic mass element in the undeformed state. Fixed in the floating reference frame	(2.10)
$\underline{\rho}_c^i$	Location for the undeformed state of the generic mass element of the deformable body relative to the deformable body center of mass. Fixed in the floating reference frame	(3.30)
$\underline{\rho}^i$	Undeformed location of body i center of mass relative to the system center of mass. Fixed in the floating reference frame	(4.5)
$\underline{\rho}_R$	Location of the rotor center of mass relative to the system center of mass	(3.33)
(ρ_1, ρ_2, ρ_3)	Components of $\underline{\rho}$ in the floating frame coordinate system	(2.7)
$[\phi]$	Rectangular modal matrix excluding rigid body modes	(4.47)
$\underline{\phi}^i$	Mode shape	(2.15)
$\underline{\phi}_i^o$	Rigid body mode shape	(3.7)
$(\phi_1^i, \phi_2^i, \phi_3^i)$	Components of $\underline{\phi}^i$ in the floating frame coordinate system	(2.14)
$\underline{\phi}^j$	Deformational mode shape corresponding to a nonzero natural frequency	(3.10)
ψ	Rotation about the beam centroid due to torsion	(5.7)
ψ_R	Rotation of the rotor about the beam centroid due to torsion	(5.14)
$\dot{\Omega}$	Rotor spin speed	(5.13)

		<u>Ref. Eq.</u>
ω_1	System natural frequency	(5.36)
$\begin{bmatrix} \omega_1 \\ \omega_n^2 \end{bmatrix}$	Diagonal angular velocity squared matrix. Nonzero frequencies only	(4.47)
ω^{bi}	Angular velocity of beam locally attached frame relative to inertial frame	(5.12)
ω^{bf}	Angular velocity of the beam locally attached frame (commonly at the rotor mounting point) relative to the system floating frame	(3.36)
$\omega^{b^i f}$	Angular velocity of body i frame relative to Tisserand frame	(4.9)
ω^{fi}	Angular velocity of the floating frame relative to an inertial frame	(2.2)
ω^{vb}	Angular velocity of rotor fixed frame relative to the beam locally attached frame at the mounting point	(3.36)
ω^{vbR}	Angular velocity of the rotor fixed frame relative to the body R frame	(4.10)
ω^{vf}	Angular velocity of the rotor frame relative to the floating frame	(3.33)

APPENDIX B

COORDINATE TRANSFORMATIONS

1-2-3 COORDINATE TRANSFORMATION

$$\{\underline{\hat{b}}\} = \begin{bmatrix} \cos\theta_3 & \sin\theta_3 & 0 \\ -\sin\theta_3 & \cos\theta_3 & 0 \\ 0 & 0 & 1 \end{bmatrix} \begin{bmatrix} \cos\theta_2 & 0 & -\sin\theta_2 \\ 0 & 1 & 0 \\ \sin\theta_2 & 0 & \cos\theta_2 \end{bmatrix} \begin{bmatrix} 1 & 0 & 0 \\ 0 & \cos\theta_1 & \sin\theta_1 \\ 0 & -\sin\theta_1 & \cos\theta_1 \end{bmatrix} \{\underline{\hat{i}}\}$$

$$\{\underline{\hat{b}}\} = \begin{bmatrix} \cos\theta_2 \cos\theta_3 & \cos\theta_1 \sin\theta_3 & \sin\theta_1 \sin\theta_3 \\ +\sin\theta_1 \sin\theta_2 \cos\theta_3 & -\cos\theta_1 \sin\theta_2 \cos\theta_3 & \\ -\cos\theta_2 \sin\theta_3 & \cos\theta_1 \cos\theta_3 & \sin\theta_1 \cos\theta_3 \\ -\sin\theta_1 \sin\theta_2 \sin\theta_3 & +\cos\theta_1 \sin\theta_2 \sin\theta_3 & \\ \sin\theta_2 & -\sin\theta_1 \cos\theta_2 & \cos\theta_1 \cos\theta_2 \end{bmatrix} \{\underline{\hat{i}}\}$$

$$\begin{aligned} \underline{\omega}^{bi} &= (\dot{\theta}_1 \cos\theta_2 \cos\theta_3 + \dot{\theta}_2 \sin\theta_3) \underline{\hat{b}}_1 \\ &+ (-\dot{\theta}_1 \cos\theta_2 \sin\theta_3 + \dot{\theta}_2 \cos\theta_3) \underline{\hat{b}}_2 \\ &+ (\dot{\theta}_1 \sin\theta_2 + \dot{\theta}_3) \underline{\hat{b}}_3 \\ &= (\dot{\theta}_1 + \dot{\theta}_3 \sin\theta_2) \underline{\hat{i}}_1 \\ &+ (\dot{\theta}_2 \cos\theta_1 - \dot{\theta}_3 \sin\theta_1 \cos\theta_2) \underline{\hat{i}}_2 \\ &+ (\dot{\theta}_2 \sin\theta_1 + \dot{\theta}_3 \cos\theta_1 \cos\theta_2) \underline{\hat{i}}_3 \end{aligned}$$

First Order Approximation

$$\{\underline{\hat{b}}\} = \begin{bmatrix} 1 & \theta_3 & -\theta_2 \\ -\theta_3 & 1 & \theta_1 \\ \theta_2 & -\theta_1 & 1 \end{bmatrix} \{\underline{\hat{i}}\} = ([E] - [\tilde{\theta}]) \{\underline{\hat{i}}\}$$

$$\underline{\omega}^{bi} = \{\hat{\underline{b}}\}^T \begin{pmatrix} \dot{\theta}_1 \\ \dot{\theta}_2 \\ \dot{\theta}_3 \end{pmatrix} = \{\hat{\underline{b}}\}^T \{\dot{\theta}\}$$

Second Order Approximation of Angular Velocity

$$\begin{aligned} \underline{\omega}^{bi} &= \{\hat{\underline{b}}\}^T \begin{pmatrix} \dot{\theta}_1 + \theta_3 \dot{\theta}_2 \\ \dot{\theta}_2 - \theta_3 \dot{\theta}_1 \\ \dot{\theta}_3 + \theta_2 \dot{\theta}_1 \end{pmatrix} \\ &= \{\hat{\underline{b}}\}^T \left([E] + \begin{bmatrix} 0 & \theta_3 & 0 \\ -\theta_3 & 0 & 0 \\ \theta_2 & 0 & 0 \end{bmatrix} \right) \{\dot{\theta}\} = \{\hat{\underline{b}}\}^T ([E] + [\theta_A]) \{\dot{\theta}\} \\ &= \{\hat{\underline{b}}\}^T \left(\{\dot{\theta}\} + \begin{bmatrix} 0 & 0 & \dot{\theta}_2 \\ 0 & 0 & -\dot{\theta}_1 \\ 0 & \dot{\theta}_1 & 0 \end{bmatrix} \{\theta\} \right) = \{\hat{\underline{b}}\}^T (\{\dot{\theta}\} + [\dot{\theta}_B] \{\theta\}) \end{aligned}$$

$$[\dot{\theta}_A]^T - [\dot{\theta}_B]^T = [\tilde{\theta}]$$

BEAM LOCALLY ATTACHED TO INERTIAL COORDINATE TRANSFORMATION

The $\hat{\underline{b}}_3$ axis is placed tangent to the centroid at each point. This accomplishes rotations 1 and 2. Rotation three is the torsional rotation, ψ , about the centroid (now $\hat{\underline{b}}_3$). Let \underline{T} be the unit vector tangent to the centroid, located at (u_1, u_2, z)

$$\underline{T} = \frac{u_1' \hat{\underline{i}}_1 + u_2' \hat{\underline{i}}_2 + \hat{\underline{i}}_3}{\sqrt{1 + (u_1')^2 + (u_2')^2}}$$

Since $\underline{T} = \hat{\underline{b}}_3$, the direction cosines of $\hat{\underline{b}}_3$ must equal the components of \underline{T} .

$$C_{31} = \sin\theta_2 = u'_1 / \sqrt{1 + (u'_1)^2 + (u'_2)^2}$$

$$C_{32} = -\sin\theta_1 \cos\theta_2 = u'_2 / \sqrt{1 + (u'_1)^2 + (u'_2)^2}$$

$$C_{33} = \cos\theta_1 \cos\theta_2 = 1 / \sqrt{1 + (u'_1)^2 + (u'_2)^2}$$

The direction cosines may then be defined in terms of

$$\sin\theta_1 = -u'_2 / \sqrt{1 + (u'_2)^2}$$

$$\cos\theta_1 = 1 / \sqrt{1 + (u'_2)^2}$$

$$\sin\theta_2 = u'_1 / \sqrt{1 + (u'_1)^2 + (u'_2)^2}$$

$$\cos\theta_2 = 1 + (u'_2)^2 / \sqrt{1 + (u'_1)^2 + (u'_2)^2}$$

The derivatives of θ_1 and θ_2 present in the angular velocity expression may be calculated by taking the derivatives $\sin\theta_1$ and $\sin\theta_2$. The binomial theorem may then be used in order to evaluate the second-order approximation of the angular velocity.

$$\underline{\omega}^{bi} = \{\hat{\underline{b}}\}^T \left\{ \begin{array}{c} -\dot{u}'_2 \\ \dot{u}'_1 \\ \dot{\psi} \end{array} \right\} + \left\{ \begin{array}{c} \psi \dot{u}'_1 \\ \psi \dot{u}'_2 \\ -u'_1 \dot{u}'_2 \end{array} \right\}$$

$$= \{\hat{\underline{b}}\}^T \left([E] + \begin{bmatrix} 0 & \psi & 0 \\ -\psi & 0 & 0 \\ u'_1 & 0 & 0 \end{bmatrix} \right) \left\{ \begin{array}{c} -\dot{u}'_2 \\ \dot{u}'_1 \\ \dot{\psi} \end{array} \right\}$$

APPENDIX C

VECTOR-DYADIC RELATIONSHIPS

Dot and Cross Products

$$\underline{u} \cdot \underline{v} = \{u\}^T \{v\}$$

$$\underline{u} \times \underline{v} = \{\hat{b}\}^T [\tilde{u}] \{v\}$$

where $\underline{u} = \{\hat{b}\}^T \{u\}$

$$\underline{v} = \{\hat{b}\}^T \{v\}$$

$$\{\hat{b}\} = \begin{Bmatrix} \hat{b}_1 \\ \hat{b}_2 \\ \hat{b}_3 \end{Bmatrix}$$

$$\{u\} = \begin{Bmatrix} u_1 \\ u_2 \\ u_3 \end{Bmatrix}$$

$$\{v\} = \begin{Bmatrix} v_1 \\ v_2 \\ v_3 \end{Bmatrix}$$

$$[\tilde{u}] = \begin{bmatrix} 0 & -u_3 & u_2 \\ u_3 & 0 & -u_1 \\ -u_2 & u_1 & 0 \end{bmatrix}$$

$$[\tilde{u}] \{v\} = - [\tilde{v}] \{u\}$$

$$\square \times \underline{u} = \{\hat{b}\}^T [I] [\tilde{u}] \{\hat{b}\}$$

where $\square = \{\hat{b}\}^T [I] \{\hat{b}\}$

$$[I] = \begin{bmatrix} I_{11} & I_{12} & I_{13} \\ I_{21} & I_{22} & I_{23} \\ I_{31} & I_{32} & I_{33} \end{bmatrix}$$

ENDING PAGE

Reference Point Transfer Theorem for an Inertia Dyadic

$$\boxed{}^o = \boxed{}^c + M[(\underline{r}_o \cdot \underline{r}_o)\mathbb{U} - \underline{r}_o \underline{r}_o]$$

where $\boxed{}^o$: Inertia dyadic about point 0.

$\boxed{}^c$: Inertia dyadic about body center of mass.

\mathbb{U} : Unit dyadic.

\underline{r}_o : Vector from 0 to C.

M : Mass of the body

$$\frac{1}{2} \underline{\omega} \cdot \boxed{}^o \cdot \underline{\omega} = \frac{1}{2} \underline{\omega} \cdot \boxed{}^c \cdot \underline{\omega} + \frac{1}{2} M[(\underline{\omega} \times \underline{r}_o) \cdot (\underline{\omega} \times \underline{r}_o)]$$

$$\boxed{}^o \cdot \underline{\omega} = \boxed{}^c \cdot \underline{\omega} + M \underline{r}_o \times (\underline{\omega} \times \underline{r}_o)$$

APPENDIX D

HYBRID COORDINATE METHOD USING ASSUMED

MODE SHAPES FOR ELASTIC CONTINUA

ABSTRACT: The hybrid coordinate method provides equations of motion of minimum dimension for a spacecraft with flexible appendages. Instead of the usual finite element approach, in which mode shapes are calculated from equations of vibration of the finite element assembly, this chapter provides an alternative formulation using assumed mode shapes. This proves useful for a class of simply modeled appendages for which mode shapes are provided by an outside agency, or are otherwise known. The results are shown to be compatible with the finite element formulation, as previously described.

I. INTRODUCTION

The hybrid-coordinate method provides equations of motion of a spacecraft with elastic (flexible) appendages. The appendages are modeled as an interconnected set of small rigid bodies interconnected by massless or massive elastic bodies (finite elements). From the Newton-Euler approach, the equations of motion for each finite element and the rigid body portion of the spacecraft are formulated. The introduction of an appropriate coordinate transformation allows the finite element equations to be represented as decoupled vibration equations, which involve mode shapes and modal coordinates. Since the vibration equations have been decoupled from each other, significant truncation of the higher order mode shapes can be accomplished. This leads to a set of equations where rotation of the rigid body portion of the spacecraft is coupled to the vibration of the flexible appendages. These equations are of great practical use because the truncation procedure has significantly reduced the number of degrees of freedom of the system without substantially sacrificing the fidelity of the results.

The purpose of this chapter is to provide an alternative formulation for the hybrid coordinate method using assumed mode shapes. This approach will prove useful for simply modeled appendages. For these the mode shapes can be determined from a continuum analysis using partial differential equation methods. The truncation procedure is accomplished at the outset by eliminating the higher order modes of vibration. The equations of motion are formulated using a Lagrangian approach and the coordinate transformation is accomplished using the assumed mode shapes. The resulting equations of motion are then seen to be compatible with those arising from the finite element method.

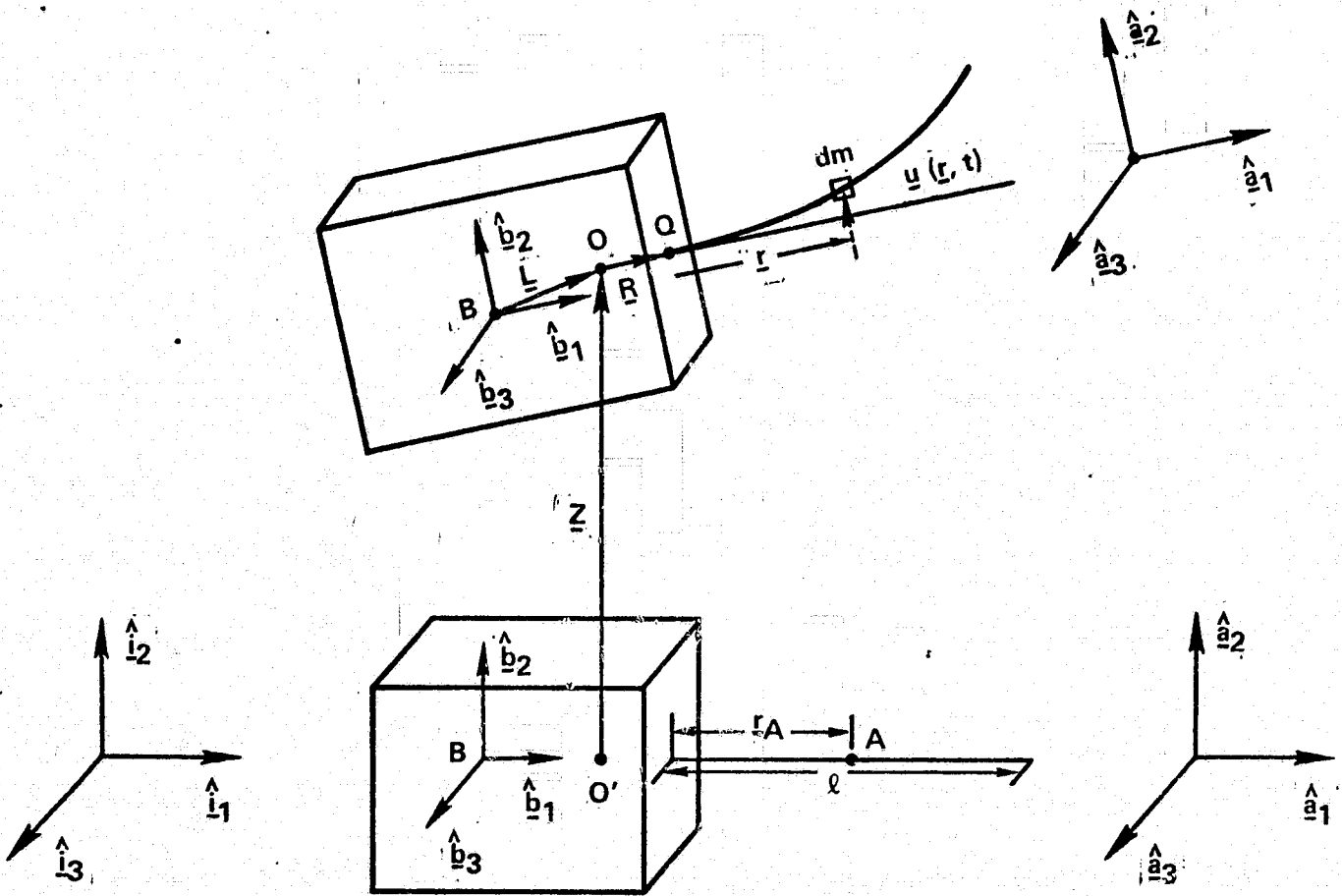


Figure 1. System Diagram.

where

- O : Center of mass of undeformed system (body fixed)
- O' : Position of O at rest (inertially fixed)
- B : Center of mass of rigid body
- A : Center of mass of undeformed appendage
- \mathcal{M} : Total System mass
- M : Appendage mass
- m : Appendage mass/length
- Q : Connection point of appendage

II. MODEL

The following derivation of equations of motion uses a model comprised of a central rigid body and a flexible cantilevered beam. Extensions to several appendages of arbitrary configurations may be made from the results of this simple model. The undeformed position of the appendage is taken to be constant relative to the rigid body. The transformation between the two is included in the derivation to facilitate the extension of the equations to cover a driven appendage. The angular rotations are assumed to be small as are the translational displacements. A diagram of the model is shown in Figure 1. To summarize, the assumptions used in the following derivation are:

- rigid body with cantilevered beam,
- beam rest position constant relative to base,
- small translations and rotations.

No orthogonality requirements have been placed on the assumed mode shapes. The vibration equations are therefore coupled. Further coordinate transformations may be employed to decouple the vibration equations or to achieve vehicle normal modes, but the truncation procedure does not require this as it does with the finite element procedure.

The vector bases employed in the derivation are:

- $\{\underline{i}\}$: Inertially fixed basis
- $\{\underline{b}\}$: Basis fixed in the rigid body
- $\{\underline{a}\}$: Basis fixed in appendage prior to deformation

where

$$\{\underline{b}\} = [\theta]\{\underline{i}\}$$

$$[\theta] = (E - \tilde{\theta}) \text{ for small rotations } \tilde{\theta} = \begin{bmatrix} 0 & -\theta_3 & \theta_2 \\ \theta_3 & 0 & -\theta_1 \\ -\theta_2 & \theta_1 & 0 \end{bmatrix}$$

$$\{\underline{a}\} = [c]\{\underline{b}\}$$

$$[c] = \text{constant for an undriven appendage.}$$

For the undeformed system, the location of the center of mass is defined by

$$\int_{\text{SYS}} \underline{\rho} \, dm = 0$$

where $\underline{\rho}$ is the generic position vector from the center of mass to the differential mass element. Evaluating this expression leads to

$$-(\mathcal{M} - M) \underline{L} + M(\underline{R} + \underline{r}_A) = 0$$

where the quantities are shown in Figure 1 with \underline{L} being the location of the rigid body center of mass and \underline{r}_A the appendage center of mass.

The dyadic of the undeformed system is defined by

$$\underline{\underline{\square}}^* = \underline{\underline{\square}}_{\text{RB}}^0 + \underline{\underline{\square}}_{\text{AP-u}}^0$$

$$\underline{\underline{\square}}_{\text{RB}}^0 = \underline{\underline{\square}}_{\text{RB}}^B + (\mathcal{M} - M)(\underline{L} \cdot \underline{L} \, \underline{\underline{U}} - \underline{\underline{L}} \underline{\underline{L}})$$

$$\underline{\underline{\square}}_{\text{AP-u}}^0 = \underline{\underline{\square}}_{\text{AP-u}}^A + M \left[(\underline{R} + \underline{r}_A) \cdot (\underline{R} + \underline{r}_A) \, \underline{\underline{U}} - (\underline{R} + \underline{r}_A)(\underline{R} + \underline{r}_A) \right]$$

III. THE LAGRANGIAN OF THE SYSTEM

The kinetic energy of the system is

$$T_{\text{SYS}} = \frac{1}{2} \int_{\text{RB}} \underline{v} \cdot \underline{v} \, dm + \frac{1}{2} \int_{\text{APP}} \underline{v} \cdot \underline{v} \, dm$$

where \underline{v} is the inertial velocity of a generic mass element. The kinetic energy for the rigid body yields

$$\frac{1}{2} \int_{\text{RB}} \underline{v} \cdot \underline{v} \, dm = \frac{1}{2} (\mathcal{M} - M) \dot{\underline{R}}^B \cdot \dot{\underline{R}}^B + \frac{1}{2} \underline{\omega} \cdot \underline{\underline{\square}}_{\text{RB}}^B \cdot \underline{\omega}$$

where \mathcal{M} is the system mass, M the appendage mass, and B is the center of mass of the rigid body with

$$\underline{R}_B = \underline{Z} - \underline{L}$$

$$\dot{\underline{R}}_B = \dot{\underline{Z}} - \underline{\omega} \times \underline{L}$$

Expanding this expression and switching the reference point of the inertia dyadic to the system mass center gives

$$\frac{1}{2} \int_{RB} \underline{v} \cdot \underline{v} \, dm = \frac{1}{2} (\mathcal{M} - M) \dot{\underline{Z}} \cdot \dot{\underline{Z}} + \frac{1}{2} \underline{\omega} \cdot \underline{\square}_{RB}^0 \cdot \underline{\omega} - (\mathcal{M} - M) \left[\dot{\underline{Z}} \cdot (\underline{\omega} \times \underline{L}) \right]$$

The kinetic energy of the appendage is

$$\frac{1}{2} \int_{APP} \underline{v} \cdot \underline{v} \, dm = \frac{1}{2} \int \dot{\underline{R}}_m \cdot \dot{\underline{R}}_m \, dm$$

where

$$\underline{R}_m = \underline{Z} + \underline{R} + \underline{r} + \underline{u}$$

$$\dot{\underline{R}}_m = \dot{\underline{Z}} + \dot{\underline{u}} + \overset{\circ}{\underline{R}} + \overset{\circ}{\underline{r}} + \underline{\omega} \times (\underline{R} + \underline{r})$$

Vector differentiation with respect to the rotating reference frame is denoted by the "circle" above the vector. Here $\overset{\circ}{\underline{R}}$ and $\overset{\circ}{\underline{r}}$ are zero since they are fixed in the frame. The "dot" denotes differentiation relative to an inertial reference frame. Expanding the expression and making use of the dyadic of the undeformed appendage about the system mass center ($\underline{\square}_{AP-u}^0$) yields.

$$\begin{aligned} \frac{1}{2} \int_{APP} \underline{v} \cdot \underline{v} \, dm &= \frac{1}{2} M \dot{\underline{Z}} \cdot \dot{\underline{Z}} + \frac{1}{2} \underline{\omega} \cdot \underline{\square}_{AP-u}^0 \cdot \underline{\omega} + \frac{1}{2} \int \dot{\underline{u}} \cdot \dot{\underline{u}} \, dm \\ &+ \dot{\underline{Z}} \cdot \int_{APP} \dot{\underline{u}} \, dm + \dot{\underline{Z}} \cdot \underline{\omega} \times \left[M(\underline{R} + \underline{r}_A) \right] \\ &+ \int_{APP} \left[\dot{\underline{u}} \cdot \underline{\omega} \times (\underline{R} + \underline{r}) \right] \, dm \end{aligned}$$

Combining the terms for kinetic energy and eliminating terms produces

$$\begin{aligned}
T_{\text{SYS}} &= \frac{1}{2} M \dot{\underline{Z}} \cdot \dot{\underline{Z}} + \frac{1}{2} \underline{\omega} \cdot \underline{\square}^* \cdot \underline{\omega} \\
&+ \frac{1}{2} \int_{\text{APP}} \dot{\underline{u}} \cdot \dot{\underline{u}} \, dm + \underline{Z} \cdot \int_{\text{APP}} \dot{\underline{u}} \, dm \\
&+ \underline{\omega} \cdot \underline{R} \times \int_{\text{APP}} \dot{\underline{u}} \, dm + \underline{\omega} \cdot \int_{\text{APP}} (\underline{r} \times \dot{\underline{u}}) \, dm.
\end{aligned}$$

The inertia dyadic of the undeformed system about the system center of mass is $\underline{\square}^*$. The center of mass expression eliminated the term in the kinetic energy containing \underline{Z} and $\underline{\omega}$.

From beam theory, the strain energy of the appendage is

$$u = \frac{1}{2} \int_{\text{APP}} EI \left(\frac{\partial^2 u}{\partial r^2} \right) \cdot \left(\frac{\partial^2 u}{\partial r^2} \right) dr$$

The Lagrangian for the system is then

$$\begin{aligned}
\mathcal{L} &= \frac{1}{2} M \dot{\underline{Z}} \cdot \dot{\underline{Z}} + \frac{1}{2} \underline{\omega} \cdot \underline{\square}^* \cdot \underline{\omega} + \frac{1}{2} \int_{\text{APP}} \dot{\underline{u}} \cdot \dot{\underline{u}} \, dm \\
&+ \dot{\underline{Z}} \cdot \int_{\text{APP}} \dot{\underline{u}} \, dm + \underline{\omega} \cdot \underline{R} \times \int_{\text{APP}} \dot{\underline{u}} \, dm \\
&+ \underline{\omega} \cdot \int_{\text{APP}} (\underline{r} \times \dot{\underline{u}}) \, dm - \frac{1}{2} \int_{\text{APP}} EI \left(\frac{\partial^2 u}{\partial r^2} \right) \cdot \left(\frac{\partial^2 u}{\partial r^2} \right) dr.
\end{aligned}$$

The formation of the above has assumed that the undeformed appendage is fixed relative to the base ($\underline{\omega}^{\text{Bi}} = \underline{\omega}^{\text{A1}}$). The next step to be taken is to assume small angle rotations and represent the Lagrangian in matrix form. The following matrices are used:

$$\begin{aligned}
\dot{\underline{Z}} &= \{\underline{i}\}^T \{\dot{Z}\} \\
\underline{\omega} &= \{\underline{b}\}^T \{\dot{\theta}\} \quad (\text{small rotations})
\end{aligned}$$

$$\underline{u} = \{\underline{a}\}^T \{u\}$$

$$\underline{I}^* = \{\underline{b}\}^T I^* \{\underline{b}\}$$

$$\underline{R} = \{\underline{b}\}^T \{R\}$$

$$\underline{r} = \{\underline{b}\}^T \{r\}$$

$$\tilde{R} = \begin{bmatrix} 0 & -R_3 & R_2 \\ R_3 & 0 & -R_1 \\ -R_2 & R_1 & 0 \end{bmatrix} ; \quad \tilde{r} = \begin{bmatrix} 0 & -r_3 & r_2 \\ r_3 & 0 & r_1 \\ -r_2 & r_1 & 0 \end{bmatrix}$$

$$\tilde{\theta} = \begin{bmatrix} 0 & -\dot{\theta}_3 & \dot{\theta}_2 \\ \dot{\theta}_3 & 0 & -\dot{\theta}_1 \\ -\dot{\theta}_2 & \dot{\theta}_1 & 0 \end{bmatrix}$$

$$[\theta] = [E - \tilde{\theta}]$$

$$\frac{\partial^2 u}{\partial r^2} = \{\underline{a}\}^T \begin{Bmatrix} \frac{\partial^2 u_1}{\partial r^2} \\ \frac{\partial^2 u_2}{\partial r^2} \\ \frac{\partial^2 u_3}{\partial r^2} \end{Bmatrix} = \{\underline{a}\}^T \{u''\}$$

Retaining second order terms in the Lagrangian produces

$$\begin{aligned} \mathcal{L} = & \frac{1}{2} M \{\dot{Z}\}^T \{\dot{Z}\} + \frac{1}{2} \{\dot{\theta}\}^T I^* \{\dot{\theta}\} \\ & + \frac{1}{2} \int_{APP} \{\dot{u}\}^T \{\dot{u}\} dm + \{\dot{Z}\} [C] \int_{APP} \{\dot{u}\} dm \\ & + \{\dot{\theta}\}^T C \tilde{R} \int_{APP} \{\dot{u}\} dm + \{\dot{\theta}\}^T C \int_{APP} \tilde{r} \{\dot{u}\} dm \\ & - \frac{1}{2} \int_{APP} EI \{u''\}^T \{u''\} dr. \end{aligned}$$

Distributed coordinates are introduced by the coordinate transformation

$$\underline{u}(r, t) = \sum_{i=1}^n \phi^i(r) \eta^i(t)$$

where n is the number of modes used to represent the displacement. In matrix form, the transformation is

$$\begin{aligned} \{u\} &= \sum_{i=1}^n \{\phi^i\} \eta^i \\ &= \begin{bmatrix} \phi^1 & \phi^2 & \dots & \phi^n \end{bmatrix} \{\eta\} \\ &= [\phi] \{\eta\} \end{aligned}$$

where $[\phi]$ is a $3 \times n$ matrix with each column corresponding to a mode shape and $\{\eta\}$ contains n modal coordinates.

This coordinate transformation yields the Lagrangian

$$\begin{aligned} \mathcal{L} &= \frac{1}{2} M \{\dot{z}\}^T \{\dot{z}\} + \frac{1}{2} \{\dot{\theta}\}^T I^* \{\dot{\theta}\} \\ &+ \frac{1}{2} \{\dot{\eta}\}^T x_2 \{\dot{\eta}\} + \{\dot{z}\}^T c x_1 \{\dot{\eta}\} \\ &+ \{\dot{\theta}\}^T c(\tilde{R} x_1 + x_3) \{\dot{\eta}\} - \frac{1}{2} \{\eta\}^T x_4 \{\eta\} \end{aligned}$$

where

$$x_1 = \int_{APP} [\phi] \, dm$$

$$x_2 = \int_{APP} [\phi]^T [\phi] \, dm$$

$$x_3 = \int_{APP} \tilde{r} [\phi] \, dm$$

$$x_4 = \int_{APP} EI [\phi'']^T [\phi''] \, dr$$

The matrices X_1 and X_3 are of dimension $3 \times n$ while the matrices X_2 and X_4 are symmetric and of dimension $n \times n$. The Lagrangian depends on $n+6$ generalized coordinates. Six coordinates describe the translation and rotation of the undeformed system and n modal coordinates describe the displacement from rest of the flexible appendage relative to the rigid base.

IV. EQUATIONS OF MOTION

The equations of motion for the system may now be derived from the Lagrangian in the traditional manner. The resulting $n+6$ equations may be represented in matrix form as

$$\mathcal{M} \{\ddot{Z}\} + X_1 \{\ddot{\eta}\} = 0$$

$$I^* \{\ddot{\theta}\} + (\tilde{R} X_1 + X_3) \{\ddot{\eta}\} = \{T\}$$

$$X_2 \{\ddot{\eta}\} + X_4 \{\eta\} = -X_1^T \{\ddot{Z}\} + (X_1^T \tilde{R} - X_3^T) \{\ddot{\theta}\}$$

where $\{T\}$ is the externally applied torque. The first matrix equation may be used to eliminate the translation from the vibration equations. This produces $n + 3$ equations of the form

$$I^* \{\ddot{\theta}\} + (\tilde{R} X_1 + X_3) \{\ddot{\eta}\} = \{T\}$$

$$\left(X_2 - \frac{1}{\mathcal{M}} X_1^T X_1 \right) \{\ddot{\eta}\} + X_4 \{\eta\} = (X_1^T \tilde{R} - X_3^T) \{\ddot{\theta}\}$$

The matrices that provide coupling between the rotation and vibration in each equation may be seen to be transposes of each other. The equations can be written as

$$I^* \{\ddot{\theta}\} - \delta^T \{\ddot{\eta}\} = \{T\}$$

$$\left(X_2 - \frac{1}{\mathcal{M}} X_1^T X_1 \right) \{\ddot{\eta}\} + X_4 \{\eta\} = \delta \{\ddot{\theta}\}$$

where

$$\delta = X_1^T \tilde{R} - X_3^T.$$

V. COMPATIBILITY WITH FINITE

ELEMENT EQUATIONS OF MOTION

The equations of motion derived from the continuum analysis are similar in structure to those derived from the finite element analysis (Ref. 1). The differences between the two appear in the assumptions made in the continuum analysis:

- No orthogonality properties
- Rotary inertia effect ignored.
(No differential rotation of appendage mass elements due to deformation)

Orthogonality properties can be applied to the continuum analysis vibration equations by a suitable coordinate transformation. The orthogonality properties are not needed to permit truncation as is the case in the finite element analysis.

The equations of motion from a finite element analysis are shown by equations (287) to (289) of Reference 1.

$$\begin{aligned} I^* \ddot{\theta} - \bar{\delta}^T \ddot{\bar{\eta}} &= T \\ \ddot{\bar{\eta}} + 2\bar{\zeta}\bar{\omega}\dot{\bar{\eta}} + \bar{\omega}^2\bar{\eta} &= \bar{\delta} \ddot{\theta} \\ \bar{\delta} &= -\phi^T M \left(\sum_{OE} - \sum_{EO} \tilde{R} - \tilde{r} \sum_{EO} \right) \end{aligned}$$

The overbar indicates truncation. If the damping is eliminated and the orthogonality condition relaxed (after truncation), the equations become

$$\begin{aligned} I^* \ddot{\theta} - \bar{\delta}^T \ddot{\bar{\eta}} &= T \\ \phi^T M' \phi \ddot{\bar{\eta}} + \phi^T K' \phi \bar{\eta} &= \bar{\delta} \ddot{\theta} \end{aligned}$$

where

$$M' = M \left(E - \sum_{EO} \sum_{EO}^T M_{/..ll} \right)$$

K' = Stiffness-matrix.

Normally, the coordinate transformation $\bar{\phi}$ includes mode shapes with translation and rotation of the finite elements. To agree with the continuum analysis, no rotations of the finite elements will be allowed. The coordinate transformation $\bar{\phi}$ will then be a $6n \times N$ matrix represented by

$$\bar{\phi} = [\{\phi^1\} \{\phi^2\} \dots \{\phi^N\}]$$

where

$$\{\phi^i\} = \begin{Bmatrix} \{\phi_{D1}^i\} \\ 0 \\ \vdots \\ \{\phi_{Dn}^i\} \\ 0 \end{Bmatrix}$$

With the above limitations, the matrix multiplication can be performed in the finite element equations and the terms may be compared with those from the continuum analysis.

For the augmented mass matrix, the finite element analysis results in

$$\begin{aligned} (\bar{\phi}^T M \bar{\phi})_{ij} &= \sum_{k=1}^n m_k \left\{ \phi_{D_k}^i \right\}^T \left\{ \phi_{D_k}^j \right\} \\ &+ \sum_{\ell=1}^n \sum_{k=1}^n \left(\frac{m_k m_\ell}{\mathcal{M}} \left\{ \phi_{D_\ell}^i \right\}^T \left\{ \phi_{D_k}^j \right\} \right). \end{aligned}$$

This is compatible with the result from the continuum analysis

$$\begin{aligned} \left(X_2 - \frac{1}{\mathcal{M}} X_1^T X_1 \right)_{ij} &= \int_{APP} m(r) \left[\phi^i \right]^T \left[\phi^j \right] dr \\ &+ \iint_{APP} \frac{m(r)m(r)}{\mathcal{M}} \left[\phi^i \right]^T \left[\phi^j \right] dr dr. \end{aligned}$$

For the δ matrix, the finite element analysis results in

$$[\delta]_j = \sum_{i=1} m_i \left\{ \phi_{D_1}^j \right\}^T (\tilde{R} + \tilde{r}_i)$$

This is compatible with the result from the continuum analysis

$$[\delta]_j = \int m(r) \left[\phi_D^j \right]^T (\tilde{R} + \tilde{r}) dr$$

Thus, if the number of finite elements were increased without limit, the finite element equations would be identical to the continuum analysis equations.

VI. CONCLUSION

With the foregoing results it becomes possible to accomplish a hybrid coordinate dynamic analysis for a system with appendages defined only in terms of modal data based on a continuum analysis.